The gene, *occ1*, is preferentially expressed in the primary visual cortex in an activity-dependent manner: a pattern of gene expression strikingly related to the functional area in macaque neocortex

by

Shiro Tochitani

Department of Molecular Biomechanics,
School of Life Science,
The Graduate University for Advanced Studies

A Thesis Submitted in a Partial Fulfillment of the Requirements for the Degree of Doctor of Philosophy

January 2001

Acknowledgements

I am grateful to Prof. Tetsuo Yamamori at National Institute for Basic Biology (NIBB) for encouragement throughout the course of the work. I am grateful also to Drs. Hashikawa and Liang at Brain Science Institute at Riken for technical advice and encouragement. I wish to express my great appreciation to Dr. Koike at Tokyo Metropolitan Institute for Neuroscience (TMIN) for encouragement and technical suggestions. I thank Dr. Watakabe at NIBB for encouragement, Ms. Ida-Hosonuma at TMIN for technical assistance, Drs. Horie, Abe and Hashizume at Japan Poliomyelitis Research Institute for providing the monkey tissues and Dr. Ono of the Corporation for Production and Research of Laboratory Primates and Dr. Terao of the Tsukuba Primate Center, National Institute of Infectious Diseases for supplying the monkeys.

Lastly, but not the least, I would like to appreciate lots of encouragement and supports given by my parents, sister and aunt.

Contents

General Introduction

The mammalian central nervous system is composed of quite various types of neurons. Nowhere is this neuronal diversity more apparent than in the cerebral neocortex. The neuronal diversity in the neocortex may be, at least in part, reflected in molecular characteristics. The discovery of molecular markers unique to specific neuronal groups can allow us to see and study those groups in isolation, which would be effective in deciphering neuronal organizations and functions in the neocortex.

The adult mammalian neocortex is subdivided into functional areas which have distinct cytoarchitectonic characteristics. With a notion that I might come across such a marker as to visualize a specific subset of neurons comparing molecular properties among the neocortical subdivisions, I started to compare genes expressed as mRNA in the functionally and structurally distinct areas of adult macaque neocortex. Macaque monkeys were selected as the samples because cortical differentiation is more fully expressed in macaques than in the other mammalian model organisms such as mice and rats. The comparison of

mRNAs was performed using differential display, with which you can compare many kinds of mRNAs at the same time with relatively small amount of mRNA. As a result of the search, a cDNA fragment which was preferentially transcribed in the occipital neocortex was obtained, and it has been named *occ1*. In part I, the identification of *occ1* and the characterization of the neurons specified by *occ1* expression will be described.

The distibution of *occ1*-expressing neurons shows a marked correlation with the cytoarchitectonic borders, which raises the following questions. What is the function of *occ1* in the neurons? How does the region-selective expression of *occ1* contribute to the function of neocortex? Answering these questions will help us to understand how the neocortex is formed to function. As a first step toward addressing these questions, the spatial and temporal expression pattern of *occ1* during the postnatal developmental events of visual cortex was examined. The description on this study will be presented in part II.

Part I

Identification and characterization of the gene *occ1*, which is preferentially expressed in the primary visual cortex in an activity-dependent manner.

Summary

Marker molecules to visualize specific subsets of neurons are useful for studying how the neocortex is organized to function. One approach to identify such molecular markers is to examine the differences in molecular properties among morphologically and physiologically distinct neuronal cell types. I applied differential display to compare mRNA expression in the anatomically and functionally distinct areas of the adult macaque neocortex. I found that a gene designated *occ1* was preferentially transcribed in the posterior region of the neocortex, especially, area 17. Complete sequencing analysis revealed that *occ1* encodes a macaque homologue of a secretable protein, TSC-36/follistatin-related protein (FRP). *In situ* hybridization histochemistry confirmed the characteristic neocortical expression pattern of *occ1* and showed that *occ1* transcription is high in layers II, III, IVA and IVC of area 17. In addition, *occ1* transcription was observed selectively in cells of the magnocellular layers in LGN and specific subset of neurons in the hippocampal formation. Dual labeling immunohistochemistry showed that the *occ1*-positive neurons in area 17 include

both GABA-positive aspiny inhibitory cells and α subunit of type II calcium/calmodulin-dependent protein kinase (CaMKII α)-positive spiny excitatory cells. With brief periods of monocular deprivation, the *occ1*-mRNA level markedly decreased in deprived ocular dominance columns of area 17. From these, I conclude that the expression of *occ1* mRNA is marked to a subset of neurons which are preferentially localized in particular laminae of area 17 and consist of various morphological and physiological neuronal types, and, furthermore, *occ1* transcription is subject to visually driven activity-dependent regulation.

Introduction

The distributions of specific molecules show striking correlations with particular physiological organizations in the primate visual system. The Cat-301 antibody, which recognizes a chondroitin sulfate proteoglycan (Zaremba et al., 1989; Hockfield et al., 1990), primarily stains the magnocellular layers (layers 1-2) of the lateral geniculate nucleus (LGN) (Hendry et al., 1984). Immunostaining for calcium/calmodulin-dependent protein kinase II α subunit (CaMK II α in combination with neuronal tracing techniques revealed that the koniocellular layers (intercalated layers) in macaque LGN send direct afferent inputs to blobs in area 17 (Hendry and Yoshioka, 1994). Although functional modules of the neocortex are even more complicated than those in thalamic nuclei, some molecules spatially coincide with the fundamental functional subdivisions of the neocortex, such as layers, columns and areas. Cytochrome oxidase (CO) is enriched in the blobs in layers II and III of the primary visual cortex (area 17) (Wong-Riley, 1979; Horton and Hubel, 1981) and in the stripe-shaped structures in the secondary visual cortex (area 18) (Livingstone and Hubel, 1982, 1983; Horton, 1984). Synaptic zinc is enriched in CO-poor interblob regions (Dyck and Cynader, 1993). The pattern of m2 muscarinic acetylcholine receptor immunoreactivity is also reciprocal to the pattern of CO histochemical staining in layers II and III, the strongest immunoreactivity being observed in layers IVA and IVCβ of area 17 where projections from the parvocellular layers (layers 3-6) of the LGN selectively terminate (Mrzljak et al., 1996). Regional variations among

higher visual areas exist in terms of density and laminar distribution of neurons marked by SMI-32, a monoclonal antibody against on the medium- and high-molecular-weight subunits of neurofilament protein (Hof and Morrison, 1995). The antigen recognized by Cat-301 is more abundantly expressed in the areas of the dorsal stream than in those of the ventral stream of the visual processing pathway (Hendry et al., 1988b).

The results of these studies provide impressive examples of molecular parcelations of the nervous system although the number of available molecular markers is still limited. It is expected that as more molecular markers that allow visualization of specific neuronal subsets in the neocortex are obtained, more information about how the neocortex is organized in relation to function will arrive. New histochemical markers may allow us to recognize new populations of neurons and/or new functional subdivisions of the neocortex. In addition, it may be noted that most of the known markers and the neurons marked by them have been discovered by chance. This implies that an extensive and systematic approach to identify such molecular markers for determining specific neuronal subsets would be more fruitful (Hendry & Calkins, 1998).

I applied differential display (DD) (Liang and Pardee, 1992) to compare mRNA expression in structurally and functionally distinct areas of the adult macaque neocortex. I cloned a cDNA named *occ1*, which showed a high transcription level in the occipital cortex. In this report, I describe the

identification of *occ1* and the characterization of the neurons specified by *occ1* expression.

Materials and methods

Tissue dissection, total RNA extraction and DD PCR.

The brains were removed from three adult macaques (*Macaca fascicularis*) under deep Nembutal anesthesia at the Japan Poliomyelitis Research Institute. The brains were dissected and frozen on dry ice. Total RNA was obtained by a single-step RNA isolation method by guanidine thiocyanate-urea-phenol-chloroform extraction (Chomczynski and Sacchi, 1987). The DD PCR was performed following the protocol of the RNA Image kit (GeneHunter, Nashville, TN, USA) with minor modifications. The reverse transcription (RT) reaction was carried out using an anchor oligo-dT primer, followed by arbitrarily primed PCR with the 5'-end-^{33}P-labeled anchor oligo-dT primer and an arbitrary 13-mer primer by KlenTaq Polymerase (Clontech Laboratories, Palo Alto, CA, USA). The PCR parameters were 1 cycle of 94°C (5 min), 40°C (5 min) and 68°C (5 min), 6 cycles of 94°C (2 min), 40°C (5 min) and 68°C (5 min), and 33 cycles of 94°C (1 min), 40°C (2 min) and 68°C (1 min), followed by the final elongation step at 72°C for 20 min. The PCR products were then separated by electrophoresis on 4% polyacrylamide sequencing gels. The bands that showed differential expressions among the areas were reamplified by PCR using the same primer set that generated them. The PCR parameters for reamplification were 95°C for 5 min, 30 cycles of 95°C (1 min), 40°C (1 min) and 68°C (1 min), and finally at 72°C for 5 min.

RT-PCR analysis.

Total RNAs (2.0 μg) from five regions (areas FDΔ, FA, TE, OA and OC; see Fig. I-1) of *Macaca fascicularis* neocortex were reverse-transcribed using Superscript II reverse transcriptase (Life Technologies, Rockville, MD, USA) with Oligo $(dT)_{12\text{-}18}$ primer (Life Technologies) in a final reaction volume of 40 μl. Simultaneously, the samples subject to the same preparations without reverse transcriptase were prepared and used as negative control samples (RT-) to show the absence of contaminated genomic DNA in the total RNAs. PCR was performed using a primer set corresponding to the end sequences of the cloned occ1 DD band (5'-GGAAGAGATTTAATCTTACAAAAGG-3' and 5'-TATACAGTCAAAGAGGTTGCAACAG-3'). PCR conditions were 95°C for 5 min, 20 cycles of 94°C (30 sec), 60°C (30 sec) and 72°C (30 sec), and finally at 72°C for 5 min. After separation on a 1.0 % agarose gel, the products were blotted and detected by hybridization to the ^{32}P-labeled *occ1* probe. RT-PCR for *glyceraldehyde-3-phosphate dehydrogenase* (*g3pdh*) was performed with primers 5'-AGCGAGATCCCTCCAAAATCAAGTG-3' and 5'-GCCATGCCAGTGAGCTTCCCGTTCA -3' as an internal control.

Northern blot analysis.

Poly $(A)^+$ RNA (12 μg) was purified from the total RNA from neocortical area OC, electrophoresed on a 1.2% agarose gel and transferred to Hybond N^+ nylon membrane (Amersham Pharmacia Biotech, Buckinghamshire, UK). The hybridization probe was prepared from an *occ1* cDNA clone (1024 bp + poly $(A)^+$

tail), firstly obtained by screening a cDNA library, and radiolabeled with (^{32}P) dCTP.

Construction of cDNA library and isolation of occ1 full-length clone.

Using poly (A)$^+$ mRNA from *Macaca fascicularis* neocortical area OC, cDNAs were synthesized with ZAP-cDNA synthesis kit (Stratagene, La Jolla, CA, USA) and ligated to EcoRI/XhoI-digested λ ZAPII vector (Stratagene), followed by packaging with Gigapack III Gold packaging extract (Stratagene). The nucleotide sequences determined on both strands are in the DDBJ/EMBL/GenBank nucleotide sequence databases with the accession number AB039661. Alignments of the sequences were performed using CLUSTAL W (Thompson et al., 1994).

Generation of antiserum against OCC1.

Rabbit OCC1 antisera were raised against a fusion protein. OCC1-GST (amino acids (aa) 87-308 of OCC1 fused to GST) was constructed by subcloning this segment of the *occ1* cDNA into pGEX 2TK (Amersham Pharmacia Biotech) and expressed in *Escherichia coli BL21*. For antiserum production, three New Zealand white rabbits were immunized, and the antisera were passed through the affinity resin Affi-gel 15 (Bio-Rad Laboratories, Hercules, CA, USA) coupled with the crude lysates of *E. coli BL21* transfected with mock pGEX2TK vector to exclude the antibodies against GST and bacterial proteins.

Construction of expression vector, transient expression of OCC1 in COS-7 cells and Western blot analysis.

The expression plasmid, pOCC1, was constructed as follows: the complete sequence of the *occ1* cDNA was amplified by PCR using a 5'-primer (5'-CCGCTCCAGATGTGGAAACGCTGGCTCGCGCTC-3') which introduced an XhoI cleavage site at the N terminus and a 3'-primer (5'-AAACTGCAGTCATTAGATCTCTTTGGTGCTCAC-3') introducing two consecutive stop codons and a PstI cleavage site at the C terminus of the *occ1* cDNA. The XhoI/PstI fragment of the PCR product was cloned into the CMV-promoter driven pEGFP-N1 (Clontech Laboratories). COS-7 cells were transiently transfected with pOCC1 using Lipofectamine Plus (Life Technologies) and cultured in DMEM/10% FCS. Two days after transfection, the cells were washed with DMEM/1% FCS and cultured for another day. Aliquots of cell lysates and conditioned medium were subjected to electrophoresis on 15% SDS-polyacrylamide gels and transferred to Immobilon P transfer membrane (Millipore, Bedford, MA, USA) using standard protocols. After blocking, the blot was incubated with anti-OCC1 antiserum (1:800). The blots were then immunoreacted with goat anti-rabbit antibody coupled to peroxidase (Organon Teknika, Durham, NC, USA; 1:2000) and the immunoreactivity was detected using an ECL detection kit (Amersham Pharmacia Biotech). The blotting performed with the antiserum that had been preabsorbed with 20 μg/ml OCC1-GST fusion protein did not display any band (data not shown).

Tissue preparation for in situ hybridization and immunohistochemistry.

Ten adult macaques (three *Macaca fascicularis* and seven *Macaca fuscata*) weighing 2.9-9.1 kg were used. In five, tetrodotoxin (TTX; 15 μg in 10 μl of normal saline) was injected under Ketamine anesthesia into the vitreous cavity of the left eye twice a week for a total of 7, 10, 14 (two monkeys) or 21 days prior to sacrifice. Retinal activity in the injected eye remains to be suppressed at least for five days following a single injection of this dose of TTX (Hendry et al., 1988a). The other five were untreated. All monkeys were given overdoses of Nembutal and perfused through the hearts with 4% paraformaldehyde in 0.1M phosphate buffer (pH 7.4). The brains were removed, post fixed 3-6 h at room temperature in the fixative, cut into blocks and cryoprotected in 30% sucrose in 0.1M phosphate buffer. The blocks were cut as frozen sections on a sliding microtome. The blocks of occipital lobes were sectioned at 30 μm thickness. In three monkeys, either parasagittal (45 μm thickness), horizontal (35 μm) or frontal (40 μm) slices were prepared through one entire hemisphere. In addition, the cortices posterior to the lunate sulcus of the right hemispheres of all monocularly-deprived and one normal monkeys were dissected out, flattened between glass slides during postfixation and cut parallel to the opercular surface at 25 μm thickness.

In situ hybridization.

Digoxigenin-labeled antisense and sense riboprobes were prepared from the nucleotide positions 333-999 (aa 87-308) of the *occ1* cDNA with digoxigenin-

dUTP labeling kit (Roche Diagnostics, Indianapolis, IN, USA). All the sections were stained with these probes, except the horizontal sections of a whole cerebral hemisphere, which were stained with the antisense and sense probes prepared from the nucleotide positions 4632-5675. *In situ* hybridization was carried out as described (Liang et al., 2000). Briefly, free-floating sections were treated with 1 μg/ml proteinase K for 30 min at 37°C. After acetylation, sections were incubated in a hybridization buffer containing 1.0 μg/ml digoxigenin-labeled riboprobes at 50°C. Hybridized sections were washed by successively immersing once (unless otherwise indicated) in 2×SSC/50% formamide/0.1% N-lauroylsarcosine (50°C, 20 min, twice), RNase A buffer (room temperature, 10 min), RNase A buffer containing 20 μg/ml RNase A (37°C, 30 min), 2×SSC/0.1% N-lauroylsarcosine (room temperature and 50℃, 15 min each), 1×SSC/0.1% N-lauroylsarcosine (room temperature, 5 min), 0.5×SSC/0.1% N-lauroylsarcosine (room temperature, 5 min) and 0.2×SSC/0.1% N-lauroylsarcosine (room temperature and 50°C, 20 min each). Hybridization signals were visualized by alkaline-phosphatase immunohistochemistry with the digoxigenin detection kit (Roche Diagnostics). In the series of parasagittal or frontal sections of whole hemisphere, every 12th section was processed with the antisense probe, every 48th (parasagittal) or 24th (frontal) section was processed with the sense probe. The series of horizontal sections at about 2 mm and 8 mm intervals were stained with the antisense probe and the sense probe, respectively. In control sections hybridized with the sense probes, the neocortex

gave no staining above background. The results obtained from both species of macaques were indistinguishable.

The signal intensity of *in situ* hybridization in the processed tissues was quantified with NIH image software by taking optical density meanings of the digitized image. Optical density readings were taken from at least 20 areas (each approximately 1100-6500 μm^2 in size) around the centers of perturbed and non-perturbed columns, which were identified by matching them to columns showing reduced and normal staining in adjacent CO-stained sections, in layer III or IVCβ of area 17 in a section. Background readings, taken from the almost-unstained regions just suprajacent to the white matter because the white matter itself exhibit the pale staining by endogenous alkaline phosphatase activity. These were subtracted and the optical densities were averaged. Data from three sections of each monocularly deprived monkey were then averaged. The significance of difference was examined using the two-tailed Student's *t* test.

Double immunohistochemical staining.

For dual labeling, two antiserum/antibody combinations were used: rabbit anti-OCC1 (1:100) and mouse anti-CaMKII α (Roche Diagnostics; 1:400), rabbit anti-OCC1 and mouse anti-GABA (GB-69, Sigma, St. Louis, MO, USA; 1:400). Selected 30 μm-thick sections of normal monkey visual cortex were preincubated in 0.25% Triton X-100 in phosphate buffered saline (PBS) at r. t. for 2 h before being placed in the blocking buffer (1% blocking reagent from Roche Diagnostics, 5% normal goat serum and 0.1% Triton X-100 in PBS) at room

temperature for at least 2 h. They were then transferred to the blocking buffer containing each primary antiserum/antibody combination. After 36-48 h at 4°C, the sections were washed and incubated in a mixture of Alexa 488 conjugated goat anti-rabbit IgG (Molecular probe, Eugene, OR, USA; 1:100) and Alexa 594 conjugated goat anti-mouse IgG (Molecular probe; 1:100) in PBS containing 5% normal goat serum and 0.1% Triton X-100. For controls, the same procedures were performed without primary antiserum or antibody. The control sections showed no fluorescent staining.

All the experiments described here were performed in compliance with the guidelines for animal experiments at Okazaki National Research Institute.

Results

Identification of *occ1*, a transcript expressed preferentially in macaque occipital neocortex.

Total RNAs from five anatomically distinct regions of the adult cynomolgus monkey neocortex (areas FDΔ, FA, TE, OA and OC according to the classification of von Bonin and Bailey (von Bonin and Bailey, 1947) shown in Fig. I-1) were converted to cDNA with anchor oligo-dT primers, and the mRNA expression in these regions was compared by DD. Among the bands of the PCR-amplified fragments, I identified a 190 base pair (bp) cDNA fragment that showed the highest transcription level in area OC (Fig. I-2a). RT-PCR analysis using a primer set corresponding to the both ends of the clone confirmed this characteristic regional expression pattern (Fig. I-2b).

The cDNA sequence of the clone obtained from DD shared no homology with any DNA sequences available on the GenBank database. Because the clone was likely to represent a 3'-noncoding region adjacent to the poly $(A)^+$ tail, I isolated a full-length cDNA from a cDNA library from area OC of cynomolgus monkey neocortex. Northern blotting showed that the full-length *occ1* mRNA is about 5.7 kb long (Fig. I-3). The first screen of a cDNA library with the DD cDNA fragment resulted in the isolation of a cDNA clone including a 1024 bp sequence upstream from the poly $(A)^+$ tail. I obtained a full-length clone after another screening of a cDNA library using the elongated clone as a probe. The entire sequence of the clone consisted of 5688 nucleotides, and a putative open

reading frame of 308 amino acids (calculated molecular mass of 34,999 Da) was found upstream from the nucleotide sequence for the DD clone (Fig. I-4 a and b).

I named the gene *occ1* (for occipital 1). Homology search revealed that this gene encodes the macaque homologue of human, rat and mouse follistatin-related protein (FRP)/TSC-36 (Fig. I-5 and I-6). The sequence comparisons showed that the identity of the coding DNA sequence of *occ1* to human, mouse and rat *frp/tsc-36* was 98.6 %, 88.8% and 88.5 %, respectively, while the deduced amino acid sequence identity of OCC1 to human, mouse and rat FRP/TSC-36 was 99.7 %, 91.6 % and 92.5 %, respectively (Table I-1). FRP/TSC-36 was originally isolated from the cells of a mouse osteoblastic cell line treated with TGF β1 (Shibanuma et al., 1993), and contains a cystein-rich follistatin motif, three putative N-glycosylation sites and various phosphorylation sites (Fig. I-6; Zwijsen, 1994; Patel, 1996; Ohashi, 1997; Tanaka, 1998; Okabayashi, 1999). The follistatin motif is shared by various proteins, such as the activin-inhibitor FOLLISTATIN, the protein which induces the aggregation of nicotinic acetylcholine receptors AGRIN, the multifunctional extracellular glycoprotein SPARC/OSTEONECTIN/BM-40, the rat brain protein SC1 and the quail retina specific protein QR1 (Johnston et al., 1990; Guermah et al., 1991; Patthy and Nikolics, 1993; Maurer et al., 1995; Phillips and de Kretser, 1998; Motamed, 1999).

The sequence analysis of the 3'-untranslated region (UTR) of the full-length clone revealed that the clone has the cytoplasmic polyadenylation element (CPE; TTTTTAT) residing 22 nucleotides upstream of the sequences similar to

the typical polyadenylation signal hexanucleotides AATAAA sequences (HEX) in its 3' end (Fig. I-7). The CPE, which usually resides about 20 nucleotides 5' of HEX, stimulates cytoplasmic polyadenylation and translation during oocyte maturation (Fox et al., 1989; McGrew et al., 1989). In neurons, the CPE is also thought to mediate polyadenylation-induced translation, which is necessary for controlling local and rapid translation of specific mRNAs in neuronal processes (Wu et al., 1998; Wells et al., 2000). As shown in Fig. I-9, the *occ1* mRNA were occasionally observed to be localized in the neuronal processes. Taking this observation and the presence of the CPE in *occ1* mRNA into consideration, it is speculated that *occ1* mRNA undergoes cytoplasmic local translation in the neuronal processes.

OCC1 has putative N-terminal signal peptides (Fig. I-6; Zwijsen, 1994 #6). I performed Western blot analysis with the cell lysates and the supernatant of conditioned medium of COS-7 cells transfected with OCC1 expression vector, and found that the molecular weight of the major product detected in the medium (arrow in Fig. I-8; about 43 kDa) is larger than that in the cell lysates (arrowhead in Fig. I-8; about 36 kDa). This result showed that OCC1 was released into the medium with posttranslational modifications.

Neocortical distribution of the cells specified by *occ1*.

In the monkey neocortex, most *occ1*-positive signals in *in situ* hybridization preparation were observed in neurons. This is judged from the following observations: i) Little signal was observed in the white matter. ii) The cells

stained by the probe had large somata in general (7-12 μm in diameter in layers III and IVC of area 17). iii) *occ1* mRNA was occasionally observed to be localized in the processes of some pyramidal cells, resulting in contoured cell shapes (Fig. I-9).

In situ hybridization histochemistry of the serial sections of the entire cerebral hemisphere demonstrated that the distribution of *occ1*-positive neurons was as expected on the basis of the results of DD and RT-PCR experiments (Fig. I-10). The strongest and densest hybridization signals were observed in area 17. The other occipital areas showed moderate expression of *occ1* (Fig. I-10a and e). *occ1*-positive neurons were distributed with relatively weak labeling basically throughout the temporal and the posterior half of the parietal cortex (Fig. I-10a, c and d). In these cortices, certain cortical areas could be identified by densities and patterns of staining. The primary somatosensory cortex (area 3b) show some dense expression in layer IV and the deeper stratum of layer III (Fig. I-10c, d and I-11a). The primary auditory cortex (AI) also exhibited relatively dense expression in layer IV and the deeper half of layer III (Fig. I-10d and I-11c). The intensity of labeling and the frequency of the signals was even lower in the areas anterior to the central sulcus than in the postcentral regions. In the precentral regions, no obvious cortical areas could be identified by the *occ1* expression pattern (Fig. I-10a and b).

Laminar distribution of *occ1*-positive neurons in visual cortex and visual thalamus.

Examination of *occ1* mRNA positive neurons in areas 17 and 18 revealed distinctive laminar distributions of *occ1*-expressing neurons in these regions. In area 17 (Fig. I-12a), signal was most densely distributed and cells were most intensely labeled in layers IVCα and IVCβ. Layers II, III and IVA exhibited many intensely labeled neurons. In the intervening layer, IVB, a relatively smaller number of moderately labeled neurons existed. The distribution of *occ1*-positive neurons divided layer V into a superficial, lightly stained sub-layer and a deeper, even more lightly stained sub-layer. In layer VI and the deeper half of layer V, a few moderately stained neurons were rather sparsely found. The positive neurons in layer I were lightly stained and sparsely present.

The laminar distribution of *occ1*-positive neurons in area 18 (Fig. I-12c) was completely different from that in area 17. Many intensely labeled neurons with large somata were found in the lower one third of layer III. In the upper two thirds of layer III and layer IV, many lightly labeled cells and some moderately labeled cells were observed. Layer II exhibited many lightly labeled neurons. In layers V and VI, a few relatively lightly labeled cells were present. Weak signal was sparsely distributed in layer I.

The subset of neurons specified by *occ1* includes functionally and morphologically distinct types.

To determine whether the neurons marked by the expression of *occ1* can be classified into a single functional and morphological class of cells, I performed dual labeling immunohistochemistry on the neurons in area 17 with the antisera

to OCC1 and a monoclonal antibody against either CaMKII α or GABA. CaMKII α immunoreactivity is found only in a population of glutamatergic, excitatory cells in the cerebral cortex (Benson et al., 1991; Benson et al., 1992; Liu and Jones, 1996), which includes the spiny stellate cells in layer IV and pyramidal cells in the other layers of area 17 (Hendry and Kennedy, 1986; Tighilet et al., 1998). On the other hand, GABAergic neurons of the primate neocortex belong to a class of inhibitory and aspiny nonpyramidal neurons (Houser et al., 1983; Jones et al., 1994). No GABA-immunoreactive neuron shows CaMKII α immunoreactivity in area 17 (Tighilet et al., 1998).

The OCC1 immunoreactivity is diffusely present within the cell bodies, especially around the cell nuclei, and seen in a punctate pattern along the neuronal processes (Fig. I-13 left panels). These observations are consistent with the possibility that the product of occ1 can be released from neurons as well as from the transfected COS-7 cells. The great majority of CaMKII α-expressing neurons show OCC1 immunoreactivity (Fig. I-13a and b). On the other hand, OCC1 immunoreactivity was found in not all, but in a large population of GABAergic neurons (Fig. I-13c). Each type of neurons, double immunoreactive for OCC1 and CaMKII α and double immunoreactive for OCC1 and GABA, was observed in all layers of area 17 except for layer I in which virtually all neurons are GABA-positive (Hendry et al., 1987). These observations show that the neuronal subset revealed by *occ1* expression includes physiologically and morphologically different classes of neurons in area 17.

***occ1* is expressed by the neurons in area 17 in an activity-dependent manner.**

The neurons marked by *occ1* expression were preferentially distributed in area 17. A question arose: does visual experience play a role in the regulation of *occ1* expression in the adult brain? Area 17 of the Old World primates is divided into alternating ocular dominance columns (Hubel and Wiesel, 1972; Wiesel et al., 1974). I can examine the alterations in neuronal phenotypes based on changes in neuronal activity in the brains of monocularly deprived animals using immunohistochemical techniques (Hendry and Jones, 1986; Hendry and Kennedy, 1986; Hendry and Jones, 1988).

Following monocular deprivation by TTX injection into the vitreous cavity (7, 10, 14 or 21 days), dramatic changes were detected in the *in situ* hybridization pattern of *occ1* in area 17. Alternating lightly and darkly stained stripes appeared (Fig. I-14a, c , e and g), irrespective of the length of deprivation. Comparison with the adjacent sections stained for CO (Wong-Riley, 1979; Horton and Hubel, 1981), which exhibited the same pattern of alternating dark and light stripes, showed that *occ1* transcription was reduced in the deprived columns. The change was observed in layers III, IVA, IVB, IVCα, IVCβ and V, being most apparent in layers III and IVCβ (Fig. I-14a). The signal intensity measurements confirmed this observation that the average level of mRNA in the perturbed columns were 57 % lower in layer III (range, 45-68 %; $p<0.0005$), and 74 % lower in layer IVCβ (66-82 %; $p<0.0001$) than those in the non-perturbed columns.

In the tangential sections cut through layer III of area 17 of TTX-injected animals, the wide row of *occ1* signal was seen along the line of blobs in the undeprived columns, and faint patchy stainings coinciding with the CO periodicities were observed in the perturbed columns (Fig. I-14c, d, e and f; arrows in e and f indicate the patchy CO and corresponding *occ1* stainings in the perturbed columns). The *occ1* expression in the undeprived columns was beyond the confines of the undeprived blobs to form an almost continuous signal, and the extent of the expression in the deprived columns was even less than that of the shrunken blobs observed in the CO sections. In the sections cut through layer IVCβ, the ocular dominance columns observed in the sections stained for *occ1* were even more obvious than those seen in the CO sections (Fig. I-14g and h). These observations also suggest that the *occ1* expression in layers III and IVC was significantly decreased by the blockade of visual input. From these results, I conclude that *occ1* mRNA is transcribed in an activity-dependent manner in area 17. An obvious change was not observed in area 18.

The characteristic distribution of *occ1*-positive neurons in the other brain regions.

I examined the *occ1* expression in LGN to ask whether *occ1* has a specific pattern of laminar distribution in the thalamic nucleus in which visual system channels are segregated into distinct layers, and found that relatively weak signal was present selectively in cells of the magnocellular layers (layers 1 and 2; Fig. I-15a, b and d).

I next examined the distribution of *occ1*-expressing neurons in the hippocampal formation which is also divided into functionally and structurally distinct subregions. I could find rather many intensely-labelled cells scattered in the stratum oriens and, occasionally, the most outer region of pyramidal cell layer in CA1 and CA2 (Fig. I-16a and c). The positive cells usually contained large somata and labelled processes (arrows in Fig. I-16e). In addition to these positive cells, quite many rather intensely-stained pyramidal cells were selectively localized in the inner fourth of the CA2 pyramidal cell layer (Fig. I-16a, c and e). In CA3, some intensely-labeled cells were scattered throughout the width of the pyramidal cell layer. The pyramidal cell layer of subiculum contained some rather intensely-labeled cells (Fig. I-16a). In the presubiculum, many rather intensely-labeled neurons were found in the lamina principalis interna, and some rather-intensely-labeled cells were sparsely present in the lamina principalis externa (Fig. I-16a). In the dentate gyrus, almost no signal was observed except for the light signals which were detected in most cells of the granule cell layer (Fig. I-16a and c).

Discussion

I have screened for genes that are transcribed differentially among structurally and functionally distinct areas of macaque neocortex, and identified *occ1*. *occ1*-positive neurons were selectively distributed in the posterior region of the neocortex, especially, in area 17.

occ1 expression and neocortical neuronal organization

It has been considered that neocortex is basically homogeneous based on the number and density (Rockel et al., 1980), and the morphology (Fairen et al., 1984) of its neuronal components. The ratios between pyramidal and nonpyramidal neurons are very similar in the motor, somatosensory and visual cortices (Sloper, 1973; Tombol, 1974; Sloper et al., 1978). In studies of the chemical properties of neurons, an extensive quantitative survey of the distribution of a major neurotransmitter, GABA, demonstrated that its distribution varies little among neocortical areas (Hendry et al., 1987). However, in these neuron counting studies, there was an exception, area 17, in which the number of neurons through the full depth of the cortex is more than twice than in the other areas (Rockel et al., 1980) and the proportion of GABAergic neurons to total neurons is lower than that in the other areas (Hendry et al., 1987). Therefore, the distribution of *occ1* mRNA, preferentially observed in the posterior region of neocortex with regional variations, is a dramatic example of neocortical neurons' heterogeneity, which coincides with the functional subdivisions, and the

high *occ1* transcription in area 17 reveals the unique neuronal organization of area 17 in the primate neocortex. Furthermore, as the results shown in Fig. I-14 demonstrate, *occ1* mRNA levels can be remarkably downregulated by blockade of afferent activity in area 17. High *occ1* expression is not only spatially coincident with area 17, but also subject to regulation dependent on neuronal activity in area 17. These results show the important features of the expression of *occ1* that can be used as a marker for neurons in area 17 as well as a good indicator of neural activities in the particular laminae of area 17.

The further characterization of the neurons specified by *occ1* in area 17 showed that they include morphologically and functionally distinct classes of neurons, spiny excitatory cells and aspiny inhibitory cells. This result suggests the other unique aspect of *occ1* expression in neocortical neurons that *occ1* is expressed not in a single type of neurons but in various types of neurons in a region-selective manner.

occ1 expression in neocortex and thalamocortical connectivity

The present results show that the transcription pattern of *occ1* relate to the cytoarchitectonic area of neocortex. At present, I cannot explain how such a difference in gene expression among neocortical neurons is generated during the brain development. In regard to the neocortical region where *occ1* shows its high transcription, however, I can find some correlation between the laminar distribution of *occ1* expressing neurons and the pattern of thalamic afferent innervation.

I found the strong *occ1* transcription in layers II, III, IVA and IVC of area 17. The major inputs to area 17 in primates and some other mammals are from the (dorsal) LGN and the minor ones are from the nuclei of the pulvinar complex. Thalamic inputs from LGN in primates terminate mainly in layer IVC and, to a lesser degree, in layer IVA of area 17 (Hubel and Wiesel, 1972; Hendrickson et al., 1978; Blasdel and Lund, 1983). The pulvinar axons and those from intercalated layers of LGN provide thalamocortical innervation to the cells in layer I and the blobs of layers II and III of area 17 (Fitzpatrick et al., 1983; Hendry and Yoshioka, 1994). In area 18, I observed strong signals in the deep stratum of layer III. The pulvinar afferent terminations in area 18 are dense in the deep part of layer III and layer IV (Curcio and Harting, 1978; Livingstone and Hubel, 1982). In addition to these thalamic recipient regions, *occ1* also shows its high transcription in the regions on which thalamic inputs have strong influences in indirect ways. *occ1* is transcribed in the interblob regions of layer II and III of area 17 where no apparent termination of direct thalamic input has been observed (Livingstone and Hubel, 1982; Itaya et al., 1984). I also found moderate and light signals in layer IVB and the upper stratum of layer V, respectively. Neither layer IVB or V receive direct geniculate inputs. On the other hand, the interblob regions of layers II and III receive indirect inputs from the LGN through layers IVA and IVC. Neurons in layer IVB receive strong inputs from layer IVCα. The upper subdivision of layer V makes prominent connections to the thalamic recipient layers IVA, IVCα, IVCβ and VI (Lund, 1988; Callaway, 1998).

***occ1* expression and a functional subdivision of visual thalamus and hippocampus.**

I observed that the *occ1* expression in LGN is observed more frequently in the magnocellular layers in which the cells with broad band spectral qualities are selectively localized (Wiesel and Hubel, 1966) than in the other layers. *occ1* is also preferentially expressed in a functional subdivision of a thalamic nucleus. Some markers, for example Cat-301 and SMI-32, are known to primarily labels the magnocellular layers (Hendry et al., 1988b; Chaudhuri et al., 1996). *occ1* can also be used as a marker to visualize a subset of neurons in those layers of LGN and contribute to the classification of neurons in LGN.

As shown in the Fig. I-16, *occ1* is expressed in a specific type of neurons in the hippocampal formation in a region-specific manner. The neuronal subtypes in the hippocampal formation can be classified by using calcium-binding proteins, Calbindin-D28K, Calretinin and Parvalbumin, as markers(Berger and Alvarez, 1996; Freund and Buzsaki, 1996). Judging from their laminar distribution and somal size, it could be infered that the population of cells in the Ammon's horn and subiculum marked by *occ1* overlaps with that of the cells specified by a calcium-binding protein parvalbumin (Ribak et al., 1990; Seress et al., 1991; Ribak et al., 1993; Berger et al., 1999). The experiments to determine the cell type which expresses *occ1* are needed. However, in any case, the *occ1*, labeling the cells in limited number with a characteristic laminar distribution, can be used as a new marker.

The function of *occ1* in cortical plasticity

The data presented here clearly indicate that *occ1* mRNA is preferentially expressed in posterior regions of the neocortex, especially in area 17, in an activity-dependent manner. Activity-dependent gene expression, resulting in changes in neuronal phenotypes, plays an important role in neuronal plasticity of brain function and development (Marty et al., 1997; Lee and Sheng, 2000). Many molecules have been reported to be expressed in an activity-dependent manner, but none of them shows such a characteristic regional expression pattern in the neocortex as that of *occ1*. Although the function of OCC1 (FRP, TSC-36) remains unknown to date, it has been suggested that follistatin motifs of follistatin, agrin and SC1 might play similar functions in the differentiation of the nervous system by accumulating, protecting and modulating the activity of growth factors (Patthy and Nikolics, 1993). This suggestion also presents the possibility that OCC1 may function by binding other molecule(s) and affecting its (their) activity(ies). The results of the expression study with COS-7 cells suggest that OCC1 may function in a secreted form. These together imply that OCC1 may work to mediate activity-dependent interactions between specific subsets of neurons through modulating the functions of other proteins in response to changes in neuronal activity in particular neuronal circuits. Furthermore, the presence of CPE sequence in 3'-UTR of *occ1* mRNA clone suggests the possibility that the *occ1* mRNA undergo the rapid local translation in the neuronal processes in response to change in the neuronal activities. Further studies on

the nature of OCC1 and to elucidate the role of the molecule in neuronal function will shed new light on the functional structure of the cerebral neocortex.

A few molecular markers for specific neuronal subtypes in the rodent brain have been identified and characterized, such as Limbic System-Associated Membrane protein (LAMP) and Latexin (Levitt, 1984; Zacco et al., 1990; Arimatsu et al., 1992; Arimatsu, 1994). LAMP is a glycoprotein that is expressed in the subsets of neurons in the adult rat brain that are associated with classic limbic structures (Reinoso et al., 1996). Latexin-immunoreactive neurons are confined essentially to the infragranular layers of lateral cortical areas in the rat neocortex (Arimatsu et al., 1999). Among these markers, the distribution of LAMP in the primate brain has been examined, and it has been shown that LAMP can also be effective in visualizing neuronal subsets in the primate limbic system (Cote et al., 1996). This result suggests that the characterization of *occ1*-positive neurons in rodents and other mammals' brains may show the similarity and the difference of the neuronal organization between the primate and other mammalian brains. This kind of knowledge will contribute to understanding the nature of *occ1*-expressing neurons in future studies.

A systematic survey for marker molecules in the primate neocortex described here presents a successful example of such an approach. Histochemical analyses using new molecular markers combined with various other techniques would become powerful tools in deciphering the functional organization of the

neocortex.

References

Arimatsu Y (1994) Latexin: a molecular marker for regional specification in the neocortex. Neurosci Res 20:131-135.

Arimatsu Y, Kojima M, Ishida M (1999) Area- and lamina-specific organization of a neuronal subpopulation defined by expression of latexin in the rat cerebral cortex. Neuroscience 88:93-105.

Arimatsu Y, Miyamoto M, Nihonmatsu I, Hirata K, Uratani Y, Hatanaka Y, Takiguchi-Hayashi K (1992) Early regional specification for a molecular neuronal phenotype in the rat neocortex. Proc Natl Acad Sci U S A 89:8879-8883.

Benson DL, Isackson PJ, Hendry SH, Jones EG (1991) Differential gene expression for glutamic acid decarboxylase and type II calcium-calmodulin-dependent protein kinase in basal ganglia, thalamus, and hypothalamus of the monkey. J Neurosci 11:1540-1564.

Benson DL, Isackson PJ, Gall CM, Jones EG (1992) Contrasting patterns in the localization of glutamic acid decarboxylase and Ca2+/calmodulin protein

kinase gene expression in the rat central nervous system. Neuroscience 46:825-849.

Berger B, Alvarez C (1996) Neurochemical development of the hippocampal region in the fetal rhesus monkey, III: calbindin-D28K, calretinin and parvalbumin with special mention of cajal-retzius cells and the retrosplenial cortex. J Comp Neurol 366:674-699.

Berger B, De Grissac N, Alvarez C (1999) Precocious development of parvalbumin-like immunoreactive interneurons in the hippocampal formation and entorhinal cortex of the fetal cynomolgus monkey. J Comp Neurol 403:309-331.

Blasdel GG, Lund JS (1983) Termination of afferent axons in macaque striate cortex. J Neurosci 3:1389-1413.

Callaway EM (1998) Local circuits in primary visual cortex of the macaque monkey. Annu Rev Neurosci 21:47-74.

Chaudhuri A, Zangenehpour S, Matsubara JA, Cynader MS (1996) Differential expression of neurofilament protein in the visual system of the vervet

monkey. Brain Res 709:17-26.

Chomczynski P, Sacchi N (1987) Single-step method of RNA isolation by acid guanidium thiocyanate-phenol-chloroform extraction. Anal Biochem 162:156-159.

Cote PY, Levitt P, Parent A (1996) Limbic system-associated membrane protein (LAMP) in primate amygdala and hippocampus. Hippocampus 6:483-494.

Curcio CA, Harting JK (1978) Organization of pulvinar afferents to area 18 in the squirrel monkey: evidence for stripes. Brain Res 143:155-161.

Dyck RH, Cynader MS (1993) An interdigitated columnar mosaic of cytochrome oxidase, zinc, and neurotransmitter-related molecules in cat and monkey visual cortex. Proc Natl Acad Sci U S A 90:9066-9069.

Fairen A, DeFelipe J, Regidor J (1984) Nonpyramidal neurons. General account. In: Cerebral Cortex, Vol. 1, Cellular Components of the Cerebral Cortex (Peters A, Jones EG, eds), pp 201-253. New York: Plenum.

Fitzpatrick D, Itoh K, Diamond IT (1983) The laminar organization of the lateral

geniculate body and the striate cortex in the squirrel monkey (Saimiri sciureus). J Neurosci 3:673-702.

Fox CA, Sheets MD, Wickens MP (1989) Poly(A) addition during maturation of frog oocytes: distinct nuclear and cytoplasmic activities and regulation by the sequence UUUUUAU. Genes Dev 3:2151-2162.

Freund TF, Buzsaki G (1996) Interneurons of the hippocampus. Hippocampus 6:347-470.

Guermah M, Crisanti P, Laugier D, Dezelee P, Bidou L, Pessac B, Calothy G (1991) Transcription of a quail gene expressed in embryonic retinal cells is shut off sharply at hatching. Proc Natl Acad Sci U S A 88:4503-4507.

Hendrickson AE, Wilson JR, Ogren MP (1978) The neuroanatomical organization of pathways between the dorsal lateral geniculate nucleus and visual cortex in Old World and New World primates. J Comp Neurol 182:123-136.

Hendry SH, Kennedy MB (1986) Immunoreactivity for a calmodulin-dependent protein kinase is selectively increased in macaque striate cortex after

monocular deprivation. Proc Natl Acad Sci U S A 83:1536-1541.

Hendry SH, Jones EG (1986) Reduction in number of immunostained GABAergic neurones in deprived-eye dominance columns of monkey area 17. Nature 320:750-753.

Hendry SH, Jones EG (1988) Activity-dependent regulation of GABA expression in the visual cortex of adult monkeys. Neuron 1:701-712.

Hendry SH, Jones EG, Burstein N (1988a) Activity-dependent regulation of tachykinin-like immunoreactivity in neurons of monkey visual cortex. J Neurosci 8:1225-1238.

Hendry SH, Schwark HD, Jones EG, Yan J (1987) Numbers and proportions of GABA-immunoreactive neurons in different areas of monkey cerebral cortex. J Neurosci 7:1503-1519.

Hendry SH, Jones EG, Hockfield S, McKay RD (1988b) Neuronal populations stained with the monoclonal antibody Cat-301 in the mammalian cerebral cortex and thalamus. J Neurosci 8:518-542.

Hendry SHC, Yoshioka T (1994) A neurochemically distinct third channel in the

macaque dorsal lateral geniculate nucleus. Science 264:575-577.

Hendry SHC, Hockfield S, Jones EG, MacKay R (1984) Monoclonal antibody that identifies subsets of neurons in the central visual system of monkey and cat. Nature 307:267-269.

Hockfield S, Kalb RG, Zaremba S, Fryer H (1990) Expression of Neural proteoglycans correlates with the acquisition of mature neuronal properties in the mammalian brain. In: Cold Spring Harbor symp on Quant Biol, pp 505-514: Cold Spring Harbor Laboratory Press.

Hof PR, Morrison JH (1995) Neurofilament protein defines regional patterns of cortical organization in the macaque monkey visual system: a quantitative immunohistochemical analysis. J Comp Neurol 352:161-186.

Horton JC (1984) Cytochrome oxidase patches: a new cytoarchitectonic feature of monkey visual cortex. Philos Trans R Soc Lond B Biol Sci 304:199-253.

Horton JC, Hubel DH (1981) Regular patchy distribution of cytochrome oxidase

staining in primary visual cortex of macaque monkey. Nature 292:762-764.

Houser CR, Hendry SH, Jones EG, Vaughn JE (1983) Morphological diversity of immunocytochemically identified GABA neurons in the monkey sensory-motor cortex. J Neurocytol 12:617-638.

Hubel DH, Wiesel TN (1972) Laminar and columnar distribution of geniculo-cortical fibers in the macaque monkey. J Comp Neurol 146:421-450.

Itaya SK, Itaya PW, Van Hoesen GW (1984) Intracortical termination of the retino-geniculo-striate pathway studied with transsynaptic tracer (wheat germ agglutinin-horseradish peroxidase) and cytochrome oxidase staining in the macaque monkey. Brain Res 304:303-310.

Johnston IG, Paladino T, Gurd JW, Brown IR (1990) Molecular cloning of SC1: a putative brain extracellular matrix glycoprotein showing partial similarity to osteonectin/BM40/SPARC [published erratum appears in Neuron 1990 Mar;4(3):477]. Neuron 4:165-176.

Jones EG, Hendry SHC, DeFelipe J, Benson DL (1994) GABA neurons and their

role in activity-dependent plasticity of adult primate visual cortex. In: Cerebral cortex, Vol. 10, Primary Visual Cortex in Primates. (Peters A, Rockland K, eds), pp 61-140. New York: Plenum.

Lee SH, Sheng M (2000) Development of neuron-neuron synapses. Curr Opin Neurobiol 10:125-131.

Levitt P (1984) A monoclonal antibody to limbic system neurons. Science 223:299-301.

Liang F, Hatanaka Y, Saito H, Yamamori T, Hashikawa T (2000) Differential expression of gamma-aminobutyric acid type B receptor-1a and -1b mRNA variants in GABA and non-GABAergic neurons of the rat brain. J Comp Neurol 416:475-495.

Liang P, Pardee AB (1992) Differential display of eukaryotic messenger RNA by means of the polymerase chain reaction [see comments]. Science 257:967-971.

Liu XB, Jones EG (1996) Localization of alpha type II calcium calmodulin-dependent protein kinase at glutamatergic but not gamma-aminobutyric

acid (GABAergic) synapses in thalamus and cerebral cortex. Proc Natl Acad Sci U S A 93:7332-7336.

Livingstone MS, Hubel DH (1982) Thalamic inputs to cytochrome oxidase-rich regions in monkey visual cortex. Proc Natl Acad Sci U S A 79:6098-6101.

Livingstone MS, Hubel DH (1983) Specificity of cortico-cortical connections in monkey visual system. Nature 304:531-534.

Lund JS (1988) Anatomical organization of macaque monkey striate visual cortex. Annu Rev Neurosci 11:253-288.

Marty S, Berzaghi Mda P, Berninger B (1997) Neurotrophins and activity-dependent plasticity of cortical interneurons. Trends Neurosci 20:198-202.

Maurer P, Hohenadl C, Hohenester E, Gohring W, Timpl R, Engel J (1995) The C-terminal portion of BM-40 (SPARC/osteonectin) is an autonomously folding and crystallisable domain that binds calcium and collagen IV. J Mol Biol 253:347-357.

McGrew LL, Dworkin-Rastl E, Dworkin MB, Richter JD (1989) Poly(A) elongation during Xenopus oocyte maturation is required for translational recruitment and is mediated by a short sequence element. Genes Dev 3:803-815.

Motamed K (1999) SPARC (osteonectin/BM-40). Int J Biochem Cell Biol 31:1363-1366.

Mrzljak L, Levey AI, Rakic P (1996) Selective expression of m2 muscarinic receptor in the parvocellular channel of the primate visual cortex. Proc Natl Acad Sci U S A 93:7337-7340.

Patthy L, Nikolics K (1993) Functions of agrin and agrin-related proteins. Trends Neurosci 16:76-81.

Phillips DJ, de Kretser DM (1998) Follistatin: a multifunctional regulatory protein. Front Neuroendocrinol 19:287-322.

Reinoso BS, Pimenta AF, Levitt P (1996) Expression of the mRNAs encoding the limbic system-associated membrane protein (LAMP): I. Adult rat brain. J Comp Neurol 375:274-288.

Ribak CE, Nitsch R, Seress L (1990) Proportion of parvalbumin-positive basket cells in the GABAergic innervation of pyramidal and granule cells of the rat hippocampal formation. J Comp Neurol 300:449-461.

Ribak CE, Seress L, Leranth C (1993) Electron microscopic immunocytochemical study of the distribution of parvalbumin-containing neurons and axon terminals in the primate dentate gyrus and Ammon's horn. J Comp Neurol 327:298-321.

Rockel AJ, Hiorns RW, Powell TP (1980) The basic uniformity in structure of the neocortex. Brain 103:221-244.

Seress L, Gulyas AI, Freund TF (1991) Parvalbumin- and calbindin D28k-immunoreactive neurons in the hippocampal formation of the macaque monkey. J Comp Neurol 313:162-177.

Shibanuma M, Mashimo J, Mita A, Kuroki T, Nose K (1993) Cloning from a mouse osteoblastic cell line of a set of transforming- growth-factor-beta 1-regulated genes, one of which seems to encode a follistatin-related polypeptide. Eur J Biochem 217:13-19.

Sloper JJ (1973) An electron microscopic study of the neurons of the primate motor and somatic sensory cortices. J Neurocytol 2:351-359.

Sloper JJ, Hirons RW, Powell TPS (1978) A qualitative and quantitative electron microscopic study of the neurons in the primate motor and somatic sensory cortices. Philos Trans R Soc Lond B Biol Sci 285:141-171.

Thompson JD, Higgins DG, Gibson TJ (1994) CLUSTAL W: improving the sensitivity of progressive multiple sequence alignment through sequence weighting, position-specific gap penalties and weight matrix choice. Nucleic Acids Res 22:4673-4680.

Tighilet B, Hashikawa T, Jones EG (1998) Cell- and lamina-specific expression and activity-dependent regulation of type II calcium/calmodulin-dependent protein kinase isoforms in monkey visual cortex. J Neurosci 18:2129-2146.

Tombol T (1974) An electron microscopic study of the neurons of the visual cortex. J Neurocytol 3:525-531.

von Bonin G, Bailey P (1947) The Neocortex of *Macaca mulatta*. Urbana:

University of Illinoi Press.

Wells DG, Richter JD, Fallon JR (2000) Molecular mechanisms for activity-regulated protein synthesis in the synapto-dendritic compartment. Curr Opin Neurobiol 10:132-137.

Wiesel TN, Hubel DH (1966) Spatial and chromatic interactions in the lateral geniculate body of the rhesus monkey. J Neurophysiol 29:1115-1156.

Wiesel TN, Hubel DH, Lam DM (1974) Autoradiographic demonstration of ocular-dominance columns in the monkey striate cortex by means of transneuronal transport. Brain Res 79:273-279.

Wong-Riley M (1979) Changes in the visual system of monocularly sutured or enucleated cats demonstrable with cytochrome oxidase histochemistry. Brain Res 171:11-28.

Wu L, Wells D, Tay J, Mendis D, Abbott MA, Barnitt A, Quinlan E, Heynen A, Fallon JR, Richter JD (1998) CPEB-mediated cytoplasmic polyadenylation and the regulation of experience-dependent translation of alpha-CaMKII mRNA at synapses. Neuron 21:1129-1139.

Zacco A, Cooper V, Chantler PD, Fisher-Hyland S, Horton HL, Levitt P (1990) Isolation, biochemical characterization and ultrastructural analysis of the limbic system-associated membrane protein (LAMP), a protein expressed by neurons comprising functional neural circuits. J Neurosci 10:73-90.

Zaremba S, Guimaraes A, Kalb RG, Hockfield S (1989) Characterization of an activity-dependent, neuronal surface proteoglycan identified with monoclonal antibody Cat-301. Neuron 2:1207-1219.

Figure legends

Fig. I-1. The five neocortical regions (areas FDΔ, FA, TE, OA and OC; colored) from which tissues were dissected. ari, inferior ramus of arcuate sulcus (s); ars, superior ramus of arcuate s; ce, central s; itp, intraparietal s; lat, lateral s; lu, lunate s; oci, inferior occipital s; oct, occipito-temporal s; prn, principal s; ti, inferior temporal s; ts, superior temporal s.

Fig. I-2. Differential display and RT-PCR analysis of *occ1* expression in the five neocortical regions. (a) Total RNAs from five areas of cynomolgous monkey neocortex were compared by differential display. A cDNA fragment, named *occ1*, was differentially detected (arrow; 190 bp). Lane 1, area FDΔ; lane 2, area FA; lane 3, area TE; lane 4, area OA; lane 5, area OC. (b) RT-PCR confirmation of differential transcription of *occ1* in the five neocortical areas. cDNAs or RT-s from area FDΔ(lane 1), area FA (lane 2), area TE (lane 3), area OA (lane 4) and area OC (lane 5) were used. *occ1* is transcribed at a high level selectively in area OC. PCR using serial dilutions (1/2-1/16) of cDNA from area OC shows the cycles employed (20 cycles for both primers) were within the range in which amplification occurred linearly. RT-PCR for *glyceraldehyde-3-phosphate dehydrogenase* (*g3pdh*), which is known to be ubiquitously expressed in various tissues and cells, was used as a control reaction to show the quantity and quality of the cDNAs applied.

Fig. I-3. Northern blot analysis of *occ1* expression in neocortical area OC. The lane contained 12 μg of poly $(A)^+$ RNA(a) purified from *Macaca fascicularis* neocortical area OC. The blot was hybridized with a probe prepared from an *occ1* cDNA clone, firstly obtained by screening a cDNA library (1024bp + poly $(A)^+$ tail). RNA length is indicated by the numbers at the left (kb). A single band, about 5.7 kb in size, was detected.

Fig. I-4. Nucleotide and deduced amino acid sequences of the full-length clone of *occ1* cDNA. (a) The entire sequence of the clone, composed of 5688 nucleotides, contained a putative open reading frame of 927 nuceotides (308 amino acids; bolded). The sequence of the band firstly detected in the differential display (208 bp.) was found at the 3' end of the clone (underlined). (b) Schematic structure of the full length clone. The open reading frame (927 bp.) is shown as a box. Sequences for the clone detected in the differential display is found at the 3' end of the full-length clone as indicated by a black bar. The nucleotide sequences are in the DDBJ/EMBL/GenBank nucleotide sequence databases with the accession number AB039661.

Fig. I-5. *occ1* is a homologue of human, mouse and rat *frp* (*follistatin-related protein*)/*tsc-36*. The coding region of *occ1* cDNA is aligned with the corresponding region of human, mouse and rat *frp*/*tsc-36*. Asterisks indicate nucleotides invariant between the sequences.

Fig. I-6. *occ1* encodes a homologue of a secretable protein, FRP/TSC-36. Alignment of OCC1 deduced amino acid sequences with human, mouse and rat FRP/TSC-36. Identical residues are indicated by asterisks. The putative signal sequences at the N-terminus are bolded. The follistatin motif is boxed and shadowed, while the common cystein residues are in bold and marked by stars. Putative recognition sites for *N*-glycosylation are marked by open triangle, for CaMKII phosphorylation by filled and inverted triangles, for protein-kinase C by open squares and for tyrosine kinase phosphorylation by closed squares.

Fig. I-7. Schematic representation of 3' untranslated region (3' UTR) of the *occ1* full-length cDNA. The CPE sequence (TTTTTAT) is localized 22 nucleotides (nt) upstream from the HEX-like sequence (ATTAAA), which resides 19 nucleotides 5' from poly $(A)^+$ tail.

Fig. I-8. Western blot analysis with anti-OCC1 antiserum of lysates and conditioned medium of COS 7 cells transfected with OCC1 expression vector. Untransfected COS 7 cells were used as a control. l, cell lysates; m, conditioned medium. The molecular weight of the major product detected in the medium of OCC1-expressing COS 7 cells (arrow; about 43 kDa) is larger than that in the cell lysates (arrowhead; about 36 kDa) indicating that the product is secreted after being modified.

Fig. I-9. A photomicrograph for neurons stained by *in situ* hybridization

histochemistry with the *occ1* antisense probe in layer IVA of area 17. *occ1* mRNA was occasionally found in the processes of some neurons, which resulted in contoured pyramidal-shaped cell bodies (arrow). Pial surface is to the top. Bar, 20 μm.

Fig. I-10. Neocortical distribution of the neurons marked by *occ1*-mRNA expression. (a-e) Parasagittal (a) and frontal (b-e) whole-brain sections processed by *in situ* hybridization. In (a), rostral is to the left, and the arrows indicate the borders between areas 17 and 18. In (b-e), medial is to the right. Arrows in (c) indicate the borders of area 3b. Arrowheads and arrows in (d) indicate the borders of area 3b and AI, respectively. (f) Lateral view of macaque neocortex, rostral is to the left. The lines indicate the coronal planes sliced for the sections (b-e). The signals were localized preferentially in the posterior region of the neocortex, in particular, area 17. Bar, 5 mm. Abbreviations are as used in Fig. 1. cc, sulcus of corpus callosum.

Fig. I-11. Area 3b and AI can be identified by densities and patterns of *occ1* expression. (a-d) Sections through area 3b (a; the region indicated by arrows in Fig. 10c at higher magnification) and AI (c; the region indicated by arrows in Fig. 10d at higher magnification), stained for *occ1* (a and c) and with thionin (b and d). Area 3b and AI show relatively dense expression of *occ1* in layer III and IV. Bar, 500 μm.

Fig. I-12. Laminar distribution of *occ1*-positive neurons in areas 17 and 18. (a-d) Sections through area 17 (a and b) and area 18 (c and d), stained for *occ1* (a and c) and with thionin (b and d). In areas 17 and 18, the strongest signals are found in layer IVC and in the deeper stratum of layer III, respectively. Bar, 200 μm.

Fig. I-13. Neuronal subset revealed by *occ1* includes two different classes of neurons. (a-c) Sections were double labeled with antiserum against OCC1 (left panels) and antibody against either CaMKII α (a and b; middle panels) or GABA (c; middle panel), and imaged to determine colocalization (right panels, OCC1 in green, CaMKII α or GABA in red). (a) from layer II, (b) and (c) from layer IVCβ of area 17. Pial surface is to the top. Arrowheads indicate the representative cells double-positive for each antiserum/antibody combination. Note that, owing to the difference of the subcellular localization pattern of OCC1 from that of GABA, the confocal images to show colocalization of them (c) had to be acquired in a slice plane in which optimal staining of OCC1 might not be yielded, which resulted in the difference of OCC1 staining patterns in layer IVCβ in the two images (b and c; left panels). Bar, 20 μm.

Fig. I-14. Change in the *occ1* transcription in adult area 17 following monocular deprivation. Sections are stained for *occ1* (left panels) and CO (right panels). (a,

b) A coronal section through area 17 of a monkey monocularly deprived for 14 days. The change was detected in layers III, IVA, IVB, IVCα, IVCβ and V. (c-f) Tangential sections through layer III. The boxed areas in (c) and (d) are magnified in (e) and (f), respectively. (g, h) Tangential sections through layer IVCβ. By comparing the positions of the same blood vessel profiles in these sections (arrowheads), the remarkable reduction of *occ1* mRNA was found in the perturbed columns. Arrows in (e, f) indicate the representative patchy stainings in the perturbed columns in each section. Bars, 500 μm.

Fig. I-15. Distribution of *occ1*-expressing neurons in the LGN. (a, c) Frontal sections through LGN, stained for *occ1* (a) and with thionin (c). (b) Drawing of the positive signals (dots) in (a). (d) The boxed area in (a) is magnified. (e) The boxed area in (c) is magnified. In LGN, *occ1* mRNA is expressed selectively in the cells of the magnocellular layers (layers 1 and 2). Bar in (c) for (a-c), 500 μm; bar in (e) for (d, e), 200 μm.

Fig. I-16. Distribution of *occ1*-expressing neurons in the hippocampal formation of the macaque monkey. Frontal sections through the hippocampus, stained for *occ1* (a, c and e) and with thionin (b,d and f). CA1-3, subfields of Ammon's horn;

DG, dentate gyrus; Sub, subiculum; Prs, presubiculum. The arrows in (a) and (b) indicate the borders between CA1 and CA2 and between CA2 and CA3. The CA2 and CA3 subregions in (a) and (b) were magnified in (c) and (d), respectively. The CA2 subregions in (a) and (b) were at further higher magnification in (e) and (f), respectively. *occ1* mRNA is observed to be localized in the processes of the positively-stained neurons ; arrows in (e) mark the cells whose processes were visualized by *in situ* hybridization. gc, granule cell layer; ml, molecular layer; pc, pyramidal cell layer; pm, polymorphic layer; s l-m, stratum lacunosum-moleculare; lpe, the lamina principalis externa; lpi, the lamina principalis interna; so, stratum oriens; sr, stratum radiatum. Bars in (b) and (d), 500 μm; bar in (f), 100 μm.

Table I-1. The sequence identity between *occ1* and human, mouse and rat FRP/TSC-36. Proportion of identical nucleotide sequences (top right) and identical amino acid sequences (bottom left), calculated with GENETYX-Mac ver 8.0 (SOFTWARE DEVELOPMENT).

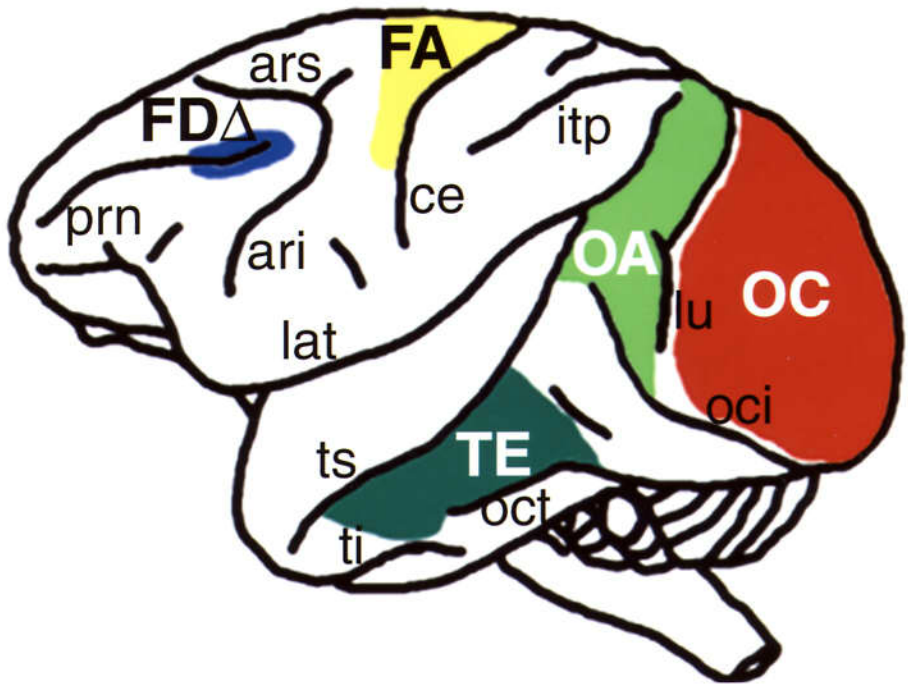

Fig. I-1

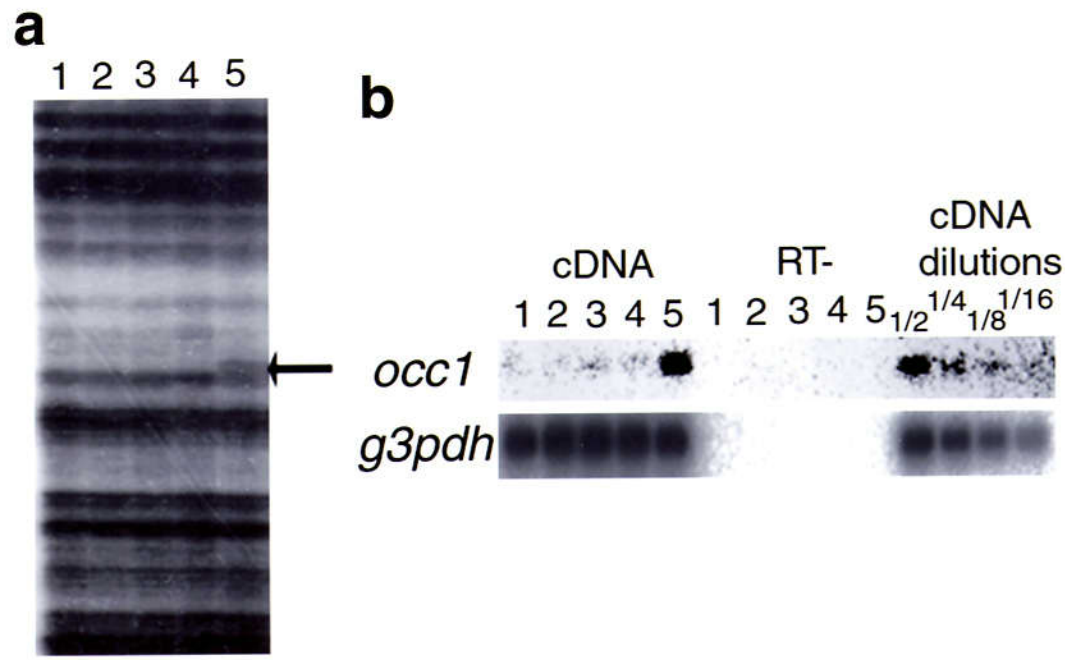
a
1 2 3 4 5
b
cDNA
RT-
cDNA dilutions
1 2 3 4 5 1 2 3 4 5 1/2 1/4 1/8 1/16
occ1
g3pdh

Fig. I-2

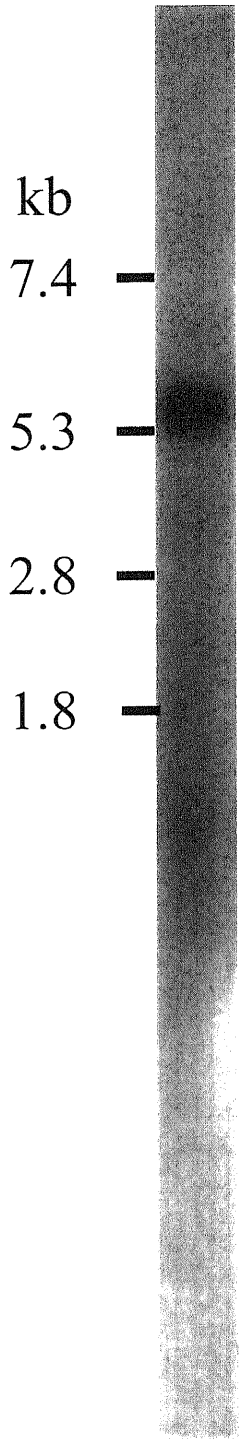

Fig. I-3

a

```
GGAGCTCCAACCTCCGCTTAGAGCTCGCTGCGGCCGTCCTGCCCCGTGCCCTCGGAGACCTGGACCGTACCACGATGTGGAAACGCTGGCTCGCGCTCGCGCTAGCGCTGGTGGCGGTCG  120
                                                                M  W  K  R  W  L  A  L  A  L  A  L  V  A  V  A

CCTGGGTCCGCGCCGAGGAAGAGCTAAGGAGCAAATCCAAGATCTGTGCCAATGTGTTTTGTGGAGCTGGCCGGGAATGTGCAGTCACAGAGAAAGGGGAACCCACCTGTCTCTGCATTG  240
   W  V  R  A  E  E  E  L  R  S  K  S  K  I  C  A  N  V  F  C  G  A  G  R  E  C  A  V  T  E  K  G  E  P  T  C  L  C  I  E

AGCAATGCAAACCTCACAAGAGGCCTGTATGTGGCAGTAACGGCAAGACCTACCTCAACCACTGTGAACTGCATCGAGATGCCTGCCTCACTGGATCCAAAATCCAGGTTGATTACGATG  360
   Q  C  K  P  H  K  R  P  V  C  G  S  N  G  K  T  Y  L  N  H  C  E  L  H  R  D  A  C  L  T  G  S  K  I  Q  V  D  Y  D  G

GACACTGCAAAGAGAAGAAATCCATAAGTCCATCTGCCAGCCCAGTTGTTTGCTATCAGTCCAACCGTGATGAGCTCCGACGTCGCATCATCCAGTGGCTGGAAGCTGAGATCATTCCAG  480
   H  C  K  E  K  K  S  I  S  P  S  A  S  P  V  V  C  Y  Q  S  N  R  D  E  L  R  R  R  I  I  Q  W  L  E  A  E  I  I  P  D

ATGGCTGGTTCTCTAAAGGCAGCAACTACAGTGAAATCCTAGACAAGTATTTTAAGAACTTTGATAATGGTGACTCTCGCCTGGACTCCAGCGAATTCCTGAAGTTTGTGGAACAGAATG  600
   G  W  F  S  K  G  S  N  Y  S  E  I  L  D  K  Y  F  K  N  F  D  N  G  D  S  R  L  D  S  S  E  F  L  K  F  V  E  Q  N  E

AAACTGCCATCAATATTACCACGTATCCAGACCAGGAGAACAACAAGTTGCTTAGGGGACTCTGTGTTGATGCTCTCATTGAACTGTCTGATGAAAATGCTGATTGGAAACTCAGCTTCC  720
   T  A  I  N  I  T  T  Y  P  D  Q  E  N  N  K  L  L  R  G  L  C  V  D  A  L  I  E  L  S  D  E  N  A  D  W  K  L  S  F  Q

AAGAGTTTCTCAAGTGCCTCAACCCATCTTTCAACCCTCCTGAGAAGAAGTGTGCCCTGGAGGATGAAACGTATGCAGATGGAGCTGAGACTGAGGTGGACTGTAACCGCTGTGTCTGTG  840
   E  F  L  K  C  L  N  P  S  F  N  P  P  E  K  K  C  A  L  E  D  E  T  Y  A  D  G  A  E  T  E  V  D  C  N  R  C  V  C  A

CCTGTGGAAACTGGGTCTGTACAGCCATGACCTGTGACGGAAAGAATCAGAAGGGGGCCCAGACTCAGACAGAGGAGGAGATGACCAGATACGTCCAGGAGCTCCAGAAGCATCAGGAAA  960
   C  G  N  W  V  C  T  A  M  T  C  D  G  K  N  Q  K  G  A  Q  T  Q  T  E  E  E  M  T  R  Y  V  Q  E  L  Q  K  H  Q  E  T

CAGCTGAAAAGACCAAGAGAGTGAGCACCAAAGAGATCTAATGAGGCGGCACAGGATAGTGTCTGGAGCCCAGCATCTTCTCTTCCACTTCAGCGCTGAGTCCAGTATACACGAGTGTCT  1080
   A  E  K  T  K  R  V  S  T  K  E  I  *
GCTACAGTCGCCAAATCACCAGTATTTGCTTATATAGCAATGAATTTCATTTTGTTTATTTGTTTTGCAATAAAGGAGATGAAGGTGGCTGGCTAGGAGGGGAAGGGCCACAGCCTTCAT  1200
TTCTAGGAGTGCTTTAAGAGACACTGCAAACGGTGCTCTGGGGCCGTTTAGTAAGGAAACTGCATCACGATTGAAAGAGGAACAAACCCAAATCTGAACCTCTTTTGAGTTTACTGCATC  1320
TGTCAGCAGGTTACAGGGAGTGCACACAATGCCAGAGAGAACTTAGCAGGGTGTCCCTGGAGGAGAGGTTTGGGAAGTTCCACAGAGAGGAACGCTCTCTGCTTCCAGCCTCTTTCCATT  1440
GCCGTCAGCATGACAGACCTCCAGCATCCACGCATCTCTTGGTCCCAATTACTGCCTCTAGATACATAGCCATCCTGCTAGTTAACCCAGTGTCCCTCAGACTTAGATGGAGTTTCTGGG  1560
AGAGTACACCCAAATGATGCAGATACTTGTATACTTTGAGGCCCTTGGCAACCTAACCAAATTTTAAAAATACTTTTGACCAAAGGTGCTATTTCTCTGTAAAACACTTTTTTTTTTTTG  1680
GCAAGTTGACTTTATTCTTCAATTATTATCATTATATTATTGTTTTTTAATATTTTATTTTCTTGACTAGGTATTAAGCTTTTTTTATTATTTTTCAATAGTCCCACCACTTCATAGGTG  1800
GAAGGAGTCTGGGGTTCTTCCTGGTGCAGGGGCTCAAATAACCCAGATGCCCCCACCCTGCCACATACTAGATGCAGCCCATAGTTGGCCCCCCCAGCTTCCAGCAGTCCACTATCTGCCA  1920
GAGGAGCAAGGGGTGCCTTAGACCGAAGCCAGGGGAGGAAGCATCTTCATAAAAAACTTTCGAGATCCAAACATTAATTTGTTTTTATTTATTCTGAGAAGTTCAGGCAAATCAGTATTC  2040
CCAAGGATGGAGATAAGTACAGCCAAGCGGGCTTAGGATATCCCAGCCTACCAATATGCTCATTGGCCTACAACTAACTAGGAGAGTGAGTTGGCCCTGTCTCTCTTCCTTTTTCTGGAC  2160
CTCAGTTTCCTCAGTAGCTGGTAAGAATGCACTAGCCTTTTGATTTGATAAGTTATAAATTCTGTGGTTCTGATCATTGGTCCAGAGGGGAAATAGGTTCCTGTGATTTTTCCTTCTTCT  2280
CTGTAGAATAAATGAAATCTCGTTGTTAGAACAAGAAATGTCAGATGGCCAAAAACAAGATGACCAAATTTGATCTCAGCCTGATGACGCTACAGGTTGTGCTGTGATACAGAGTCCTCA  2400
TGGGTAAAGCAGAAAGAGAGTGGGAAAGAGAACCACCCCACTCTGTCTTCATATTTGCATTTCATGTTTAACCTCCGGCTGGAAATAGAAAGCATTCCCTTAGCGATGAGGATAAAAGAA  2520
AGTTTGTAATTCAACAGGGGGAAGAAAATGGAGATTTAATCCTAAAACTATGACTTGGGGAGGTCAGTCATTTACAGTTAGTCTTGTGTCTTTTGACTTCTGTGATAGTTAACCCCACTC  2640
ACTACCCTGTTTAAGATGCATTTGGAATACCAAAGATTAAAGCCTTGACATAAGATCTCATTTGTAGAAAGTAGATTAAAGACCATCAGAAGGAAATTATTTAGGTTGTAATGCACAAGC  2760
AACTGTGAGAAACTGTTGTGCCAAAAATATAATTCCTTCTAGTTTTCCTTGTTCTTATTTGAAAGGAGAAAATCCCACTTTGTTCAGCATTTTAAGCTTTTGTGTATCAATCCCATCTAA  2880
AAACTCTCTTCAAACTCCACTTGTTCAGTCTGAAATGCAGCTCCCTGTCCAAGTGCCTTGGAGAACTCACAGCAGCATGCCTTAATCAAAAGTTTTGCCAGCCCTTGGACACTATGGGAG  3000
GAGGGCAAGAGTATCAGTTTGTTAAAAGCAAAAAAACCACAGTGTCTCTTCACTAGCCATATTTAGAACAGTGGTTACCATCCAAGACTACTCTATCCTGCAACACTGAACTCTCAAGAG  3120
CAAATCCACATTCCTCTGCTTCTGTGTAAATAGGGCAGCTGTTGTCTATGCCATAGAATCACATGATCTGAGGACCATTCATGGAAAGCTGCTAAATAGCCTAGTCTGGGAAGTCTTGCA  3240
TAAAGTTTTGCATGAAGCAAACAGGATTAAATCAGGTTTGGTTCCTTCAGCCCTCTAAAGGCATAGGGCTTAGCCTGCAGGCTTCCTTGGGCATTCTCTGTGTGTGTAGTTTTGTAAACA  3360
CTATAGCATCTGTTAAGATCCAGTGTCCATGGAAACCTTCCCACATGCCGTGACTCTGGACTCTCAGTTTTTGAAAGCAGGGTTCCTCTGCCTGCTAACAAGCCCACGAGGACCAGTCTG  3480
AATGTCTTTCCTTTACACCTATGTTTTTAAATAGTCAAACTTCAAGAAACAATCTAAACAAGTTTCTGTTGCATATGTGTTTGTGAACTTGTATTTGTATTTAGTAGGCTTCCATATTGC  3600
ATTTAACTTGTTTTTGTAACTCCTGATTCTTTCTTTTCGGATACTATTGATGAATAAAGAAATTAAAGTGATAGTTTTATTGGTTTCCTTTCCCCCAATTAAGGCCAAATAAAGTTGTGA  3720
GAACATTACCCATTTACTTCCTAAGAGTGGATTGGAGTTTCAGGAGCCTTACAAAGGACTGAAGAGTTTCTCCTGGGACTGCAGCTTGGATGGGAAGTTTACTCGGGGACTGGCAGAACA  3840
AGTTTCTTTGAAAGGATCATGGATGATGGGTCTGGAGTAGAAGGTGATGACAAGTCAGAGAGTGTCTTAGTCCCTTCAGGTTGCTATAACAAAATGCCTCAGACTGGGTAATTATAGACA  3960
ACAGAAATGTATTGCTCACAGTTCTGAAGGCTGGGAAGCCTAAGATTAAGGTACCAACAGATTTAATGTCTGATAAGGGCTTGTTGAAGCTTGTCTGCTTCAAAGAATGCACCTTCTTGA  4080
TGCATCCCCACATGGTGGAAAGGGTGAACAAACTCCCTTAGGCCTCTTTTATAAGGGCACGAGGGTTAAACTTTTGATGACCTAATCATCTCCCAAGAGCCTCACCTCTCAATACCATTG  4200
CTTTGGGGGATTCAATTTTATCATGAATTTTGGGGGGACATAAACATTCAAACCATAGCAGGGTGCATTCCTGTATTGGGAAGATGTTAAATTAAATGACTTCTAAATCCCCCATACGAT  4320
TTAGGAGACTAAATGGCATCCTGTGAGGCTGACTGCAGTGGCCTGTGAGAAGGCAAATAAACATGGGAAGGTAGTACAGGGAACATGGAATCGTTGCCAGGGACAGGCTAAATAACCTTA  4440
ATGGCACTTCCTTGATACACACATTCCATGGGGATAAACATTTCCAAGTGGGCTGAATGTTGGCTGGTTAAAACCTCTTCTGCTCCATCTTGGGGACACATGACTAATGTTTTCCAACCT  4560
GCCATTTTCATATGTATCGTGCACTCTCCACCCCCAATAATTCTGCCTCCCAAAAGAGCATATAGTCGATGAGGTTTAAGGTTTCTTCAGTTCAGTCATGTGGAAGTGTTGCTATCCTAA  4680
AATTATAGCTGGATCACTTTGATTGGATTTGGGATATAACCCAAATACTAATCAAATATTAAAAGGCAATCTTTTTTGTTACGTGATTGCTACAGATTACTGATCTCATTTGTCACAGTT  4800
TGATTCTTCAAATTTTCATTCTCAGAAGGGAATCTTAAACCCAGTTTGAAGGGTACCTTGTCCACAACCACTTTTAAATTTTGGCTAACTACTCCCAACCTTCTACTGTGTTCTGGGAAA  4920
ACTTTTTCTGCTGTTATGTATGTATTCAGGAAGTGCAACATTATTAAAATAACCTAAACTAAGCATAATTCAGAAGTTAAGTTTCCTTTCATCAAAATTTAATATTATGAATTGTGCAGA  5040
GAAGTATGTTACTTTGATCCACTTTATTTTAGAACTTCTTTATCAAGTTATCAGTCCTCTTGAACTATTTCTGAAATAAGGGGAAGGAAGGAAGGGAAAAAATATGAATGTGTAGATAGA  5160
TCTAAGCAGATGCCCTCAGAGCCCTGGAATAATCCTAGCCGGGATGTGGGACATGAAAACAACTCTGGCCTACTGCTGCTGGGGGCTGCTTCATGGTGTGACATAGGAAGTAAAATGTTG  5280
CTGTATGAATAGGAAGGAGGGTCTTCCTGTCAATGAGAATTAATGTTTTTCTAATGATTTAACTTTTTTACTGAAGAAATAATATGTATACGTGGTAAAAATCCAAATTGTATCAAGGAA  5400
AATACAGTGAATAAAACCATCCTCTTAGAGGGTATGTCCATTTATAAATTTGCCTATGATTGCCTATACAGTCAAAGAGGTTGCACCAGTATGCATGCCTGCCGAAAGTACATAAACTGA  5520
GCATATCTATTTCCCTACATTTTTGCAAACATTACACCTTCAAGTTTTTTGGCCTCTGATAGAGGAAAAATGGTAACTCCTTGTTTTATTTTTTATATTCATTATTCCTTTTGTAAGATT  5640
AAATCTCTTCCCATGAAAAATTAAAAAAAAAAAAAAAAAAAAAAAAAA                                                                          5688
```

b

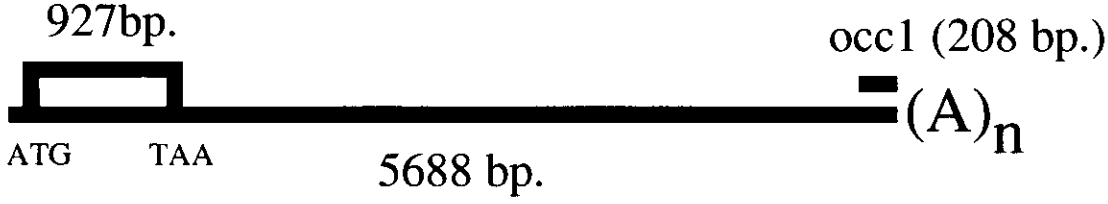

Fig. I-4

```
occl            ATGTGGAAACGCTGGCTCGCGCTCGCGCTAGCGCTGGTGGCGGTCGCCTGGGTCCGCGCC
human frp       ATGTGGAAACGCTGGCTCGCGCTCGCGCTCGCGCTGGTGGCGGTCGCCTGGGTCCGCGCC
mouse tsc-36    ATGTGGAAACGATGGCTGGCGCTCTCGCT------GGTGACCATCGCCCTGGTCCACGGC
rat frp         ATGTGGAAACGCTGGCTGGCGCTCGCGCT------GGTGACCATCGCCCTGGTCCACGGC
                *********** ***** ****** ****      **** * *****  ***** ** *

occl            GAGGAAGAGCTAAGGAGCAAATCCAAGATCTGTGCCAATGTGTTTTGTGGAGCTGGCCGG
human frp       GAGGAAGAGCTAAGGAGCAAATCCAAGATCTGTGCCAATGTGTTTTGTGGAGCCGGCCGG
mouse tsc-36    GAGGAGGAACCTAGAAGCAAATCCAAGATCTGCGCCAATGTGTTTTGTGGAGCTGGCAGG
rat frp         GAGGAGGAACAAAGAAGCAAATCCAAGATCTGCGCCAATGTGTTTTGTGGAGCTGGCCGG
                ***** ** *  ** ***************** ******************** *** **

occl            GAATGTGCAGTCACAGAGAAAGGGGAACCCACCTGTCTCTGCATTGAGCAATGCAAACCT
human frp       GAATGTGCAGTCACAGAGAAAGGGGAACCCACCTGTCTCTGCATTGAGCAATGCAAACCT
mouse tsc-36    GAATGTGCCGTCACAGAGAAGGGGGAGCCCACGTGCCTCTGCATTGAGCAATGCAAACCT
rat frp         GAATGCGCCGTCACGGAGAAGGGGGAGCCAACGTGCCTCTGCATTGAGCAATGCAAACCT
                ***** ** ***** ***** ***** ** ** ** ************************

occl            CACAAGAGGCCTGTATGTGGCAGTAACGGCAAGACCTACCTCAACCACTGTGAACTGCAT
human frp       CACAAGAGGCCTGTGTGTGGCAGTAATGGCAAGACCTACCTCAACCACTGTGAACTGCAT
mouse tsc-36    CACAAGAGGCCTGTGTGTGGCAGTAATGGCAAGACCTACCTCAACCACTGTGAACTTCAT
rat frp         CACAAGAGGCCTGTGTGTGGCAGTAATGGCAAGACCTACCTCAACCATTGTGAACTTCAC
                ************** ********** ******************** ******** **

occl            CGAGATGCCTGCCTCACTGGATCCAAAATCCAGGTTGATTACGATGGACACTGCAAAGAG
human frp       CGAGATGCCTGCCTCACTGGATCCAAAATCCAGGTTGATTACGATGGACACTGCAAAGAG
mouse tsc-36    AGAGATGCCTGCCTCACTGGATCCAAGATCCAGGTTGATTATGATGGGCACTGCAAAGAA
rat frp         AGAGACGCCTGCCTCACTGGATCCAAGATCCAGGTTGATTATGATGGGCACTGCAAAGAA
                 **** ******************** ************** ***** ***********

occl            AAGAAATCCATAAGTCCATCTGCCAGCCCAGTTGTTTGCTATCAGTCCAACCGTGATGAG
human frp       AAGAAATCCGTAAGTCCATCTGCCAGCCCAGTTGTTTGCTATCAGTCCAACCGTGATGAG
mouse tsc-36    AAGAAGTCTGCGAGTCCATCTGCCAGCCCAGTTGTCTGCTATCAAGCTAACCGGCGATGAG
rat frp         AAGAAGTCTGTGAGTCCATCCGCCAGCCCCGTTGTCTGCTATCAGGCTAACCGTGATGAG
                ***** **    ******** ******** ***** ********  * ***** ******

occl            CTCCGACGTCGCATCATCCAGTGGCTGGAAGCTGAGATCATTCCAGATGGCTGGTTCTCT
human frp       CTCCGACGTCGCATCATCCAGTGGCTGGAAGCTGAGATCATTCCAGATGGCTGGTTCTCT
mouse tsc-36    CTCCGACGGCGCCTCATCCAGTGGCTGGAAGCTGAGATCATTCCAGATGGCTGGTTCTCT
rat frp         CTGCGGCGCCGGATCATCCAGTGGCTGGAAGCCGAGATCATTCCAGATGGCTGGTTCTCT
                ** ** ** **  ******************** ************************

occl            AAAGGCAGCAACTACAGTGAAATCCTAGACAAGTATTTTAAGAACTTTGATAATGGTGAC
human frp       AAAGGCAGCAACTACAGTGAAATCCTAGACAAGTATTTTAAGAACTTTGATAATGGTGAT
mouse tsc-36    AAAGGCAGTAACTACAGTGAGATCCTAGACAAGTACTTTAAGAGCTTTGATAATGGCGAC
rat frp         AAAGGCAGTAACTACAGTGAGATCCTAGACAAGTACTTTAAGAGCTTTGATAATGGTGAC
                ******** *********** ************** ******* ************ **

occl            TCTCGCCTGGACTCCAGCGAATTCCTGAAGTTTGTGGAACAGAATGAAACTGCCATCAAT
human frp       TCTCGCCTGGACTCCAGTGAATTCCTGAAGTTTGTGGAACAGAATGAAACTGCCATCAAT
mouse tsc-36    TCTCACCTGGACTCCAGTGAATTCCTGAAATTCGTGGAGCAGAATGAAACAGCCATCAAC
rat frp         TCTCACCTGGACTCCAGCGAATTCCTGAAATTCGTGGAGCAGAATGAAACAGCCGTCAAC
                **** ************ *********** ** ***** *********** *** ****

occl            ATTACCACGTATCCAGACCAGGAGAACAACAAGTTGCTTAGGGGACTCTGTGTTGATGCT
human frp       ATTACAACGTATCCAGACCAGGAGAACAACAAGTTGCTTAGGGGACTCTGTGTTGATGCT
mouse tsc-36    ATCACCACTTATGCAGATCAGGAGAACAACAAACTGCTCAGAAGCCTCTGTGTTGACGCC
rat frp         ATCACCGCTTACCCCAATCAGGAGAACAACAAACTGCTCAGAGGCCTCTGTGTTGATGCC
                ** **  * **  *  * ***************  **** **  * *********** **

occl            CTCATTGAACTGTCTGATGAAAATGCTGATTGGAAACTCAGCTTCCAAGAGTTTCTCAAG
human frp       CTCATTGAACTGTCTGATGAAAATGCTGATTGGAAACTCAGCTTCCAAGAGTTTCTCAAG
mouse tsc-36    CTCATTGAACTGTCTGATGAGAACGCTGACTGGAAACTCAGCTTCCAAGAGTTCCTCAAG
rat frp         CTCATTGAACTGTCCGATGAGAACGCTGACTGGAAACTCAGCTTCCAAGAGTTCCTCAAG
                ************** ***** ** ***** ************************ ******

occl            TGCCTCAACCCATCTTTCAACCCTCCTGAGAAGAAGTGTGCCCTGGAGGATGAAACGTAT
human frp       TGCCTCAACCCATCTTTCAACCCTCCTGAGAAGAAGTGTGCCCTGGAGGATGAAACGTAT
mouse tsc-36    TGCCTCAACCCATCCTTCAACCCTCCTGAGAAGAAGTGTGCCCTGGAGGTCGAAACCTAT
rat frp         TGCCTCAACCCATCCTTCAACCCTCCTGAGAAGAAGTGCGCCCTGGAGGACGAAACCTAT
                ************** ************************ **********  ***** ***

occl            GCAGATGGAGCTGAGACTGAGGTGGACTGTAACCGCTGTGTCTGTGCCTGTGGAAACTGG
human frp       GCAGATGGAGCTGAGACCGAGGTGGACTGTAACCGCTGTGTCTGTGCCTGTGGAAATTGG
mouse tsc-36    GCAGATGGAGCTGAGACTGAGGTGGACTGCAATCGCTGTGTCTGTTCCTGTGGCCACTGG
rat frp         GCAGATGGAGCTGAGACCGAGGTGGACTGCAATCGCTGTGTCTGTTCCTGTGGACACTGG
                ***************** ************ ** ************ *******  * ***

occl            GTCTGTACAGCCATGACCTGTGACGGAAAGAATCAGAAGGGGGCCCAGACTCAGACAGAG
human frp       GTCTGTACAGCCATGACCTGTGACGGAAAGAATCAGAAGGGGGCCCAGACCCAGACAGAG
mouse tsc-36    GTCTGCACAGCAATGACCTGTGATGGAAAGAATCAGAAGGGGGTCCAGACCCACACAGAG
rat frp         GTCTGCACAGCGATGACCTGTGATGGAAAGAATCAGAAGGGGGTCCAGACCCACACAGAG
                ***** ***** ************ ********************** ****** ** ******

occl            GAGGAGATGACCAGATACGTCCAGGAGCTCCAGAAGCATCAGGAAACAGCTGAAAAGACC
human frp       GAGGAGATGACCAGATATGTCCAGGAGCTCCAAAAGCATCAGGAAACAGCTGAAAAGACC
mouse tsc-36    GAGGAGAAGACAGGATATGTCCAGGAACTCCAGAAGCACCAGGGCACAGCAGAAAAGACC
rat frp         GAGGAGATGACGAGATATGCCCAGGAACTCCAGAAGCACCAGGGAACAGCAGAAAAGACC
                ******* ***  **** * ****** ***** ***** **** ***** *********

occl            AAGAGAGTGAGCACCAAAGAGATCTAA*
human frp       AAGAGAGTGAGCACCAAAGAGATCTAA*
mouse tsc-36    AAGAAGGTGAACACCAAAGAGATCTAA*
rat frp         AAGAAGGTGAACACCAAAGAGATCTAA*
                **** **** ****************
```

Fig. I-5

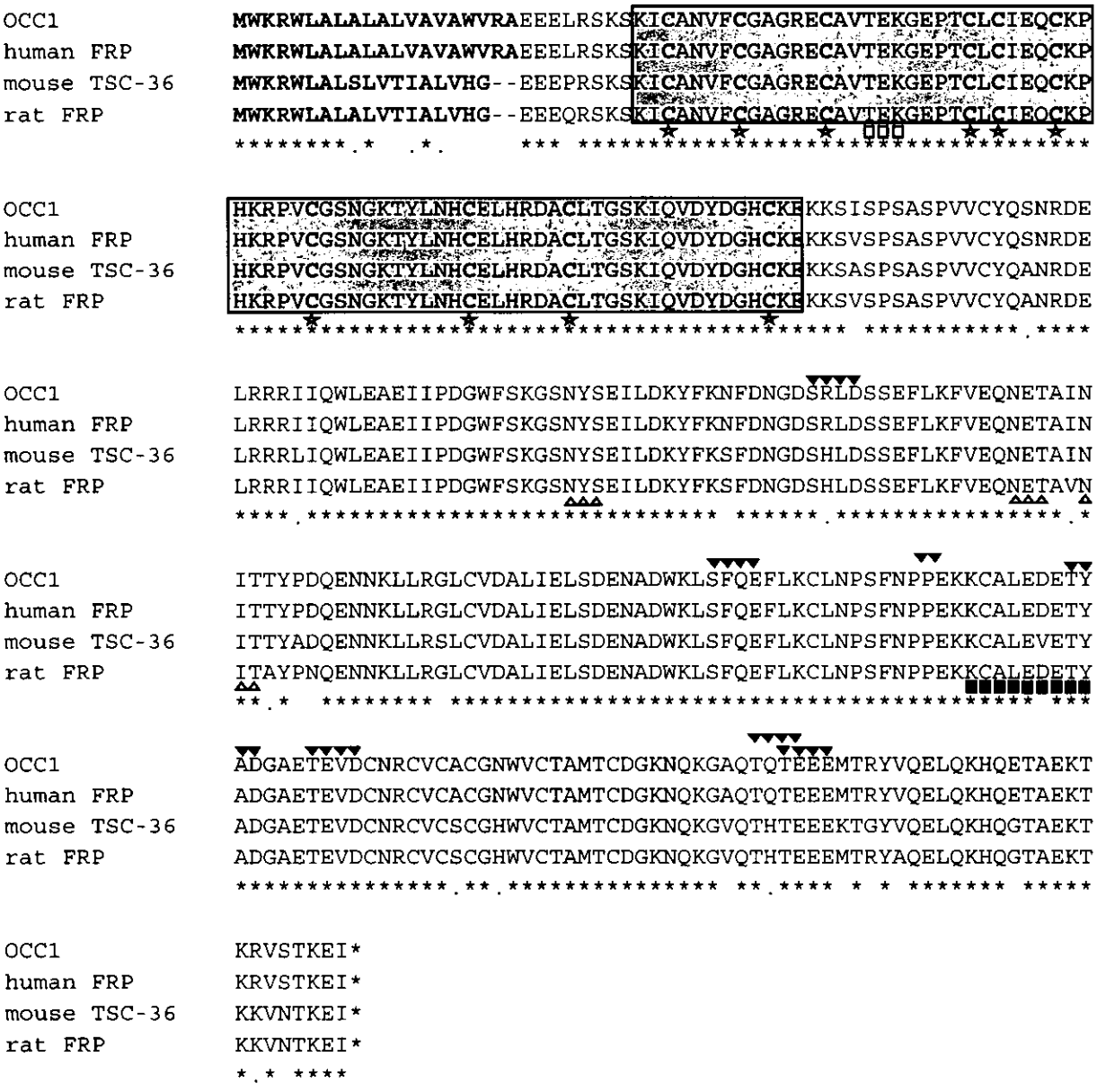
OCC1
human FRP
mouse TSC-36
rat FRP
MWKRWLALALALVAVAWVRAEEELRSKSKICANVFCGAGRECAVTEKGEPTCLCIEQCKP
MWKRWLALALALVAVAWVRAEEELRSKSKICANVFCGAGRECAVTEKGEPTCLCIEQCKP
MWKRWLALSLVTIALVHG--EEEPRSKSKICANVFCGAGRECAVTEKGEPTCLCIEQCKP
MWKRWLALALVTIALVHG--EEEQRSKSKICANVFCGAGRECAVTEKGEPTCLCIEQCKP
HKRPVCGSNGKTYLNHCELHRDACLTGSKIQVDYDGHCKEKKSISPSASPVVCYQSNRDE
HKRPVCGSNGKTYLNHCELHRDACLTGSKIQVDYDGHCKEKKSVSPSASPVVCYQSNRDE
HKRPVCGSNGKTYLNHCELHRDACLTGSKIQVDYDGHCKEKKSASPSASPVVCYQANRDE
HKRPVCGSNGKTYLNHCELHRDACLTGSKIQVDYDGHCKEKKSVSPSASPVVCYQANRDE
LRRRIIQWLEAEIIPDGWFSKGSNYSEILDKYFKNFDNGDSRLDSSEFLKFVEQNETAIN
LRRRIIQWLEAEIIPDGWFSKGSNYSEILDKYFKNFDNGDSRLDSSEFLKFVEQNETAIN
LRRRLIQWLEAEIIPDGWFSKGSNYSEILDKYFKSFDNGDSHLDSSEFLKFVEQNETAIN
LRRRIIQWLEAEIIPDGWFSKGSNYSEILDKYFKSFDNGDSHLDSSEFLKFVEQNETAVN
ITTYPDQENNKLLRGLCVDALIELSDENADWKLSFQEFLKCLNPSFNPPEKKCALEDETY
ITTYPDQENNKLLRGLCVDALIELSDENADWKLSFQEFLKCLNPSFNPPEKKCALEDETY
ITTYADQENNKLLRSLCVDALIELSDENADWKLSFQEFLKCLNPSFNPPEKKCALEVETY
ITAYPNQENNKLLRGLCVDALIELSDENADWKLSFQEFLKCLNPSFNPPEKKCALEDETY
ADGAETEVDCNRCVCACGNWVCTAMTCDGKNQKGAQTQTEEEMTRYVQELQKHQETAEKT
ADGAETEVDCNRCVCACGNWVCTAMTCDGKNQKGAQTQTEEEMTRYVQELQKHQETAEKT
ADGAETEVDCNRCVCSCGHWVCTAMTCDGKNQKGVQTHTEEEKTGYVQELQKHQGTAEKT
ADGAETEVDCNRCVCSCGHWVCTAMTCDGKNQKGVQTHTEEEMTRYAQELQKHQGTAEKT
KRVSTKEI*
KRVSTKEI*
KKVNTKEI*
KKVNTKEI*

Fig. I-6

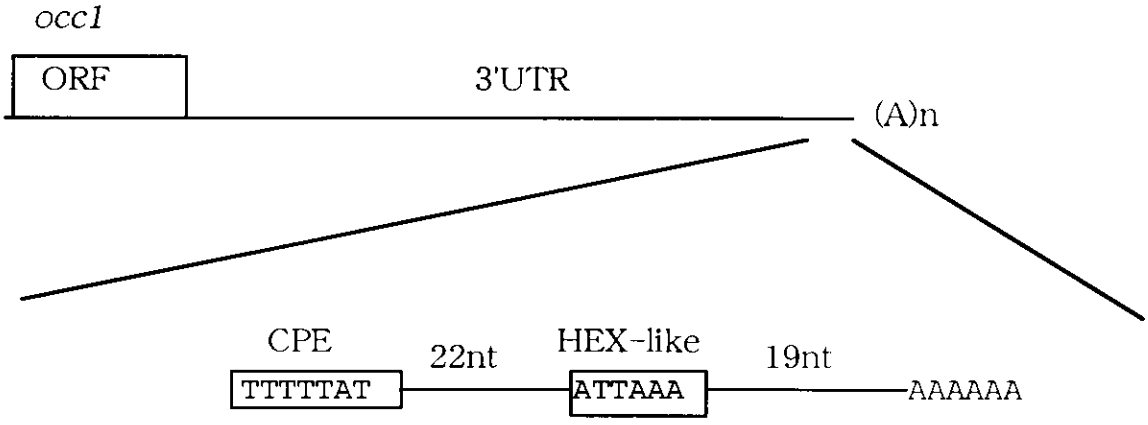
occ1
ORF
3'UTR
(A)n
CPE
22nt
HEX-like
19nt
TTTTTAT
ATTAAA
AAAAAA

Fig. I-7

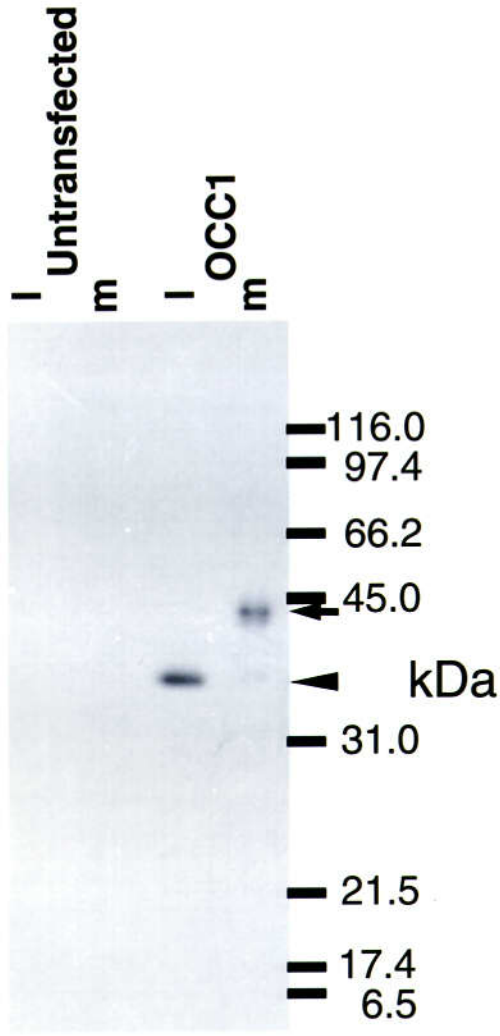

Fig. I-8

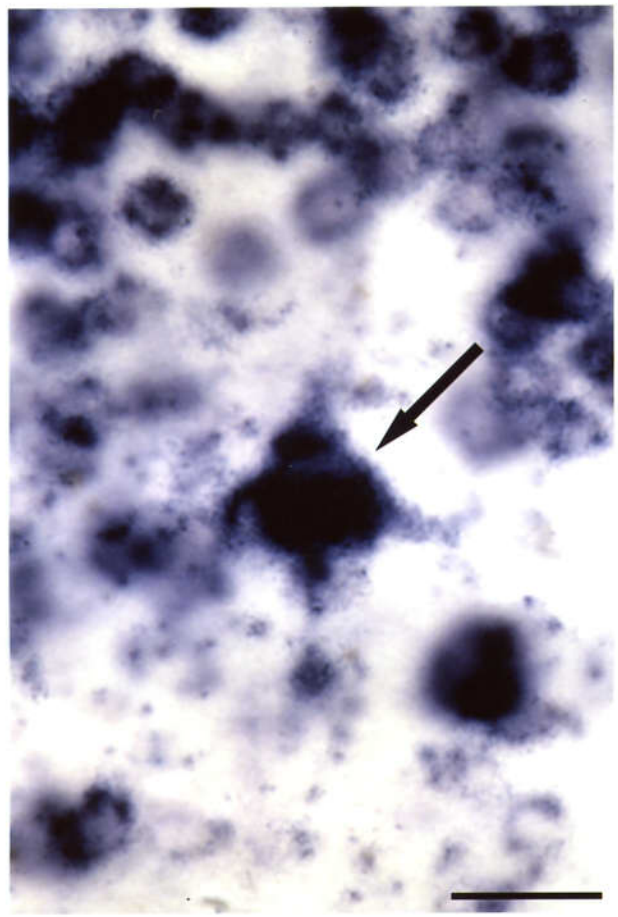

Fig. I-9

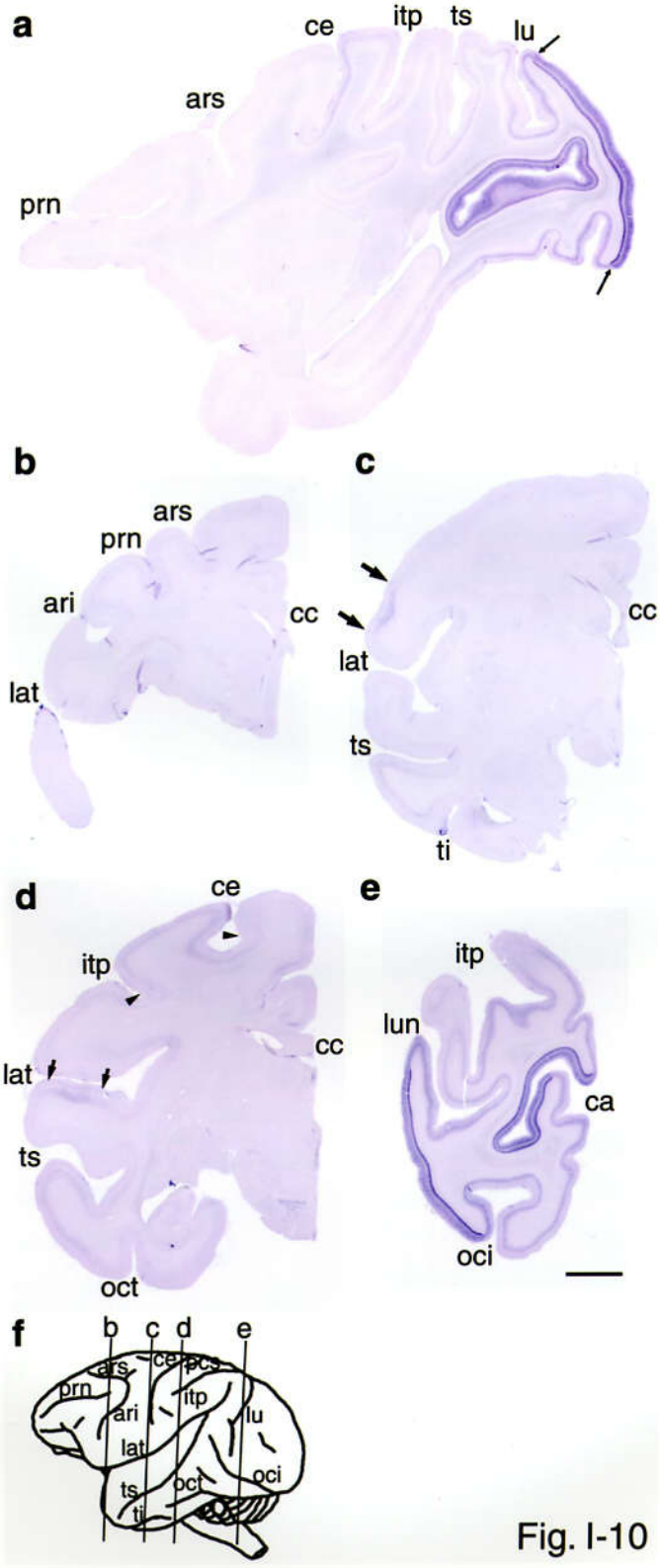
a
ce
itp
ts
lu
ars
prn
b
ars
prn
ari
cc
lat
c
cc
lat
ts
ti
d
ce
itp
cc
lat
ts
oct
e
itp
lun
ca
oci
f
b
c
d
e
ars
ce
pcs
prn
itp
ari
lu
lat
ts
pct
oci
ti

Fig. I-10

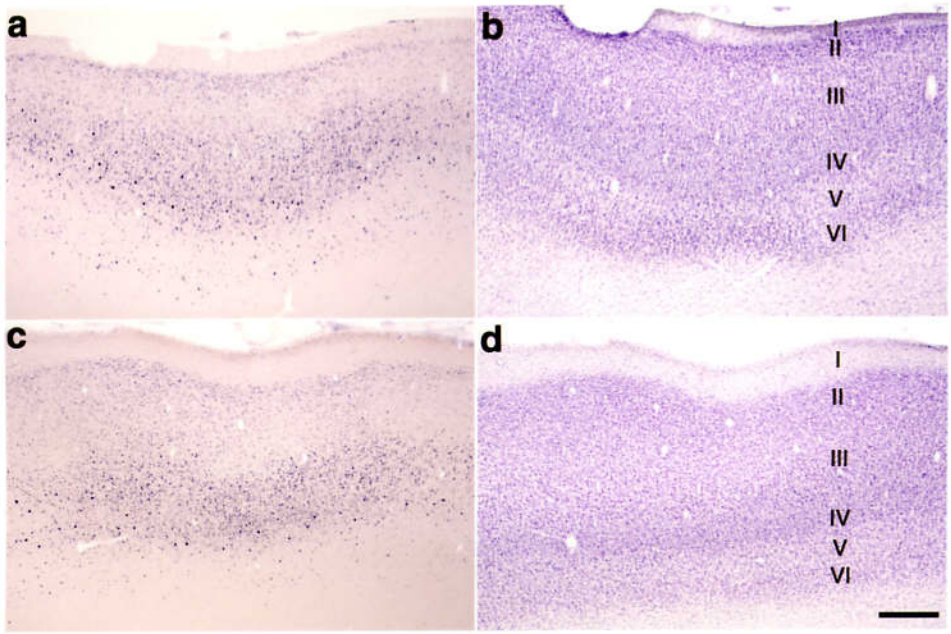

Fig. I-11

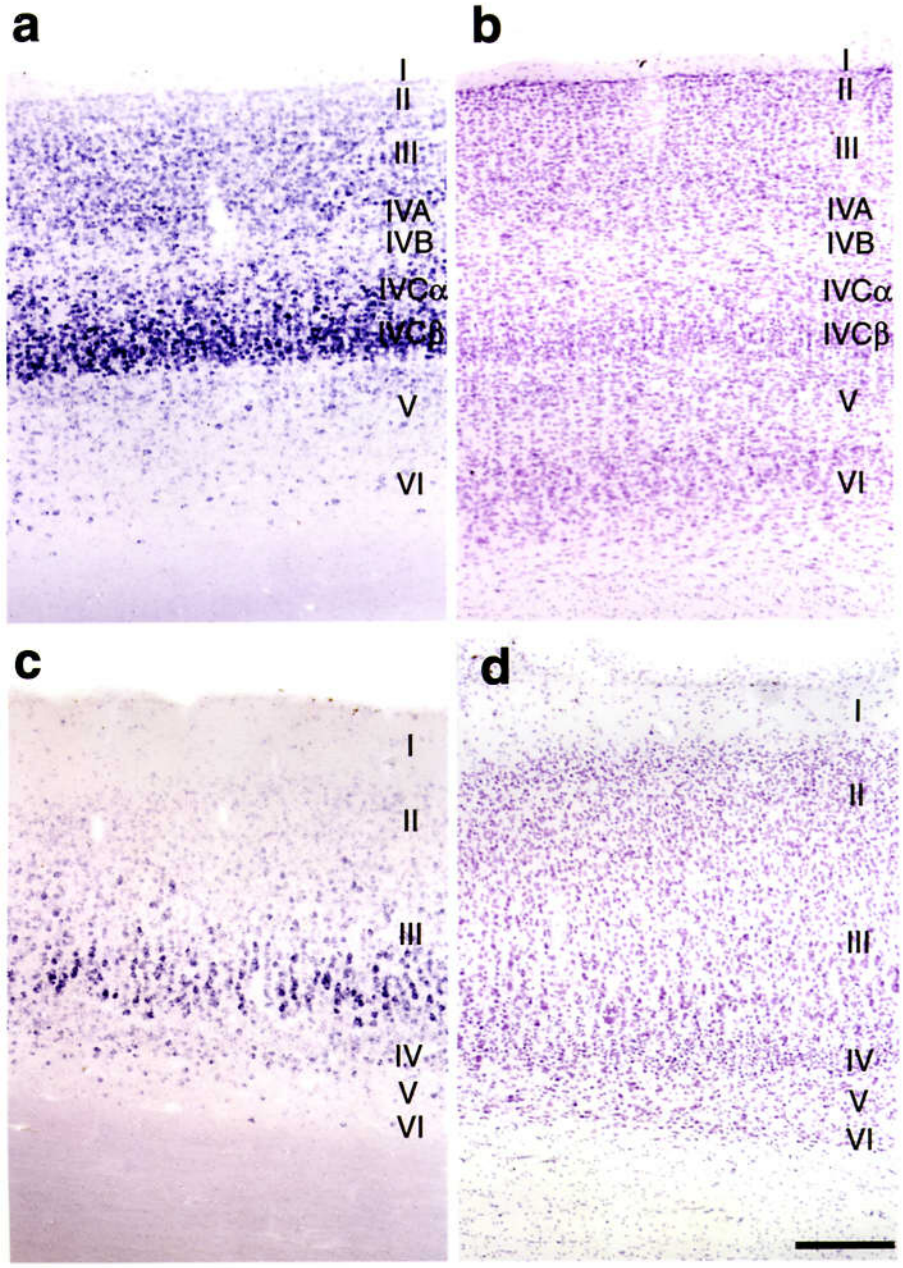
a
I
II
III
IVA
IVB
IVCα
IVCβ
V
VI
b
I
II
III
IVA
IVB
IVCα
IVCβ
V
VI
c
I
II
III
IV
V
VI
d
I
II
III
IV
V
VI

Fig. I-12

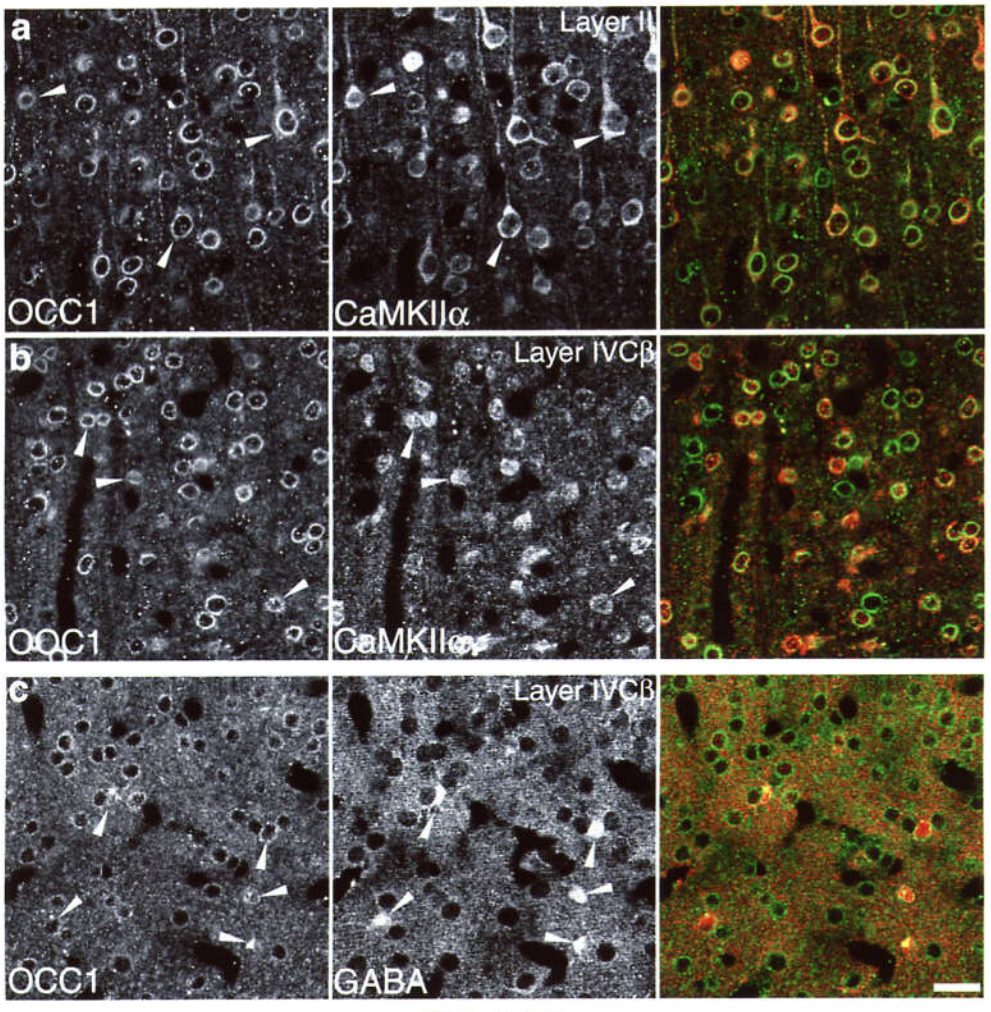
a
Layer II
OCC1
CaMKIIα
b
Layer IVCβ
OCC1
CaMKIIα
c
Layer IVCβ
OCC1
GABA

Fig. I-13

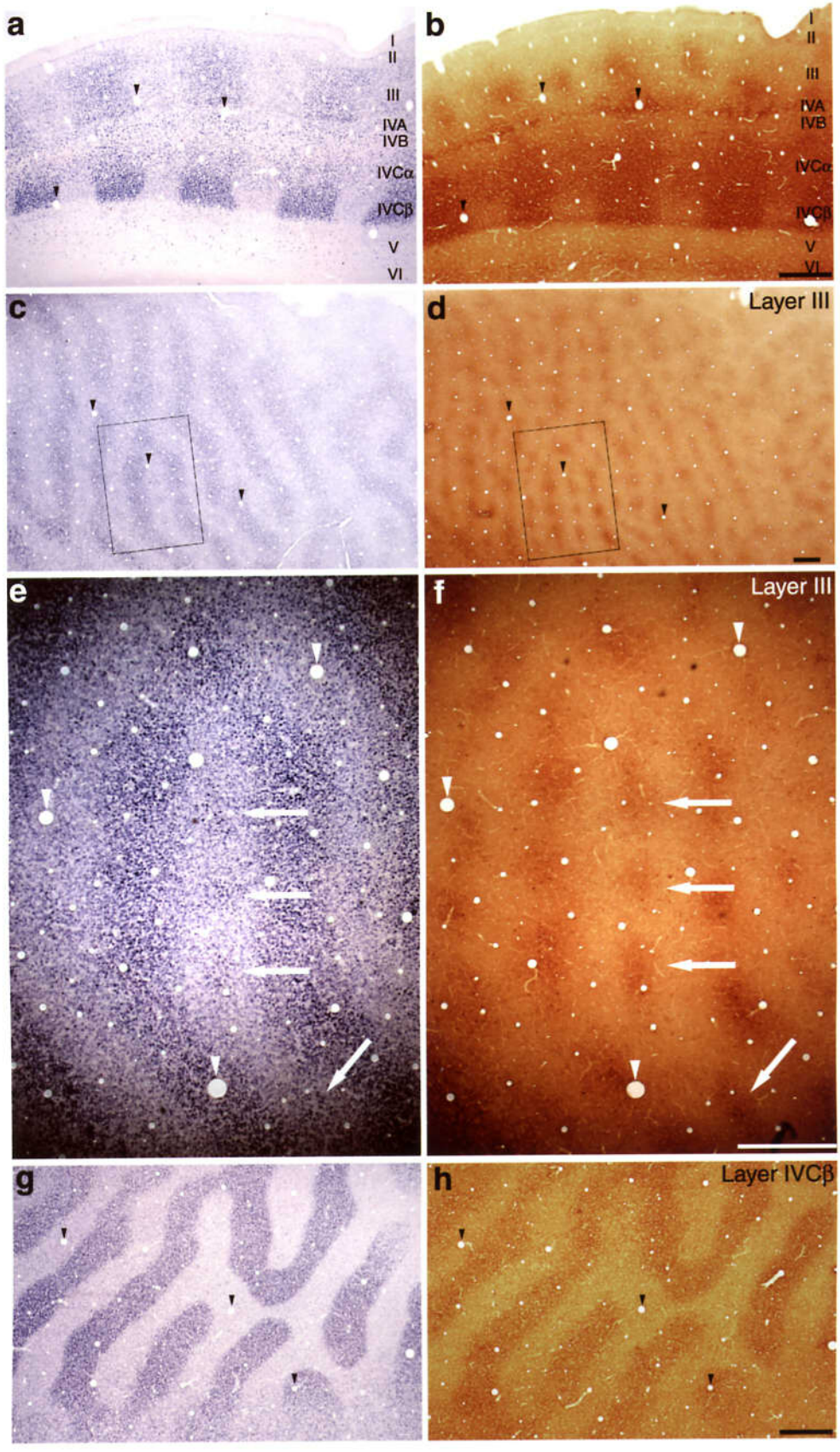
a
I
II
III
IVA
IVB
IVCα
IVCβ
V
VI
b
I
II
III
IVA
IVB
IVCα
IVCβ
V
VI
c
d
Layer III
e
f
Layer III
g
h
Layer IVCβ

Fig. I-14

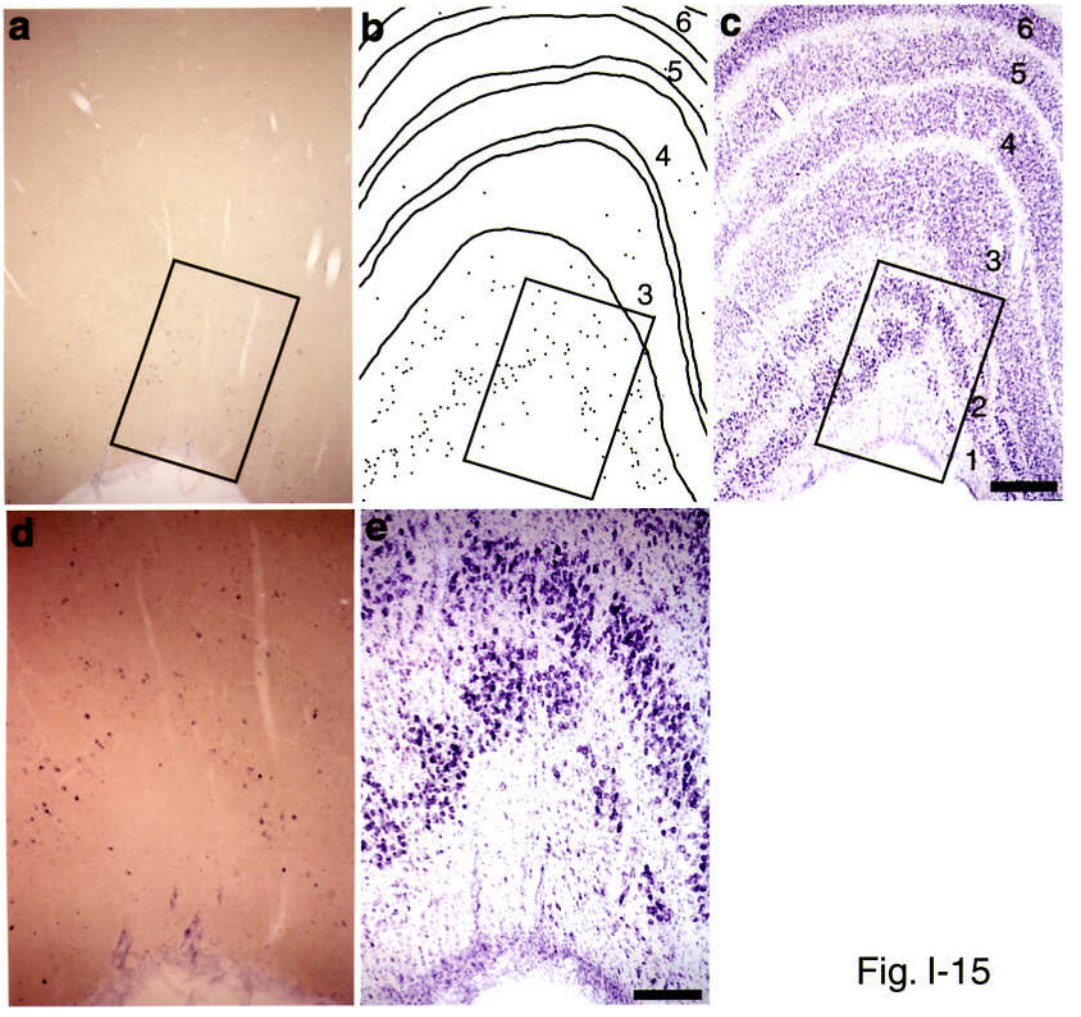

Fig. I-15

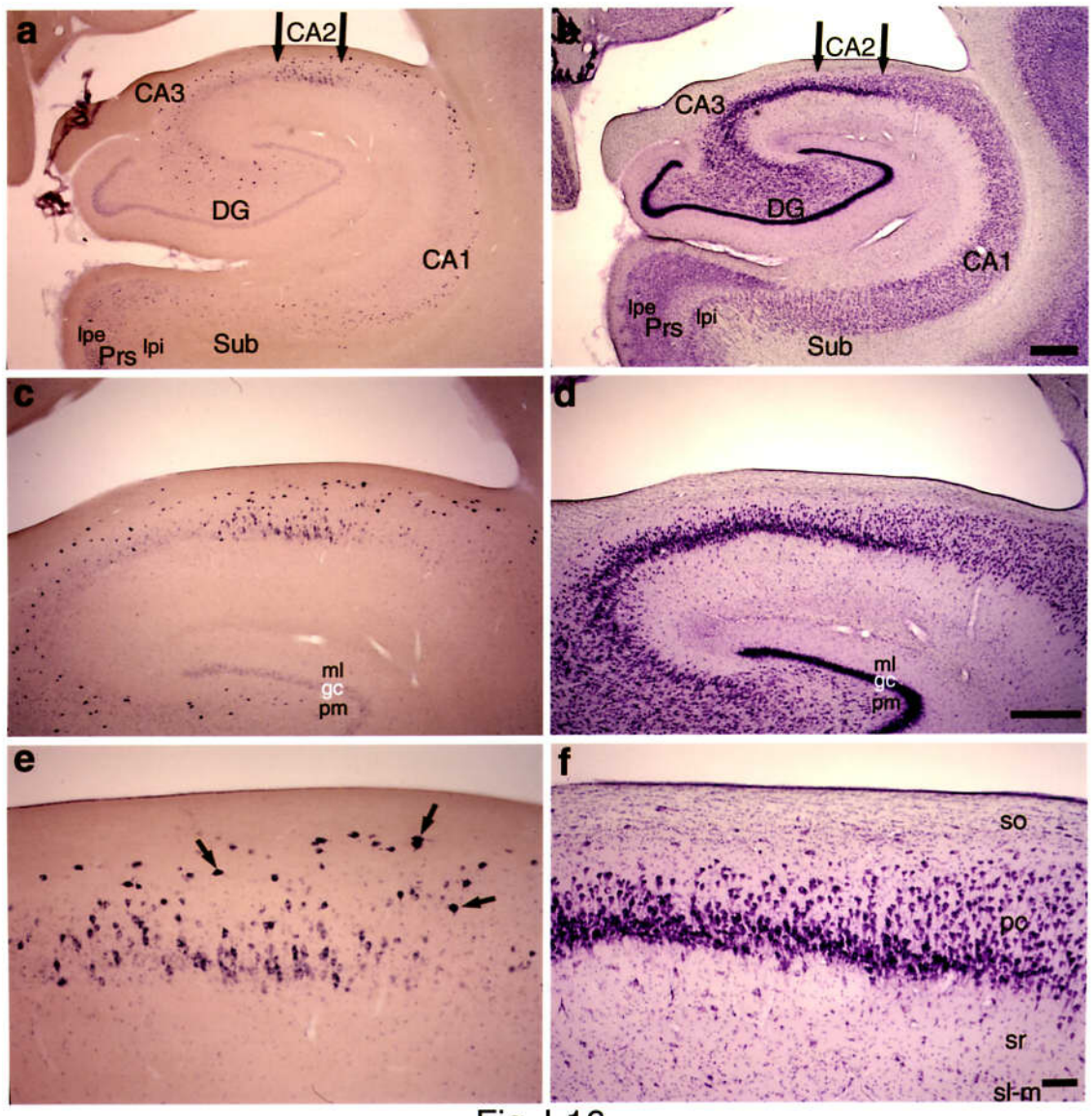
a
CA2
CA3
DG
CA1
lpe
Prs
lpi
Sub
b
CA2
CA3
DG
CA1
lpe
Prs
lpi
Sub
c
ml
gc
pm
d
ml
gc
pm
e
f
so
pc
sr
sl-m

Fig. I-16

	occ1	human FRP	mouse FRP	rat FRP
occ1		98.6	88.8	88.5
human FRP	99.7		88.9	88.6
mouse FRP	91.6	91.6		95.3
rat FRP	92.5	92.9	95.8	

Table I-1.

Part II

The expression pattern of *occ1* in neonatal and adult monkeys: *occ1* mRNA expression increases in macaque primary visual cortex during postnatal development.

Summary

As shown in part I, *occ1* is preferentially expressed in the primary visual cortex of adult monkeys in an activity-dependent manner. How does the region-selective expression of *occ1* contribute to the function of neocortex? Before answering the question, it is necessary to examine the function of this molecule in neurons. It is known that there happen two major developmental events in the primary visual cortex of macaque during the first several months after birth, the duration of the sensitivity of ocular dominance columns to monocular deprivation and the increase and peak of synaptogenesis. If *occ1* is involved in these postnatal developmental events, these events become good model systems to clarify the function of *occ1* in neurons. I analyzed the expression pattern of *occ1* mRNA in the primary visual cortex in newborn (1-2 day old), 3-month old (92-97 day old) and adult monkeys in order to examine whether there is a periodical correlation between these events and the change in *occ1* mRNA expression. *In situ* hybridization experiment showed that the laminar expression pattern of *occ1* changes during development. Optical density measurements showed that the

relative amount of *occ1* mRNA ever increases gradually during postnatal development and get the highest at adult. These data suggest the possibility that *occ1* expression is increased in an activity-dependent manner during postnatal development, and further imply that *occ1* plays a role in the postnatal developmental events. Further examination on the *occ1* expression pattern in area 18 of newborn and 3-month old monkeys suggested that the boundaries between areas 17 and 18 can be revealed by *occ1* expression at early stages as they are in adult monkeys, and the relative mRNA level and the laminar pattern of *occ1* expression change also in area 18 during postnatal development.

Introduction

It is well known that sensory experience in early postnatal life influence the maturation of the mammalian brain (Berardi et al., 2000). In the visual system, after a brief period of monocular deprivation during an early postnatal period, input from the deprived eye to the primary visual cortex is physiologically weakened and morphologically decreased in size (Shatz and Stryker, 1978; LeVay et al., 1980; Antonini and Stryker, 1993). It has been reported that some secretable molecules, such as neurotorophic factors, are involved in establishing this experience-dependent plasticity (Lo, 1995; Thoenen, 1995; Bonhoeffer, 1996). The facts that the expressions and secretions of neurotrophins are influenced by neuronal activity raise the hypothesis that a reciprocal relation between neurotrophin, functioning as a retrograde messenger, and neural activity may give an instructive factor by which frequently used neuronal connections are selectively strengthened (Isackson et al., 1991; Castren et al., 1992; Goodman et al., 1996; Heymach et al., 1996; Marty et al., 1997)).

In primates, the ocular dominance columns with an adult-like pattern emerge

within the last few weeks in gestation and are already formed at birth (Rakic, 1977; Horton and Hocking, 1996). The already-segregated columns are most vulnerable to shrinkage due to monocular deprivation for the first week of life, and the vulnerability is gradually decreased and disappears at latest by age 12 weeks (Horton and Hocking, 1997).

During the development of nervous system, the synapses are transiently overproduced and, the density of synapses then declines as the development proceeds, which is caused by both neuronal cell death and pruning the useless connections (Lund et al., 1977; Oppenheim, 1985; Acebes and Ferrus, 2000). In the development of macaque neocortex, the density of synapse increases at a rapid rate, reaches the highest level at 2-4 months after birth and, thereafter, declines gradually (Rakic et al., 1986; Hayashi, 1992).

As shown in Part I, the gene, *occ1*, which encodes a secretable protein , is selectively expressed in adult area 17 at high level, and its expression is subject to the activity-dependent regulation. It might be possible that *occ1* plays a role in the visual cortex during the early postnatal development. As a first step toward

addressing this possibility, I examined the expression pattern of *occ1* in area 17 of newborn (1-2 postnatal days), 3 month-old (92-97 postnatal days) and adult monkeys. *In situ* hybridization experiment showed that the laminar patterns of *occ1* expression were different at the stages examined. I compared the change of *occ1* mRNA level in each layer at these developmental stages. The results showed that the expression of *occ1* ever increases gradually as the development proceeds.

Materials and methods

Animals and tissue preparation.

Brain tissues were obtained from nine macaques(*Macaca fascicularis* or *Macaca fuscata*) : three adult monkeys weighing 3.0 kg-9.2 kg, three newborn monkeys (postnatal day(s) 1, 1 and 2) and three 3-month old monkeys (postnatal days 92, 96 and 97). The animals were given an overdose of Nembutal and transcardially perfused with normal saline followed by 4% paraformaldehyde in 0.1 M phosphate buffer (pH 7.4). The brains were blocked and cryoproected in 30% sucrose in 0.1 M phosphate buffer. Sections from blocks that included the primary visual cortex were cut at 40 μm thickness. Every third section was processed with the *occ1* antisense probe, for Nissl staining or with the *occ1* sense probe.

In situ hybridization histochemistry.

The *occ1* digoxigenin-labeled antisense and sense riboprobes were transcribed from a cDNA that corresponds to nucleotide positions 333-999 (aa 87-308) of the

occ1 full-length mRNA (in the DDBJ/EMBL/GenBank nucleotide sequence databases with the accession number AB039661) with digoxigenin-dUTP labeling kit (Roche Diagnostics, Indianapolis, IN, USA). *In situ* hybridization was carried out as described (Liang et al., 2000). Free-floating sections were rinsed three times in phosphate buffered saline (PBS, pH 7.4) and then treated once at room temperature (unless otherwise indicated) successively in 0.75% glycine in PBS (15 min, three times), 0.3% Triton X 100 in PBS (5 min), 1 μg/ml proteinase K in protease K buffer (0.1 M Tris-HCl, pH 8.0 and 50 mM EDTA; 30 min, 37°C) and 0.25% acetic anhydrate in 0.1 M triethanolamine, pH 8.0 (10 min). After two washes in 2× saline sodium citrate (SSC), the sections were incubated in the hybridization buffer containing 50% deionized formamide, 5× SSC, 2% blocking reagent (Roche Diagnostics) and 0.1% N-lauroylsarcosine at least for 1 hr at 50°C, transferred to the hybridization buffer containing 1.2 μg/ml digoxigenin-labeled riboprobes and incubated for at least 40 hr at 50°C. Following hybridization, sections were washed sequentially in 2× SSC/50% formamide/0.1% N-lauroylsarcosine (20 min, 50°C, twice), RNase A buffer (10

mM Tris-HCl, pH 8.0, 0.5 M NaCl and 1 mM EDTA; 10 min, room temperature), RNase A buffer containing 20 μg/ml RNase A (30 min, 37°C), 2× SSC/0.1% N-lauroylsarcosine (15 min, room temperature), 2× SSC/0.1% N-lauroylsarcosine (15 min, 50°C, 1× SSC/0.1% N-lauroylsarcosine (5 min, room temperature), 0.5× SSC/0.1% N-lauroylsarcosine (5 min, room temperature,), 0.2× SSC/0.1% N-lauroylsarcosine (20 min, room temperature) and 0.2× SSC/0.1% N-lauroylsarcosine (20 min, 50°C).

Hybridization signals were visualized by alkaline-phosphatase immunohistochemistry. The sections were rinsed twice in 0.1% Tween 20 in Tris-HCl buffered saline (TBS; 0.1 M Tris-HCl, pH 7.4 and 0.1 M NaCl), incubated in the blocking buffer (1% blocking reagent, 3% normal sheep serum and 2mM levamisole in TBS) for at least 60 min, and then incubated in anti-digoxigenin Fab-fragments conjugated with alkaline phosphatase (Roche Diagnostics) diluted (1:500) in the blocking buffer for 2 hr. After extensive wash in TBS, the sections were preincubated in TBS (pH 9.5) containing 0.1% Tween 20, 5 mM $MgCl_2$ and 2 mM levamisole followed by incubation in the color

development solution (0.033% nitroblue tetrazolium, 0.017% 5-bromo-4-chloro-3-indolyl phosphate, 5 mM MgCl2 , 4 mM levamisole in TBS, pH 9.5) for 24 hours in the dark.

For quantification, tissues from nine monkeys at three different ages were processed simultaneously.

Quantification.

The relative amount of mRNA in each cortical layer was quantified by taking optical density meanings of the digitized image. Images were obtained using a digital camera (DP11; Olympus, Tokyo, Japan) with a microscope (BX50; Olmpus). Optical density readings were taken in each layer of 200 μm width in the sections hybridized with the *occ1* antisense probe using NIH image software. Background readings were taken from the neighboring sections stained with the *occ1* sense probe. The signal intensity (SI) of a given cortical layer was determined as the optical density of the layer expressed as a percentage of the optical density of the background staining as Meberg and Routtenberg's

presented (Meberg and Routtenberg, 1991). Twelve areas (four areas from each of three sections) in each layer were measured for each animal. The significance of difference was examined using the two-tailed Student's *t* test.

All the experiments described here were performed in compliance with the guidelines for animal experiments at Okazaki National Research Institute.

Results

I examined the *occ1* mRNA expression in the primary visual cortex (area 17) of newborn monkeys (postnatal day(s) 1, 1 and 2), 3-month old monkeys (postnatal days 92, 96 and 97) and adult monkeys weighing 3.0 kg-9.2 kg by *in situ* hybridization. To confirm the changes in the *occ1* mRNA level and the distribution in the cortical layers, I quantified the relative mRNA level in the cortical layers by taking optical density meanings of the digitized images of the sections processed by *in situ* hybridization.

occ1 mRNA expression patterns in area 17 of newborn monkey.

In situ hybridization showed that *occ1* is expressed in area 17 of newborn monkey at a certain level with a characteristic laminar pattern (Fig. II-1 a). Many neurons hybridized with antisense *occ1* cRNA probe with moderate intensity were found in layers IVCα and IVCβ. Layers II and III contained many rather moderately labeled neurons. In layer IVB, some relatively moderately-labeled neurons were present. In layers V and VI, a few moderately stained neurons

were sparsely present, and very light signals were observed throughout the layers. The positive signals in layer I were lightly stained and sparsely present.

***occ1* mRNA expression patterns in area 17 of 3-month old monkey.**

The pattern of *occ1* expression in 3-month old monkey appeared basically similar to that observed in newborn monkeys, while some changes in laminar pattern were observed (Fig. II-1c). Many moderate signals were observed in layers IVCα and IVCβ. Some rather intensely-labeled neurons were also scattered in layers IVCα and IVCβ. In layers II, III and IVA, I observed moderately labeled neurons. In layer IVB, rather moderate hybridization signals were distributed with relatively low density . Layers V and VI contained a few relatively moderately-stained cells. Very light signals which were equivalent to those I observed throughout layers V and VI of newborn monkeys were even weaker. In layer I, only a few very lightly-labeled neurons were observed.

occ1 mRNA expression patterns in area 17 of adult monkey.

occ1 is expressed in a pattern different from that in newborn or 3-month old monkey (Fig. II-1e). The major difference was found in the striking dense signals of layer IVC. _occ1_ hybridization signals were most preferentially localized in layers IVCα and IVCβ, in which signals were very dense and intense. Many intensely labeled neurons were found in layers II, III and IVA . In layer IVB, relatively intense signals were observed. Moderate _occ1_ hybridization signals were present throughout the upper half of layer V. In layer VI and the deeper half of layer V, a few moderately stained neurons were rather sparsely found. Very light signals which I observed in layers V and VI of newborn monkeys were not observed. The positive neurons in layer I were light and sparse.

Change of level of _occ1_ mRNA in area 17 during development.

To clarify the change in the level of _occ1_ mRNA, I measured the optical densities of the sections hybridized with the _occ1_ riboprobes. I then introduced the signal intensity (SI) defined by Meberg and Routtenberg (Meberg and Routtenberg,

1991) to analyze the differences in the intensities of hybridization signals in layers II-IVCβ of area 17 at newborn, 3-month old and adult stages (Fig. II-2). For quantification, tissues from nine monkeys at three different stages were processed simultaneously with the same condition of hybridization. The calculated standard deviation (SD) of the average of SI in each layer at each stage was generally less than 10% of the value of each average, ranging from 5.8% to 12.1% (Fig. II-2). I then judged that the SIs were enough reliable to analyze the differences of the signal intensities at the stages examined, and the difference in the value of SI reflect that of the amount of the expressed *occ1* mRNA . The SIs in layers IVCα and IVCβ in 3-month old monkeys were significantly higher than those at newborn stage (Fig. II-2 double asterisks, $P<0.01$). The SIs in the other layers in 3-month old monkeys appeared to change slightly comparing to those in the same layers in newborn monkeys, although the differences in the levels did not reach statistical significance.

I observed the marked increase in the intensity of the *occ1* hybridization signals in adult monkeys comparing to the signals detected in newborn or 3-

month old monkey. The SIs in layers III-IVCβ were significantly higher than those in the same layers at early developmental stages (Fig. II-2 asterisks, $P<0.01$). The intensity in layer II was slightly higher than that in newborn or 3-month old monkey, while the level was significantly higher only than that in 3-month old monkey ($P=0.025$; between newborn and adult monkeys, $P=0.222$).

Change of laminar pattern of *occ1* expression during development.

To clarify the difference in the laminar expression pattern of *occ1* at the stages examined, I employed the SI ratio. The SI ratio of a given cortical layer was determined as the SI of each layer divided by the SI of layer IVCβ. Thus, I can gain the relative intensity of each layer to that of layer IVCβ at each stage (Fig. II-3). Comparing the ratios between the stages examined, I can know the difference in the laminar patterns. In newborn monkeys, the SI ratios were relatively similar, ranging from 0.881 (IVB/IVCβ) to 0.960 (II/IVCβ). In 3-month old monkey, the SI ratios of layers II, III, IVA and IVB were significantly lower than those in newborn monkeys (Fig. II-3 double asterisks, $P<0.01$). In adult, the

ratios in all the layers examined were even lower than those in 3-month old or newborn monkeys (Fig. II-3 asterisks, $P<0.01$). These data suggest that the levels of the expressed *occ1* mRNA at layers II-IVCβ are rather similar at the newborn stage, and the levels in these layers increase gradually as development proceeds while the increase in layer IVCβ is the largest.

Differential pattern of *occ1* expression in areas 17 and 18 in newborn, 3-month old and adult monkeys.

As shown in Part I or Fig. II-4e, area 17 in adult monkeys displayed a characteristic pattern of *occ1* mRNA expression that allowed for its well-defined discrimination from the adjacent area 18. The intense signals were observed in layers II, III, IVA and IVC of area 17, while intensely stained neurons with large somata were observed in the lower one third of layer III in area 18. I examined the patterns of *occ1* mRNA expression in area 18 in newborn and 3-month old monkeys (Fig. II-4). The signal intensity throughout the layers in area 18 of newborn or 3-month old monkey was much lower than that in area 17, which

allowed us to define the border between the areas easily at these stages (Fig. II-4a and c).

In area 18 of newborn monkeys, a few moderately labeled neurons were found in layer III, V and VI (Fig. II-4a). Some rather moderately-labeled neurons were present in layer II. Many light signals were observed in layer IV. Light signals were sparsely distributed in layer I.

In area 18 of 3-month old monkeys, the signals throughout the layers appeared to be slightly weaker than those observed in newborn monkeys (Fig. II-4c). Some moderate signals were observed in layers II and the lower one third of layer III. The upper two thirds of layer III exhibited many light signals. A few rather moderate signals were present in layer IV, V and VI. The signals in layer I were sparse and light.

These data showed that the difference in the relative amount and laminar pattern of *occ1* expression between areas 17 and 18 allow for clear definition of the cortical field both in newborn and 3-month old monkeys. Furthermore, these data also suggest that the changes in laminar expression pattern of *occ1* during

postnatal development occur in area 18, and the expression level changes in area 18 as the neocortical development proceeds.

Discussion

I examined the change in *occ1* mRNA expression pattern and the relative amount of *occ1* expression during postnatal development of the macaque. The measurements of signal intensity suggested that *occ1* mRNA increases in its level during the first three postnatal months. In the later development, *occ1* expression further increases and gets the highest level at adult.

Change in the laminar pattern of *occ1* expression in area 17 during postnatal development.

The sections hybridized with *occ1* cRNA probe showed differential laminar pattern of *occ1* mRNA expression at the stages examined. As shown in Fig. II-2, the signal intensities in all the layers examined except for layer II in adult monkeys are significantly higher than those at the earlier developmental stages, which suggests that the *occ1* mRNA level increases during postnatal development. The change of signal intensity in layer IVCβ during postnatal development was the most marked among the changes. The ratio of signal

intensity in each layer to that in layer IVCβ examined in Fig. II-3 confirmed that the increase of *occ1* expression during development is the largest in layer IVCβ, which is reflected by the SI ratio much smaller than 1.0 in each layer at adult while the ratios are relatively close to 1.0 in all layers examined at newborn. The difference in the level of increase in *occ1* mRNA expression in each layers appeared to result in the differences in the laminar pattern of *in situ* hybridization at the stages examined. Then, how does the differential increase happen during development in *occ1* mRNA level in each layer? As presented in Part I, I applied *in situ* hybridization to the monocularly-deprived animals. I observed that apparent decrease in *occ1* mRNA expression occurred only in layers III, IVA, IVB, IVCα, IVCβ and V. Furthermore, the extent of decrease is different in each layer such as 57% and 74% in layer III and layer IVCβ, respectively. These observations suggest that the extent of dependence of *occ1* expression on neuronal activity is different in each layer at adult. The change in layer IVCβ by monocular deprivation was the largest, which indicates that the extent of the dependency of *occ1* mRNA expression on neuronal activity is the largest in the

layer. To answer the question presented above, being hypothesized that the increase in *occ1* expression during postnatal development would be mainly due to increase in neuronal activity in area 17, the differential increase in each layer is conceivable. In other words, *occ1* expression during postnatal development increases mostly in an activity-dependent manner, and the increase during development is the largest in layer IVCβ, therefore the extent of activity-dependent expression of *occ1* becomes the largest in layer IVCβ at adult. There is another fact supporting this hypothesis. The SI in layer II are almost constant throughout development (Fig. II-2). On the other hand, in monocularly-deprived adult animals, almost no apparent change was observed in layer II, which implied that the extent of dependence of *occ1* expression on neuronal activity is little in layer II. Provided that the increase of *occ1* expression during development is dependent on activity, it can make sense that there was little increase of *occ1* expression in layer II. From these, I should suggest that the increase in *occ1* expression is principally due to increase in neuronal activity in area 17 during postnatal development, which resulted in the differential increase

of *occ1* expression in each layer during development.

Temporal correlation between change in *occ1* mRNA level and postnatal development.

In primates, among the developmental events of the visual cortex, the ocular dominance plasticity and synaptogenesis are well examined. Visual deprivation during early postnatal life causes shrinkage in the ocular dominance column serving the deprived eye and expansion in the column serving the other normal eye in area 17. The shrinkage and expansion of the ocular dominance columns by retraction and sprouting of their geniculocortical terminal arbors occur only for the early period in postnatal development, which is called 'critical period'. In monkeys, this plasticity of ocular dominance columns peaks at the first postnatal week and halts at latest by postnatal 3 months (Horton and Hocking, 1997). On the other hand, synaptic density in area 17 increase during the last 2 months of gestation and the first postnatal months, get the highest level at postnatal 4 months and gradually decrease (Lund et al., 1977; Rakic et al., 1986).

The results of signal intensity measurements shown in Fig. II-2 suggested that the expression of *occ1* mRNA in area 17 increases gradually during the postnatal development, and its level becomes the highest at adult. The increase of *occ1* expression does not show such a clear periodical correlation with the postnatal developments described above as the peak of expression is timed with the events and the expression declines later. But it is certain that the level increases during postnatal development, especially during the postnatal developmental events. And, as discussed in the previous section, the increase of *occ1* expression during postnatal development is thought to be basically dependent on the increase of neuronal activity in area 17. Regarding the involvement of neurotorofic factors in activity-dependent plasticity or synaptogenesis, the expression and the retrograde release of neurotrophic factors stimulated by neuronal activity lead to selective strengthening of specific active synapses and circuits (Lo, 1995; Wang et al., 1995). The results suggest that *occ1* expression is stimulated by neuronal activity in area 17 during the developmental events. Therefore, I should present the possibility that *occ1* is

involved in the postnatal development of visual cortex.

The data presented in Fig. II-4 showed that *occ1* is preferentially expressed in area 17 of newborn and 3-month old monkeys. These data show that *occ1* can be used as a molecular marker to reveal a specific neuronal subset in neocortex in newborn and 3-month old monkeys as it can be in adult neocortex. Furthermore, the data support the possibility that *occ1* plays a role in the development of the visual cortex because it shows *occ1* is preferentially expressed in area 17 while the developmental events occur in area 17.

However, many important questions remain to be answered. How and where is the product released? Is the product is released in an activity-dependent manner? If so, from what subcellular region is the product released? Furthermore, most importantly, does the product have the effect on the efficacy of neuronal synapse or neuronal morphologies? It is necessary to answer each questions utilizing appropriate biological systems.

References

Acebes A, Ferrus A (2000) Cellular and molecular features of axon collaterals and dendrites [In Process Citation]. Trends Neurosci 23:557-565.

Antonini A, Stryker MP (1993) Rapid remodeling of axonal arbors in the visual cortex. Science 260:1819-1821.

Berardi N, Pizzorusso T, Maffei L (2000) Critical periods during sensory development. Curr Opin Neurobiol 10:138-145.

Bonhoeffer T (1996) Neurotrophins and activity-dependent development of the neocortex. Curr Opin Neurobiol 6:119-126.

Castren E, Zafra F, Thoenen H, Lindholm D (1992) Light regulates expression of brain-derived neurotrophic factor mRNA in rat visual cortex. Proc Natl Acad Sci U S A 89:9444-9448.

Goodman LJ, Valverde J, Lim F, Geschwind MD, Federoff HJ, Geller AI, Hefti F (1996) Regulated release and polarized localization of brain-derived neurotrophic factor in hippocampal neurons. Mol Cell Neurosci 7:222-238.

Hayashi M (1992) Ontogeny of some neuropeptides in the primate brain. Prog

Neurobiol 38:231-260.

Heymach JV, Jr., Kruttgen A, Suter U, Shooter EM (1996) The regulated secretion and vectorial targeting of neurotrophins in neuroendocrine and epithelial cells. J Biol Chem 271:25430-25437.

Horton JC, Hocking DR (1996) An adult-like pattern of ocular dominance columns in striate cortex of newborn monkeys prior to visual experience. J Neurosci 16:1791-1807.

Horton JC, Hocking DR (1997) Timing of the critical period for plasticity of ocular dominance columns in macaque striate cortex. J Neurosci 17:3684-3709.

Isackson PJ, Huntsman MM, Murray KD, Gall CM (1991) BDNF mRNA expression is increased in adult rat forebrain after limbic seizures: temporal patterns of induction distinct from NGF. Neuron 6:937-948.

LeVay S, Wiesel TN, Hubel DH (1980) The development of ocular dominance columns in normal and visually deprived monkeys. J Comp Neurol 191:1-51.

Lo DC (1995) Neurotrophic factors and synaptic plasticity. Neuron 15:979-981.

Lund JS, Boothe RG, Lund RD (1977) Development of neurons in the visual cortex (area 17) of the monkey (Macaca nemestrina): a Golgi study from fetal day 127 to postnatal maturity. J Comp Neurol 176:149-188.

Marty S, Berzaghi Mda P, Berninger B (1997) Neurotrophins and activity-dependent plasticity of cortical interneurons. Trends Neurosci 20:198-202.

Meberg PJ, Routtenberg A (1991) Selective expression of protein F1/(GAP-43) mRNA in pyramidal but not granule cells of the hippocampus. Neuroscience 45:721-733.

Oppenheim RW (1985) Naturally occuring cell death during neural development. Trends Neurosci 8:487-493.

Rakic P (1977) Prenatal development of the visual system in rhesus monkey. Philos Trans R Soc Lond B Biol Sci 278:245-260.

Rakic P, Bourgeois JP, Eckenhoff MF, Zecevic N, Goldman-Rakic PS (1986) Concurrent overproduction of synapses in diverse regions of the primate cerebral cortex. Science 232:232-235.

Shatz CJ, Stryker MP (1978) Ocular dominance in layer IV of the cat's visual

cortex and the effects of monocular deprivation. J Physiol (Lond) 281:267-283.

Thoenen H (1995) Neurotrophins and neuronal plasticity. Science 270:593-598.

Wang T, Xie K, Lu B (1995) Neurotrophins promote maturation of developing neuromuscular synapses. J Neurosci 15:4796-4805.

Figure legends

Fig. II-1. Laminar distribution of *occ1* mRNA-expressing neurons in area 17 in newborn (a and b), 3 month-old (c and d) and adult (e and f) monkeys. Sections through area 17, stained for *occ1* (a, c and e) and with thionin (b, d and f). The laminar expression pattern was observed to change slightly as the development proceeds. Bar, 200 μm.

Fig. II-2. Histograms of signal intensity (SI) of *occ1 in situ* hybridization in layer II-IVCβ at three different developmental stages. Means ± Standard Deviations are shown. NB, new born; 3M, 3 month-old; AD, adult. The SIs in layers III-IVCβ in adult monkeys are higher than in new born monkeys (*, $P<0.01$; Student't t test), and the intensities in layers IVCα and IVCβ in 3 month-monkey are higher than those in newborn monkey (**, $P<0.01$).

Fig. II-3. Histograms of the ratio of SI in each layer to SI in layer IVCβ at each developmental stage. Means ± Standard Deviations. NB, new born; 3M, 3

month-old; AD, adult. Asterisks (*) and double asteriskes (**) denote the significant differences from 3 month-old and adult and from newborn and adult monkeys, respectively ($P<0.01$; Student's *t* test).

Fig. II-4. Staining patterns at the boundary between areas 17 and 18 in newborn (a and b), 3 month-old (c and d) and adult (e and f) monkeys. Sections were stained for *occ1* (a, c and e) and with thionin (b, d and f). Contrasting patterns in areas 17 and 18 were observed at all the stages examined. Arrows indicate the boundaries between areas 17 and 18. Bar, 200 μm.

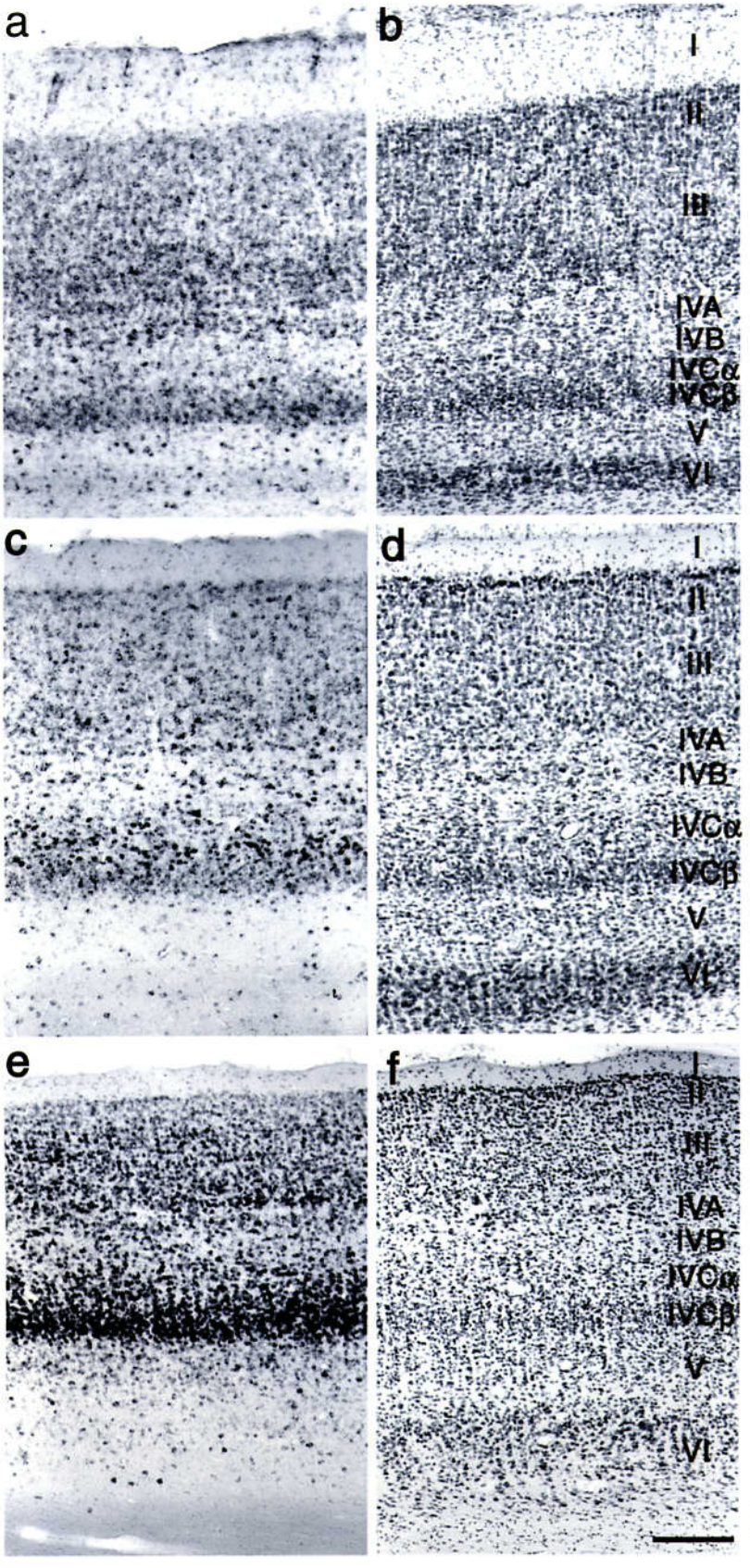
a
b
I
II
III
IVA
IVB
IVCα
IVCβ
V
VI
c
d
I
II
III
IVA
IVB
IVCα
IVCβ
V
VI
e
f
I
II
III
IVA
IVB
IVCα
IVCβ
V
VI

Fig. II-1

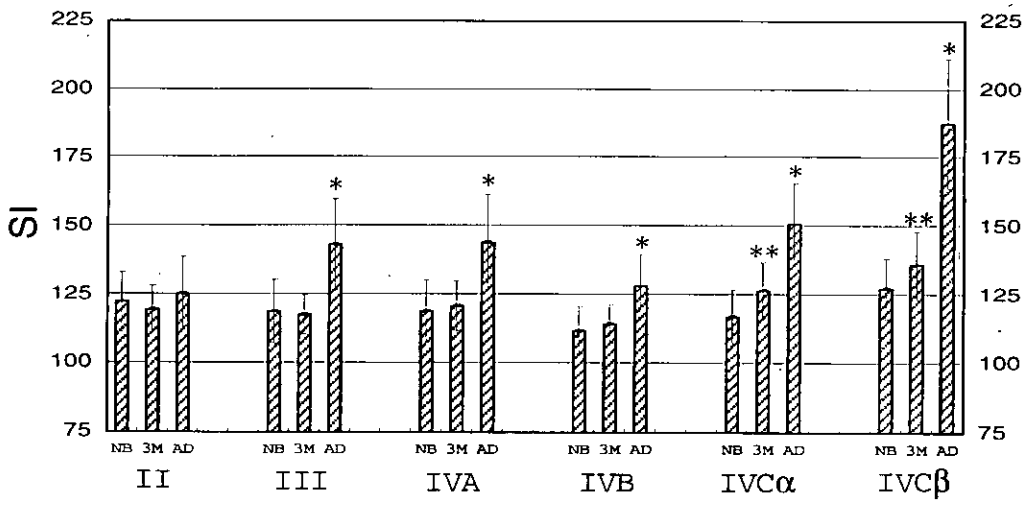

Fig. II-2

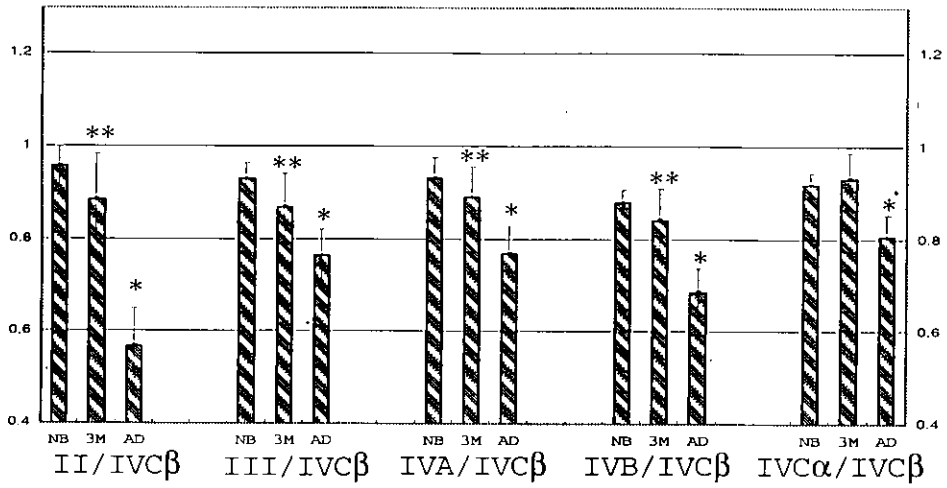
1.2
1
0.8
0.6
0.4
NB 3M AD
II/IVCβ
III/IVCβ
IVA/IVCβ
IVB/IVCβ
IVCα/IVCβ

Fig. II-3

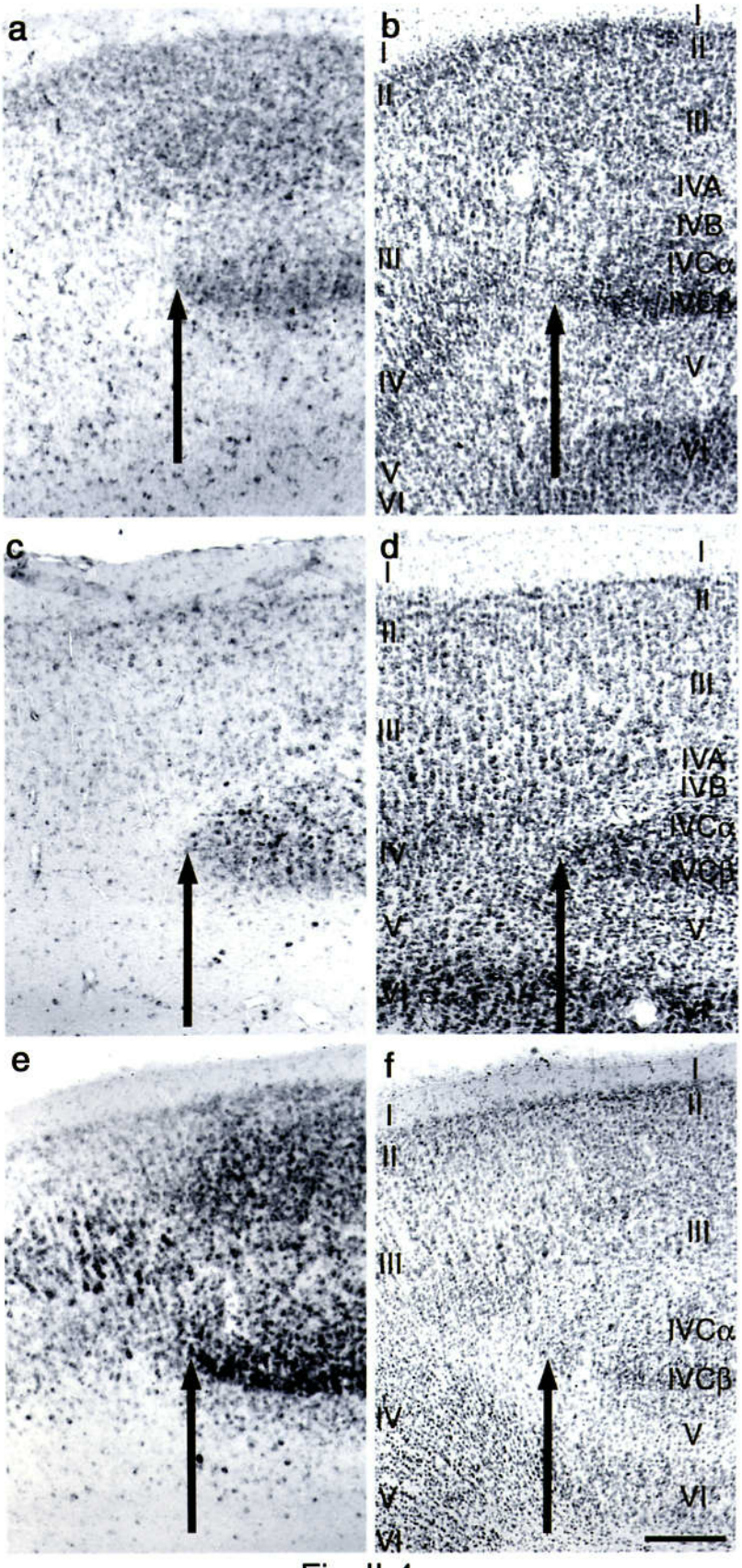

Fig. II-4

General discussion and conclusion

In part I, the identification of the gene, *occ1*, was described. I applied differential display to compare mRNAs expressed in the distinct neocortical areas in macaque neocortex and found that *occ1* was preferentially expressed in the occipital cortex. Further histological analysis showed that *occ1* is selectively expressed in area 17. Although I have already known some molecules which show regional localization in the mammalian neocortex, none of them shows such a spatial pattern strikingly related to the known cytoarchitectonic borders as that of *occ1*. It is surprising that there is a regulation of gene expression which spatially correlates with a specific functional area within neocortex. The further histochemical analysis revealed the other aspect of *occ1* expression in area 17 that *occ1* is expressed in various types of neurons in an activity-dependent manner. This feature, at least, makes *occ1* as an good indicator of neuronal activity in visual cortex because the change of *occ1* expression due to molecular deprivation was prominent among the conventional histochemical markers such as cytochrome oxidase and zif268. Moreover, many molecules have been

reported to be expressed in an activity-dependent manner, but none of them shows such a characteristic regional expression pattern in the neocortex as that of *occ1*. Activity-dependent gene expression, resulting in changes in neuronal phenotypes, plays an important role in neuronal plasticity of brain function and development. So, *occ1* is all the more outstanding in this feature of expression. Furthermore, it was shown that *occ1* labels specific types of neurons in the areas other than neocortex such as LGN and hippocampus. These results show that *occ1* will be useful as the markers not only for neurons in area 17, but for specific subsets of neurons in the other regions of the brain.

In part II, it was shown that the level of *occ1* mRNA is increased during postnatal development. The laminar pattern of *occ1* mRNA expression changes as the development proceeds. As discussed in Part II, these data suggest that *occ1* might be involved in the events of the development of visual cortex. It is necessary to further examine the effects of *occ1* in the developmental events by overproduction or disruption of the product. To examine the function of *occ1* in development will provide an information which would help us to answer the

essential question about the *occ1* localization in adult neocortex, 'how does the region-selective expression of *occ1* in neocortex contribute to the function of neocortex?' If the function of *occ1* had been clarified, an insight into the functional organization of neocortex would be obtained.

To conclude the present thesis, I would like to mention that the first systematic survey for marker molecules in the neocortex could give a successful example of such an approach. I should like to also emphasize that the further investigation on the function of *occ1* will provide a clue to understanding how the neocortex is organized in relation to function.

Publication

Tochitani, S., Liang, F., Watakabe, A., Hashikawa, T. and Yamamori, T. (2001). The *occ1* gene is preferentially expressed in the primary visual cortex in an activity-dependent manner: a pattern of gene expression related to the cytoarchitectonic area in adult macaque neocortex. European Journal of Neuroscience 13, 297-307.

Abstracts

Tochitani, S., Liang, F., Watakabe, A., Hashikawa, T. and Yamamori, T. (2000). *occ1* is transcribed preferentially in the macaque primary visual cortex in visually driven activity-dependent manner. Neuroscience Research Supplement 24, S23.

Tochitani, S., Liang, F., Watakabe, A., Hashikawa, T. and Yamamori, T. (2000). The unique neuronal organization of the primary visual cortex, revealed by *occ1* mRNA activity-dependent expression. Society for Neuroscience Abstracts 26, 1614.

Tochitani, S., Watakabe, A., Liang, F., Hashikawa, T. and Yamamori, T. (1999). A molecular marker for a neuronal population dominantly distributed in the macaque occipital neocortex. Society for Neuroscience Abstracts 25, 2190.

Tochitani, S., Watakabe, S., Liang, F., Shionoya, K., Hashikawa T. and Yamamori, T. (1999). A molecular marker for a neuronal population distributed preferentially in the macaque occipital neocortex. Neuroscience Research Supplement 23, S129.

Offprint from

European Journal of Neuroscience

Volume 13 Number 2
February 2001 pages 297–307

The *occ1* gene is preferentially expressed in the primary visual cortex in an activity-dependent manner: a pattern of gene expression related to the cytoarchitectonic area in adult macaque neocortex

Shiro Tochitani, Fengyi Liang, Akiya Watakabe,
Tsutomu Hashikawa and Tetsuo Yamamori

b
Blackwell
Science

European Journal of Neuroscience, Vol. 13, pp. 297–307, 2001

The *occ1* gene is preferentially expressed in the primary visual cortex in an activity-dependent manner: a pattern of gene expression related to the cytoarchitectonic area in adult macaque neocortex

Shiro Tochitani[1,2], Fengyi Liang[3], Akiya Watakabe[1,2], Tsutomu Hashikawa[3] and Tetsuo Yamamori[1,2]
[1]Division of Speciation Mechanisms I, National Institute for Basic Biology, Aichi 444–8585, Japan
[2]Department of Molecular Biomechanics, The Graduate University for Advanced Studies, Aichi 444–8585, Japan
[3]Laboratory for Neural Architecture, Brain Science Institute, RIKEN, Saitama 351–0198, Japan

Keywords: differential display, *occ1* (TSC-36/ FRP), ocular dominance column, region-selective expression, visual deprivation

Abstract

Marker molecules to visualize specific subsets of neurons are useful for studying the functional organization of the neocortex. One approach to identify such molecular markers is to examine the differences in molecular properties among morphologically and physiologically distinct neuronal cell types. We used differential display to compare mRNA expression in the anatomically and functionally distinct areas of the adult macaque neocortex. We found that a gene, designated *occ1*, was preferentially transcribed in the posterior region of the neocortex, especially in area 17. Complete sequence analysis revealed that *occ1* encodes a macaque homolog of a secretable protein, TSC-36/follistatin-related protein (FRP). *In situ* hybridization histochemistry confirmed the characteristic neocortical expression pattern of *occ1* and showed that *occ1* transcription is high in layers II, III, IVA and IVC of area 17. In addition, *occ1* transcription was observed selectively in cells of the magnocellular layers in the lateral geniculate nucleus (LGN). Dual labeling immunohistochemistry showed that the *occ1*-positive neurons in area 17 include both γ-aminobutyric acid (GABA)-positive aspiny inhibitory cells and the α-subunit of type II calcium/calmodulin-dependent protein kinase (CaMKII α)-positive spiny excitatory cells. With brief periods of monocular deprivation, the *occ1* mRNA level decreased markedly in deprived ocular dominance columns of area 17. From this we conclude that the expression of *occ1* mRNA is present in a subset of neurons that are preferentially localized in particular laminae of area 17 and consist of various morphological and physiological neuronal types, and, furthermore, *occ1* transcription is subject to visually driven activity-dependent regulation.

Introduction

The distribution of specific molecules shows a striking correlation with particular physiological organizations in the primate visual system. The Cat-301 antibody, which recognizes a chondroitin sulfate proteoglycan (Hockfield *et al.*, 1990; Zaremba *et al.*, 1989) primarily stains the magnocellular layers (layers 1–2) of the lateral geniculate nucleus (LGN; Hendry *et al.*, 1984). Immunostaining for calcium/calmodulin-dependent protein kinase II α-subunit (CaMKII α) in combination with neuronal tracing techniques revealed that the koniocellular layers (intercalated layers) in macaque LGN send direct afferent inputs to area 17 (Hendry & Yoshioka, 1994). Although the functional modules of the neocortex are even more complicated than those of the thalamic nuclei, some molecules coincide spatially with the fundamental functional subdivisions of the neocortex, such as layers, columns and areas. Cytochrome oxidase (CO) is enriched in the blobs in layers II and III of the primary visual cortex (area 17) (Wong-Riley, 1979; Horton & Hubel, 1981) and in the stripe-shaped structures in the secondary visual cortex (area 18) (Livingstone & Hubel, 1982, 1983; Horton, 1984). Synaptic zinc is enriched in CO-deficient interblob regions (Dyck & Cynader, 1993). The pattern of m2 muscarinic acetylcholine receptor immunoreactivity is also reciprocal to the pattern of CO histochemical staining in layers II and III, the strongest immunoreactivity being observed in layers IVA and IVCβ of area 17 where projections from the parvocellular layers (layers 3–6) of the LGN terminate selectively (Mrzljak *et al.*, 1996). Regional variations in higher visual areas exist in terms of density and laminar distribution of neurons marked by SMI-32, a monoclonal antibody against the medium and high molecular weight subunits of neurofilament protein (Hof & Morrison, 1995). The antigen recognized by Cat-301 is expressed more abundantly in the areas of the dorsal stream than in those of the ventral stream of the visual processing pathway (Hendry *et al.*, 1988b).

These studies provide impressive examples of molecular bundles of the nervous system, although the number of available molecular markers is still limited. It is expected that as more molecular markers that allow visualization of specific neuronal subsets in the neocortex are obtained, more information on how the neocortex is organized in relation to function will be gained. New histochemical markers could allow us to recognize new populations of neurons and/or new functional subdivisions of the neocortex. In addition, it should be

Correspondence: Dr T. Yamamori, as above.
E-mail: yamamori@nibb.ac.jp

Received 17 August 2000, revised 27 October 2000, accepted 3 November 2000

noted that most of the known markers and the neurons marked by them have been discovered by chance. This implies that an extensive and systematic approach to identify such molecular markers for determining specific neuronal subsets would be more fruitful (Hendry & Calkins, 1998).

We applied differential display (DD; Liang & Pardee, 1992) to compare mRNA expression in structurally and functionally distinct areas of the adult macaque neocortex. We cloned a cDNA named *occ1*, which showed a high transcription level in the occipital cortex. In this report, we describe the identification of *occ1* and the characterization of the neurons specified by *occ1* expression.

FIG. 1. Differential display and RT-PCR analysis of *occ1* expression in the five neocortical regions. (a) Total RNAs from five areas of cynomolgus monkey neocortex were compared by differential display. A cDNA fragment, named *occ1*, was differentially detected (arrow; 190 bp). Lane 1, area FDΔ; lane 2, area FA; lane 3, area TE; lane 4, area OA; lane 5, area OC. (b) RT-PCR confirmation of differential transcription of *occ1* in the five neocortical areas. cDNAs or RT-s from area FDΔ (lane 1), area FA (lane 2), area TE (lane 3), area OA (lane 4) and area OC (lane 5) were used. *occ1* is transcribed at a high level selectively in area OC. PCR using serial dilutions (1/2–1/16) of cDNA from area OC shows the cycles employed (20 cycles for both primers) were within the range in which amplification occurred linearly. RT-PCR for glyceraldehyde-3-phosphate dehydrogenase (*g3pdh*), which is expressed ubiquitously in various tissues and cells, was used as a control reaction to show the quantity and quality of the cDNAs applied.

Materials and methods

Tissue dissection, total RNA extraction and DD polymerase chain reaction

The brains of three adult macaques (*Macaca fascicularis*) were removed under deep Nembutal anesthesia at the Japan Poliomyelitis Research Institute. The brains were dissected and frozen on dry ice. Total RNA was obtained by a single-step RNA isolation method by guanidine thiocyanate–urea–phenol–chloroform extraction (Chomczynski & Sacchi, 1987). The DD polymerase chain reaction (PCR) was performed following the protocol of the RNA Image kit (GeneHunter, Nashville, TN, USA) with minor modifications. The reverse transcription (RT) reaction was carried out using an anchor oligo-dT primer, followed by arbitrarily primed PCR with the 5′-end-^{33}P-labelled anchor oligo-dT primer and an arbitrary 13-mer primer by KlenTaq polymerase (Clontech Laboratories, Palo Alto, CA, USA). The PCR parameters were 1 cycle at 94 °C (5 min), 40 °C (5 min) and 68 °C (5 min), 6 cycles at 94 °C (2 min), 40 °C (5 min) and 68 °C (5 min), and 33 cycles at 94 °C (1 min), 40 °C (2 min) and 68 °C (1 min), followed by the final elongation step at 72 °C for 20 min. The PCR products were then separated by electrophoresis on 4% polyacrylamide sequencing gels. The bands that showed differential expressions among the areas were reamplified by PCR using the same primer set used to generate them. The PCR parameters for reamplification were 95 °C for 5 min, 30 cycles at 95 °C (1 min), 40 °C (1 min) and 68 °C (1 min), and finally 5 min at 72 °C.

RT–PCR analysis

Total RNAs (2.0 μg) from five regions (areas FDΔ, FA, TE, OA and OC; see Fig. 4) of *Macaca fascicularis* neocortex were reverse-transcribed using Superscript II reverse transcriptase (Life Technologies, Rockville, MD, USA) with Oligo $(dT)_{12-18}$ primer (Life Technologies) in a final reaction volume of 40 μL. Simultaneously, the samples subject to the same preparations without reverse transcriptase were prepared and used as negative control samples (RT-) to show the absence of contaminated genomic DNA in the total RNAs. PCR was performed using a primer set corresponding to the end sequences of the cloned *occ1* DD band (5′-GGAAGA-GATTTAATCTTACAAAAGG-3′ and 5′-TATACAGTCAAAGAG-GTTGCAACAG-3′). PCR conditions were 95 °C for 5 min, 20 cycles of 94 °C (30 s), 60 °C (30 s) and 72 °C (30 s), and finally at 72 °C for 5 min. After separation on a 1.0% agarose gel, the products were blotted and detected by hybridization to the ^{32}P-labeled *occ1* probe. RT-PCR for glyceraldehyde-3-phosphate dehydrogenase (g3pdh) was performed with primers 5′-AGCGAGATCCCTCCA-AAATCAAGTG-3′ and 5′-GCCATGCCAGTGAGCTTCCCGT-TCA-3′ as an internal control.

Northern blot analysis

Poly $(A)^+$ RNA (12 μg) was purified from the total RNA from neocortical area OC, electrophoresed on a 1.2% agarose gel and transferred to Hybond N^+ nylon membrane (Amersham Pharmacia Biotech, Buckinghamshire, UK). The hybridization probe was prepared from an *occ1* cDNA clone (1024 bp + poly $(A)^+$ tail), firstly obtained by screening a cDNA library, and radiolabeled with [^{32}P]dCTP.

Construction of cDNA library and isolation of occ1 *full-length clone*

Using poly $(A)^+$ mRNA from *Macaca fascicularis* neocortical area OC, cDNAs were synthesized with ZAP-cDNA synthesis kit (Stratagene, La Jolla, CA, USA) and ligated to *Eco*RI/*Xho*I-digested λ ZAPII vector (Stratagene), followed by packaging with Gigapack III Gold packaging extract (Stratagene). The nucleotide sequences determined on both strands are in the DDBJ/EMBL/GenBank nucleotide sequence databases with the accession number AB039661.

Generation of antiserum against OCC1

Rabbit OCC1 antisera were raised against a fusion protein. OCC1–glutathione-S-transferase (OCC1–GST) (amino acids 87–308 of OCC1 fused to GST) was constructed by subcloning this segment of the *occ1* cDNA into pGEX 2TK (Amersham Pharmacia Biotech) and expressed in *Escherichia coli* (*E. coli*) *BL21*. For the production of antiserum, three New Zealand white rabbits were immunized and the antisera passed through Affigel 15 affinity resin (Bio-Rad Laboratories, Hercules, CA, USA) coupled with the crude lysates of *E. coli BL21* transfected with mock pGEX2TK vector to exclude the antibodies against GST and bacterial proteins.

Construction of expression vector, transient expression of OCC1 in COS-7 cells and Western blot analysis

The expression plasmid, pOCC1, was constructed as follows: the complete sequence of the *occ1* cDNA was amplified by PCR using a 5'-primer (5'-CCGCTCCAGATGTGGAAACGCTGGCTCGCG-CTC-3') which introduced an *Xho*I cleavage site at the N-terminus and a 3'-primer (5'-AAACTGCAGTCATTAGATCTCTTTGGT-GCTCAC-3') introducing a *Pst*I cleavage site and two consecutive stop codons at the C terminus of the *occ1* cDNA. The *Xho*I/*Pst*I fragment of the PCR product was cloned into the CMV-promoter driven pEGFP-N1 (Clontech Laboratories). COS-7 cells were transiently transfected with pOCC1 using Lipofectamine Plus (Life Technologies) and cultured in DMEM/10% fetal calf serum (FCS). Two days after transfection, the cells were washed with DMEM/1% FCS and cultured for another day. Aliquots of cell lysates and conditioned medium were subjected to electrophoresis on 15% SDS-polyacrylamide gels and transferred to Immobilon P transfer membrane (Millipore, Bedford, MA, USA) using standard protocols. After blocking, the blot was incubated with anti-OCC1 antiserum (1 : 800). The blots were then immunoreacted with goat anti-rabbit antibody coupled to peroxidase (Organon Teknika, Durham, NC, USA; 1 : 2000) and the immunoreactivity was detected using an ECL detection kit (Amersham Pharmacia Biotech). The blotting performed with the antiserum that had been preabsorbed with 20 μg/mL OCC1–GST fusion protein did not display any band (data not shown).

Tissue preparation for in situ *hybridization and immunohistochemistry*

Ten adult macaques (three *Macaca fascicularis* and seven *Macaca fuscata*) weighing 2.9–9.1 kg were used. In five, tetrodotoxin (TTX; 15 μg in 10 μL of normal saline) was injected under ketamine anesthesia into the vitreous cavity of the left eye twice a week for a total of 7, 10, 14 (two monkeys) or 21 days prior to the animals being killed. Retinal activity in the injected eye was suppressed for at least 5 days following a single injection of this dose of TTX (Hendry *et al.*, 1988a). The other five were untreated. All monkeys were given overdoses of Nembutal and perfused through the hearts with 4% paraformaldehyde in 0.1 M phosphate buffer (pH 7.4). The brains were removed, post fixed 3–6 h at room temperature in the fixative, cut into blocks and cryoprotected in 30% sucrose in 0.1 M phosphate buffer. The blocks were cut as frozen sections on a sliding microtome. The blocks of occipital lobes were sectioned at 30 μm thickness. In three monkeys, either parasagittal (45 μm thickness), horizontal (35 μm) or frontal (40 μm) slices were prepared through one entire hemisphere. In addition, the cortices posterior to the lunate sulcus of the right hemispheres of all monocularly deprived and one normal monkeys were dissected out, flattened between glass slides during postfixation and cut parallel to the opercular surface at 25 μm thickness.

In situ *hybridization*

Digoxigenin-labelled antisense and sense riboprobes were prepared from the nucleotide positions 333–999 (amino acids 87–308) of the *occ1* cDNA with a digoxigenin–dUTP labeling kit (Roche Diagnostics, Indianapolis, IN, USA). All the sections were stained with these probes, except the horizontal sections of a whole cerebral hemisphere, which were stained with the antisense and sense probes prepared from the nucleotide positions 4632–5675. *In situ* hybridization was carried out as described (Liang *et al.*, 2000). Briefly, free-floating sections were treated with 1 μg/mL proteinase K for 30 min at 37 °C. After acetylation, sections were incubated in a hybridization buffer containing 1.0 μg/mL digoxigenin-labeled riboprobes at 50 °C. Hybridized sections were washed by successively immersing once (unless otherwise indicated) in 2 × SSC/50% formamide/0.1% N-lauroylsarcosine (50 °C, 20 min, twice), RNase A buffer (room temperature, 10 min), RNase A buffer containing 20 μg/mL RNase A (37 °C, 30 min), 2 × SSC/0.1% N-lauroylsarcosine (room temperature and 50 °C, 15 min each), 1 × SSC/0.1% N-lauroylsarcosine (room temperature, 5 min), 0.5 × SSC/0.1% N-lauroylsarcosine (room temperature, 5 min) and 0.2 × SSC/0.1% N-lauroylsarcosine (room temperature and 50 °C, 20 min each). Hybridization signals were visualized by alkaline phosphatase immunohistochemistry with the digoxigenin detection kit (Roche Diagnostics). In the series of parasagittal or frontal sections of the whole hemisphere, every 12th section was processed with the antisense probe, and every 48th (parasagittal) or 24th (frontal) section was processed with the sense probe. The series of horizontal sections at about 2 mm and 8 mm intervals were stained with the antisense probe and the sense probe, respectively. In control sections hybridized with the sense probes, the neocortex gave no staining above background. The results obtained from both species of macaques were indistinguishable. The signal intensity of *in situ* hybridization was quantified with NIH image software by taking optical density meanings of the digitized image. Optical density readings were taken from at least 20 areas (each approximately 1100–6500 μm^2 in size) around the centers of perturbed and nonperturbed columns, which were identified by matching them to columns showing reduced and normal staining in adjacent CO-stained sections, in layer III or IVCβ of area 17 in a section. Background readings were taken from the almost unstained regions just suprajacent to the white matter because the white matter itself exhibited pale staining by endogenous alkaline phosphatase activity. These were subtracted and the optical densities were averaged. Data from three sections of each monocularly deprived monkey were then averaged. The significance of difference was calculated using the two-tailed Student's *t*-test.

Double immunohistochemical staining

For dual labeling, two antiserum–antibody combinations were used: rabbit anti-OCC1 (1 : 100) and mouse anti-CaMKII α (Roche Diagnostics; 1 : 400), rabbit anti-OCC1 and mouse anti-γ-aminobutyric acid (GABA; GB-69, Sigma, St. Louis, MO, USA; 1 : 400). Selected 30 μm-thick sections of normal monkey visual cortex were preincubated in 0.25% Triton X-100 in phosphate buffered saline (PBS) at room temperature for 2 h before being placed in the blocking buffer (1% blocking reagent from Roche Diagnostics, 5% normal goat serum and 0.1% Triton X-100 in PBS) at room temperature for at least 2 h. The sections were then transferred to the blocking buffer containing each primary antiserum–antibody combination. After 36–48 h at 4 °C, the sections were washed and incubated in a mixture of Alexa 488 conjugated goat anti-rabbit IgG (Molecular Probe, Eugene, OR, USA; 1 : 100) and Alexa 594 conjugated goat anti-mouse IgG (Molecular probe; 1 : 100) in PBS containing 5% normal goat serum and 0.1% Triton X-100. For controls, the same procedures were performed without primary antiserum or antibody. The control sections showed no fluorescent staining.

All the experiments described here were performed in compliance with the guidelines for animal experiments at Okazaki National Research Institute.

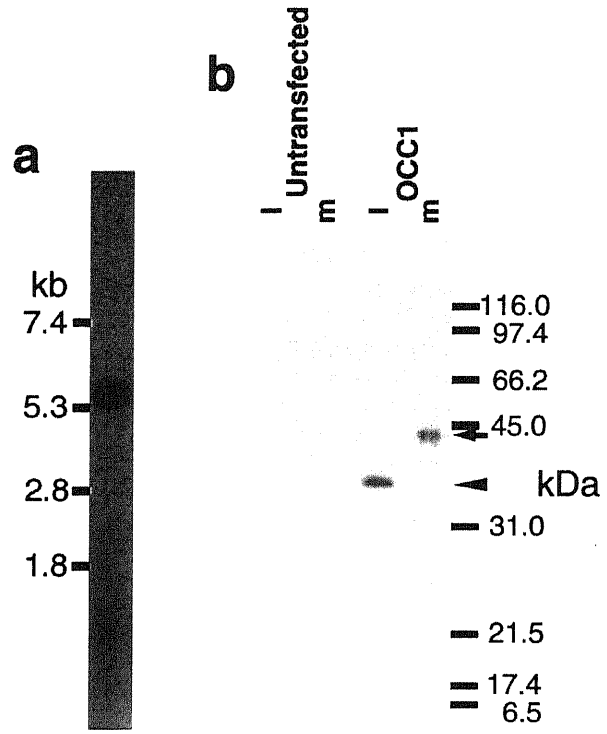

FIG. 2. Identification of *occ1* as a macaque homolog of a secretable protein. (a) Northern blotting with an *occ1* probe displayed a band at approximately 5.7 kb. (b) Western blot analysis with anti-OCC1 antiserum of lysates and conditioned medium of COS-7 cells transfected with OCC1 expression vector. Untransfected COS 7 cells were used as a control. l, cell lysates; m, conditioned medium. The molecular weight of the major product detected in the medium of OCC1-expressing COS-7 cells (arrow; approximately 43 kDa) is larger than that in the cell lysates (arrowhead; approximately 36 kDa) indicating that the product is secreted after being modified.

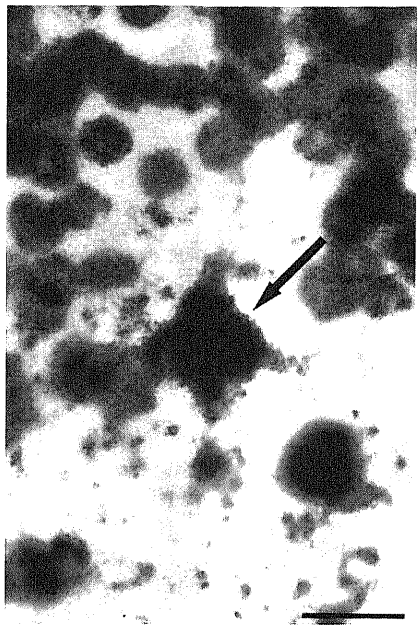

FIG. 3. A photomicrograph for neurons stained by *in situ* hybridization histochemistry with the *occ1* antisense probe in layer IVA of area 17. *occ1* mRNA was occasionally found in the processes of some neurons, which resulted in contoured pyramidal-shaped cell bodies (arrow). Pial surface is to the top. Scale bar, 20 μm.

Results

Identification of occ1

Total RNAs from five anatomically distinct regions of the adult cynomolgus monkey neocortex (areas FDΔ, FA, TE, OA and OC according to the classification of von Bonin & Bailey (1947) (see Fig. 4) were converted to cDNA with anchor oligo-dT primers, and the mRNA expression in these regions was compared by DD. Among the bands of the PCR-amplified fragments, we identified a 190 base pair (bp) cDNA fragment that showed the highest transcription level in area OC (Fig. 1a). RT-PCR analysis using a primer set corresponding to the both ends of the clone confirmed this characteristic regional expression pattern (Fig. 1b). The cDNA sequence of the clone obtained from DD shared no homology with any DNA sequences available on the GenBank database. Because the clone was likely to represent a 3′-noncoding region adjacent to the poly (A) $^+$ tail, we isolated a full-length cDNA from a cDNA library from area OC of cynomolgus monkey neocortex. Northern blotting showed that the full-length *occ1* mRNA is about 5.7 kb long (Fig. 2a). The first screen of a cDNA library with the DD cDNA fragment resulted in the isolation of a cDNA clone including a 1024-bp sequence upstream from the poly $(A)^+$ tail. We obtained a full-length clone after another screening of a cDNA library using the elongated clone as a probe. The entire sequence of the clone consisted of 5688 nucleotides, and a putative open reading frame of 308 amino acids (calculated molecular mass of 34.999 kDa) was found upstream from the nucleotide sequence for the DD clone. We named the gene *occ1*. Homology search revealed that this gene encodes the macaque homolog of human, rat and mouse follistatin-related protein (FRP)/TSC-36, which was originally isolated from the cells of a mouse osteoblastic cell line treated with transforming growth factor β1 (Shibanuma *et al.*, 1993), and contains a cysteine-rich follistatin motif, three putative N-glycosylation sites and several phosphorylation sites (Zwijsen *et al.*, 1994; Patel *et al.*, 1996; Ohashi *et al.*, 1997; Tanaka *et al.*, 1998; Okabayashi *et al.*, 1999). The follistatin motif is shared by various proteins, such as the activin inhibitor follistatin, agrin, the protein that induces the aggregation of nicotinic acetylcholine receptors, the multifunctional extracellular glycoprotein SPARC/osteonectin/BM-40, the rat brain protein SC1 and the quail retina-specific protein QR1 (Johnston *et al.*, 1990; Guermah *et al.*, 1991; Patthy & Nikolics, 1993; Maurer *et al.*, 1995; Phillips & de Kretser, 1998; Motamed, 1999). Compatible with the prediction that OCC1 has N-terminal signal peptides (Zwijsen *et al.*, 1994), Western blot analysis of cell lysates and the supernatant of conditioned medium of COS-7 cells transfected with OCC1 expression vector showed that OCC1 was released into the medium with post-translational modifications (Fig. 2b).

Neocortical distribution of the cells specified by occ1

In the monkey neocortex, most *occ1*-positive signals in *in situ* hybridization preparations were observed in neurons. This was judged from the following observations: (i) little signal was observed in the white matter; (ii) the cells stained by the probe had large somata in general (7–12 μm in diameter in layers III and IVC of area 17); and (iii) *occ1* mRNA was occasionally observed to be localized in the processes of some pyramidal cells, resulting in contoured cell shapes (Fig. 3). *In situ* hybridization histochemistry of the serial sections of the entire cerebral hemisphere demonstrated that the distribution of *occ1*-positive neurons was as expected on the basis of the results of

DD and RT-PCR experiments in which samples were taken from the cytoarchitectonic areas shown in Fig. 4. The strongest and densest hybridization signals were observed in area 17. The other occipital areas showed moderate expression of *occ1* (Fig. 5a and e). Neurons positive for *occ1* were distributed with relatively weak labeling basically throughout the temporal and the posterior half of the parietal cortex (Fig. 5a, c and d). In these cortices, certain areas could be identified by densities and patterns of staining. The primary somatosensory cortex (area 3b) show some dense expression in layer IV and the deeper stratum of layer III (Figs 5c and d, and 6a). The primary auditory cortex (AI) also exhibited relatively dense expression in layer IV and the deeper half of layer III (Figs 5d and 6c). The intensity of labeling and the frequency of the signals were even lower in the areas anterior to the central sulcus than in the postcentral regions. In the precentral regions, no obvious cortical areas could be identified by the *occ1* expression pattern (Fig. 5a and b).

Laminar distribution of occ1*-positive neurons in the visual cortex and visual thalamus*

Examination of neurons positive for *occ1* mRNA in areas 17 and 18 revealed distinctive laminar distributions of neurons expressing *occ1* in these regions. In area 17 (Fig. 7a), signal was most densely distributed and cells were most intensely labeled in layers IVCα and IVCβ. Layers II, III and IVA exhibited many intensely labeled neurons. In the intervening layer, IVB, a lower number of moderately labeled neurons were present. The distribution of *occ1*-positive neurons divided layer V into a superficial, lightly stained sublayer and a deeper, even more lightly stained sublayer. In layer VI and the deeper half of layer V, sparse moderately stained neurons were found. The positive neurons in layer I were lightly stained and sparsely present.

The laminar distribution of *occ1*-positive neurons in area 18 (Fig. 7c) was different from that in area 17. Many intensely labeled neurons with large somata were found in the lower one-third of layer III. In the upper two-thirds of layer III and layer IV, many lightly

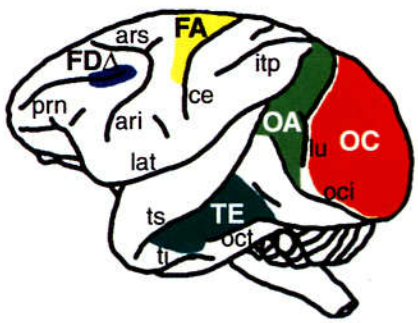

FIG. 4. The five neocortical regions (areas FDΔ, FA, TE, OA and OC; colored) from which tissues were dissected and used as samples for differential display and RT-PCR experiments. ari, inferior ramus of arcuate sulcus; ars, superior ramus of arcuate sulcus; ce, central sulcus; itp, intraparietal sulcus; lat, lateral sulcus; lu, lunate sulcus; oci, inferior occipital sulcus; oct, occipito-temporal sulcus; prn, principal sulcus; ti, inferior temporal sulcus; ts, superior temporal sulcus.

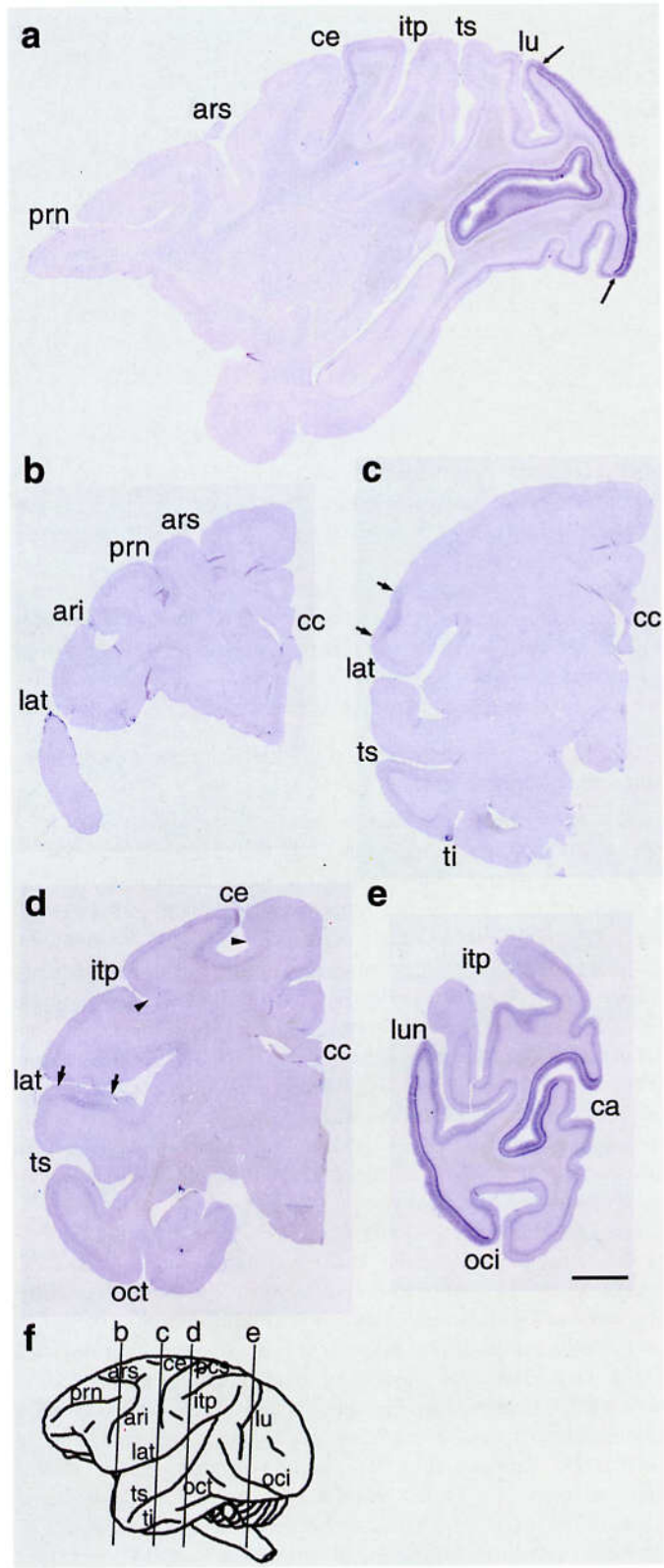

FIG. 5. Neocortical distribution of the neurons marked by *occ1*-mRNA expression. Parasagittal (a) and frontal (b–e) whole-brain sections processed by *in situ* hybridization. In (a), rostral is to the left, and the arrows indicate the borders between areas 17 and 18. In (b) to (e), medial is to the right. Arrows in (c) indicate the borders of area 3b. Arrowheads and arrows in (d) indicate the borders of area 3b and AI, respectively. (f) Lateral view of macaque neocortex, rostral is to the left. The lines indicate the coronal planes sliced for the sections (b–e). The signals were localized preferentially in the posterior region of the neocortex, in particular, area 17. Abbreviations are as used in Fig. 4. cc, sulcus of corpus callosum. Scale bar, 5 mm.

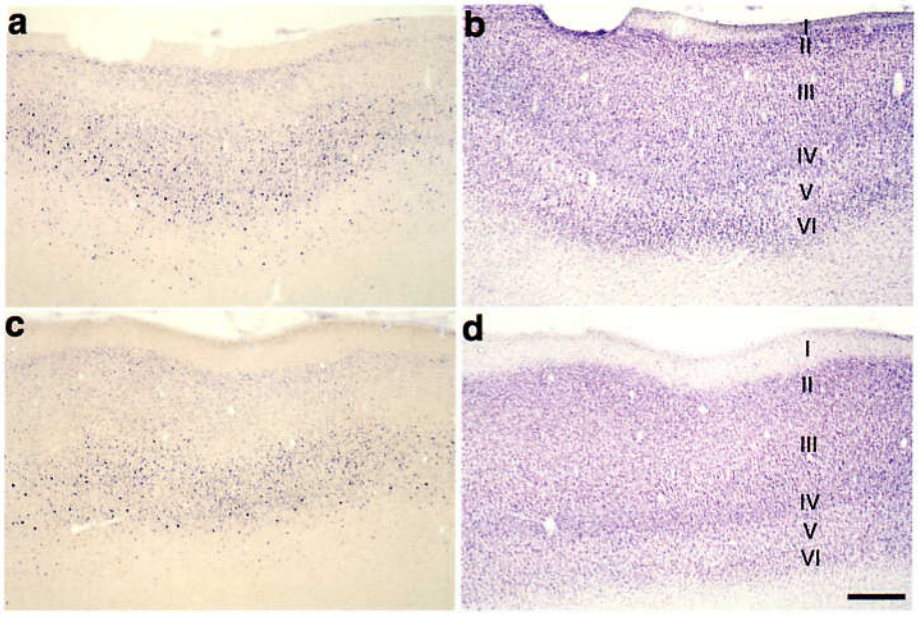

FIG. 6. Area 3b and AI can be identified by densities and patterns of *occ1* expression. (a–d) Sections through area 3b (a; the region indicated by arrows in Fig. 5c at higher magnification) and AI (c; the region indicated by arrows in Fig. 5d at higher magnification), stained for *occ1* (a and c) and with thionin (b and d). Area 3b and AI show relatively dense expression of *occ1* in layer III and IV. Scale bar, 500 μm.

labeled cells and some moderately labeled cells were observed. Layer II exhibited many lightly labeled neurons. In layers V and VI, a few relatively lightly labeled cells were present. Weak signal was sparsely distributed in layer I.

We further examined the *occ1* expression in LGN to ask whether *occ1* has a specific pattern of laminar distribution in the thalamic nucleus in which visual system channels are segregated into distinct layers, and found that relatively weak signal was present selectively in cells of the magnocellular layers (layers 1 and 2; Fig. 8a, b and d).

The subset of neurons specified by occ1 *includes functionally and morphologically distinct types*

To determine whether the neurons marked by the expression of *occ1* can be classified into a single functional and morphological class of cells, we performed dual labeling immunohistochemistry on the neurons in area 17 with the antisera to OCC1 and a monoclonal antibody against either CaMKII α or GABA. CaMKII α immunoreactivity is found only in a population of glutamatergic, excitatory cells in the cerebral cortex (Benson *et al.*, 1991, 1992; Liu & Jones, 1996), which includes the spiny stellate cells in layer IV and pyramidal cells in the other layers of area 17 (Hendry & Kennedy, 1986; Tighilet *et al.*, 1998). By contrast, GABAergic neurons of the primate neocortex belong to a class of inhibitory and aspiny nonpyramidal neurons (Houser *et al.*, 1983; Jones *et al.*, 1994). No GABA-immunoreactive neurons showed CaMKII α immunoreactivity in area 17 (Tighilet *et al.*, 1998).

The OCC1 immunoreactivity is diffusely present within the cell bodies, especially around the cell nuclei, and seen in a punctate pattern along the neuronal processes (Fig. 9 left panels). These observations are consistent with the possibility that the product of *occ1* can be released from neurons as well as from the transfected COS-7 cells. The great majority of neurons expressing CaMKII α show OCC1 immunoreactivity (Fig. 9a and b). By contrast, OCC1 immunoreactivity was found in not all, but in a large population of GABAergic neurons (Fig. 9c). Each type of neuron, double immunoreactive for OCC1 and CaMKII α and double immunoreactive for OCC1 and GABA, were observed in all layers of area 17 except for layer I in which virtually all neurons are GABA-positive

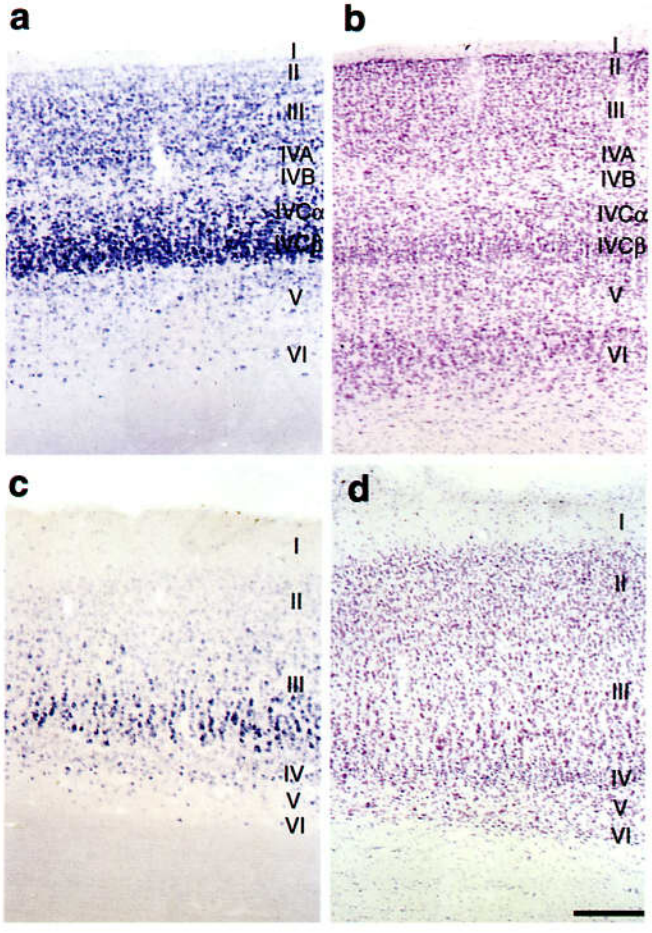

FIG. 7. Laminar distribution of *occ1*-positive neurons in areas 17 and 18. (a–d) Sections through area 17 (a and b) and area 18 (c and d), stained for *occ1* (a and c) and with thionin (b and d). In areas 17 and 18, the strongest signals are found in layer IVC and in the deeper stratum of layer III, respectively. Scale bar, 200 μm.

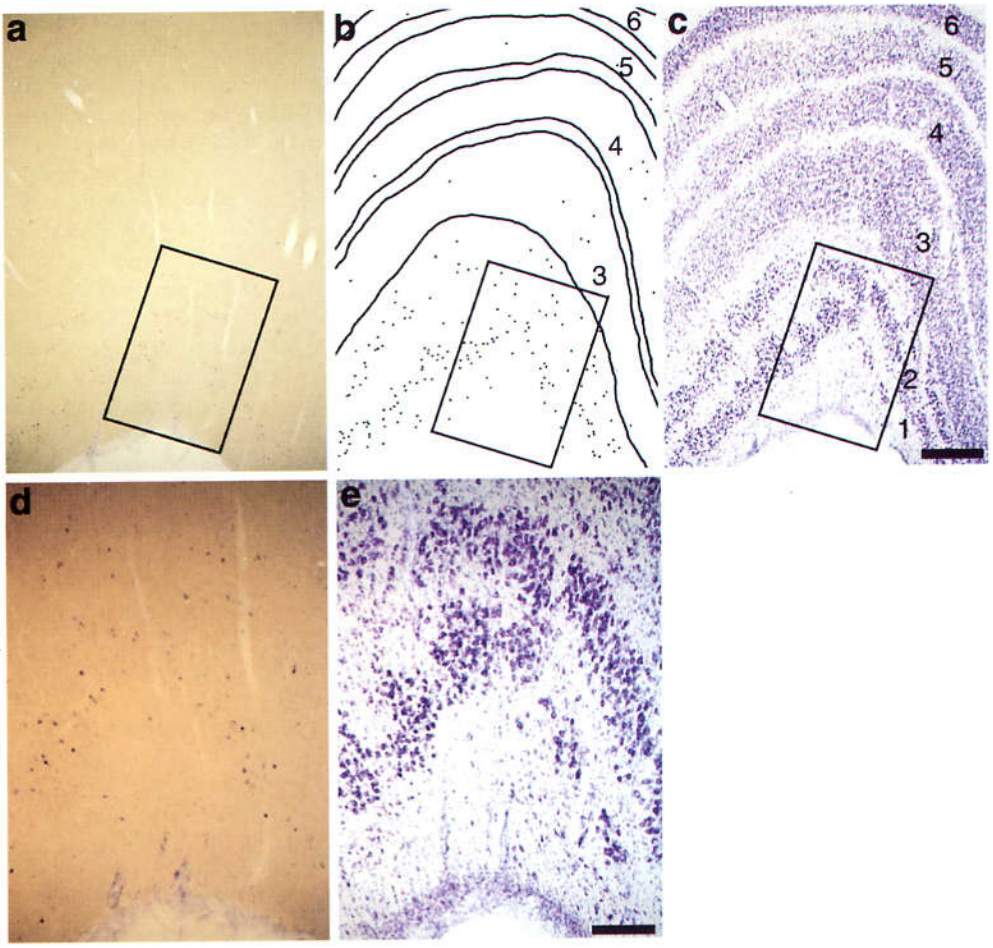

FIG. 8. Distribution of *occ1*-expressing neurons in the LGN. (a and c) Frontal sections through LGN, stained for *occ1* (a) and with thionin (c). (b) Drawing of the positive signals (dots) in (a). (d) The boxed area in (a) is magnified. (e) The boxed area in (c) is magnified. In LGN, *occ1* mRNA is expressed selectively in the cells of the magnocellular layers (layers 1 and 2). Scale bar, 500 μm (a–c) and 200 μm (d and e).

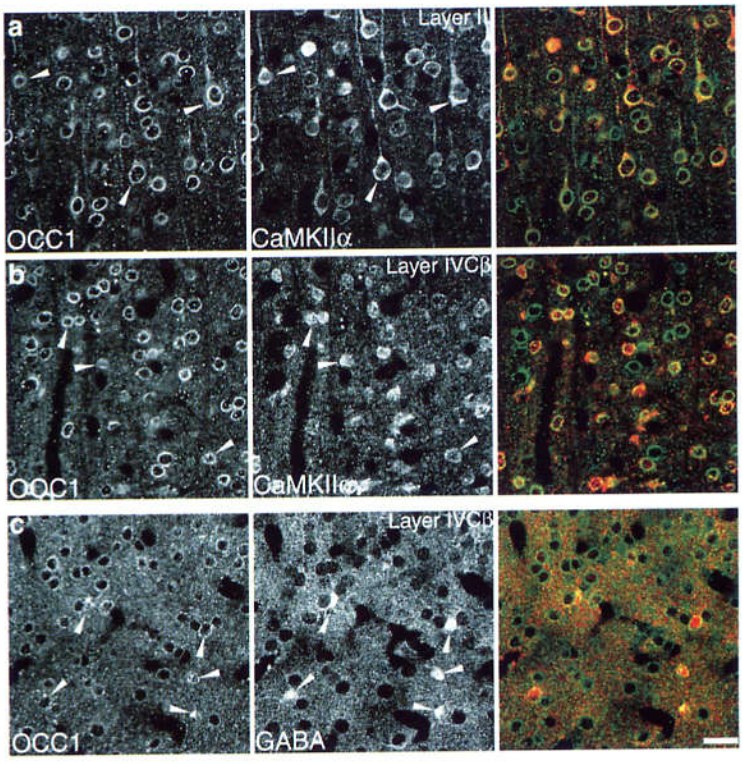

FIG. 9. Neuronal subset revealed by *occ1* includes two different classes of neurons. (a–c) Sections were double labelled with antiserum against OCC1 (left panels) and antibody against either CaMKII α (a and b; middle panels) or GABA (c; middle panel), and imaged to determine colocalization (right panels, OCC1 in green, CaMKII α or GABA in red). (a) From layer II; (b and c) from layer IVCβ of area 17 double stained with OCC1/CaMKII and OCC1/GABA, respectively. Pial surface is to the top. Arrowheads indicate the representative cells double-positive for each antiserum–antibody combination. Note that owing to the difference of the subcellular localization pattern of OCC1 from that of GABA in (c), the confocal images to show colocalization of these markers had to be acquired in a slice plane in which optimal staining of OCC1 might not be yielded; this resulted in the difference of OCC1 staining patterns in layer IVCβ in the two images (b and c; left panels). Scale bar, 20 μm.

(Hendry *et al.*, 1987). These observations show that the neuronal subset revealed by *occ1* expression includes physiologically and morphologically different classes of neurons in area 17.

occ1 *is expressed by the neurons in area 17 in an activity-dependent manner*

The neurons marked by *occ1* expression were preferentially distributed in area 17. This posed the question of whether visual experience plays a role in the regulation of *occ1* expression in the adult brain. Area 17 of the Old World primates is divided into alternating ocular dominance columns (Hubel & Wiesel, 1972; Wiesel *et al.*, 1974). We examined the alterations in neuronal phenotypes based on changes in neuronal activity in the brains of monocularly deprived animals using immunohistochemical techniques (Hendry & Jones, 1986; Hendry & Kennedy, 1986; Hendry and Jones, 1988).

Following monocular deprivation by TTX injection into the vitreous cavity (7, 10, 14 or 21 days), dramatic changes were detected in the *in situ* hybridization pattern of *occ1* in area 17. Alternating lightly and darkly stained stripes appeared (Fig. 10a, c, e and g), irrespective of the length of deprivation. Comparison with the adjacent sections stained for CO (Wong-Riley, 1979; Horton & Hubel, 1981), which exhibited the same pattern of alternating dark and light stripes, showed that *occ1* transcription was reduced in the deprived columns. The change was observed in layers III, IVA, IVB, IVCα, IVCβ and V, being most apparent in layers III and IVCβ (Fig. 10a). The signal intensity measurements confirmed this observation that the average level of mRNA in the perturbed columns were 57% lower in layer III (range, 45–68%; $P < 0.0005$), and 74% lower in layer IVCβ (66–82%; $P < 0.0001$) than those in the nonperturbed columns.

In the tangential sections cut through layer III of area 17 of TTX-injected animals, the *occ1* signal was seen along the line of blobs in the undeprived columns, and faint patchy stainings coinciding with the CO periodicities were observed in the perturbed columns (Fig. 10c–f; arrows in e and f indicate the patchy CO and corresponding *occ1* stainings in the perturbed columns). The *occ1* expression in the undeprived columns was beyond the confines of the undeprived blobs to form an almost continuous signal, and the extent of the expression in the deprived columns was even less than that of the shrunken blobs observed in the CO sections. In the sections cut through layer IVCβ, the ocular dominance columns observed in the sections stained for *occ1* were even more obvious than those seen in the CO sections (Fig. 10g and h). These observations also suggest that the *occ1* expression in layers III and IVC was significantly decreased by the blockade of visual input. From these results, we conclude that *occ1* mRNA is transcribed in an activity-dependent manner in area 17. An obvious change was not observed in area 18.

Discussion

We have screened for genes that are transcribed differentially among structurally and functionally distinct areas of macaque neocortex and identified *occ1*. Neurons positive for *occ1* were selectively distributed in the posterior region of the neocortex, especially in area 17.

Occ1 *expression and neocortical neuronal organization*

It has been considered that the neocortex is basically homogeneous on the basis of the number and density (Rockel *et al.*, 1980), and morphology (Fairen *et al.*, 1984) of its neuronal components. The ratios between pyramidal and nonpyramidal neurons are very similar in the motor, somatosensory and visual cortices (Sloper, 1973; Tombol, 1974; Sloper *et al.*, 1978). In studies of the chemical properties of neurons, an extensive quantitative survey of the distribution of a major neurotransmitter, GABA, demonstrated that its distribution varies little among neocortical areas (Hendry *et al.*, 1987). However, in these neuron counting studies, there was an exception; in area 17 the number of neurons through the full depth of the cortex is more than twice than in the other areas (Rockel *et al.*, 1980) and the proportion of GABAergic neurons to total neurons is lower than in the other areas (Hendry *et al.*, 1987). Therefore, the distribution of *occ1* mRNA, preferentially observed in the posterior region of neocortex with regional variations, is a dramatic example of the heterogeneity of neocortical neurons, which coincides with the functional subdivisions, and the high *occ1* transcription in area 17 reveals the unique neuronal organization of area 17 in the primate neocortex. Furthermore, as the results shown in Fig. 10 demonstrate, *occ1* mRNA levels can be downregulated remarkably by blockade of afferent activity in area 17. High *occ1* expression is not only spatially coincident with area 17, but also subject to regulation dependent on neuronal activity in area 17. These results show the important features of the expression of *occ1* that can be used as a marker for neurons in area 17 as well as a good indicator of neural activities in the particular laminae of area 17.

The further characterization of the neurons specified by *occ1* in area 17 showed that they include morphologically and functionally distinct classes of neurons, spiny excitatory cells and aspiny inhibitory cells. This result suggests the other unique aspect of *occ1* expression in neocortical neurons that *occ1* is expressed not in a single type of neurons but in various types of neurons in a region-selective manner.

occ1 *expression in neocortex and thalamocortical connectivity*

The present results show that the transcription pattern of *occ1* relates to the cytoarchitectonic area of the neocortex. At present, we cannot explain how such a difference in gene expression among neocortical neurons is generated during brain development. In regard to the neocortical region where *occ1* shows its high transcription, however, we can find some correlation between the laminar distribution of *occ1* expressing neurons and the pattern of thalamic afferent innervation.

We found strong *occ1* transcription in layers II, III, IVA and IVC of area 17. The major inputs to area 17 in primates and some other mammals are from the (dorsal) LGN and the minor inputs are from the nuclei of the pulvinar complex. Thalamic inputs from LGN in primates terminate mainly in layer IVC and, to a lesser degree, in layer IVA of area 17 (Hubel & Wiesel, 1972; Hendrickson *et al.*, 1978; Blasdel & Lund, 1983). The pulvinar axons and those from intercalated layers of the LGN provide thalamocortical innervation to the cells in layer I and the blobs of layers II and III of area 17 (Fitzpatrick *et al.*, 1983; Hendry & Yoshioka, 1994). In area 18, we observed strong signals in the deep stratum of layer III. The pulvinar afferent terminations in area 18 are dense in the deep levels of layer III and layer IV (Curcio & Harting, 1978; Livingstone & Hubel, 1982). In addition to these thalamic recipient regions, *occ1* also shows high transcription in the regions on which thalamic inputs have strong influences in indirect ways. *occ1* is transcribed in the interblob regions of layer II and III of area 17 where no apparent termination of direct thalamic input has been observed (Livingstone & Hubel, 1982; Itaya *et al.*, 1984). We also found moderate and light signals in layer IVB and the upper stratum of layer V, respectively. Neither layer IV B nor V receives direct geniculate inputs. On the other hand, the interblob regions of layers II and III receive indirect inputs from the LGN through layers IVA and IVC. Neurons in layer IVB receive strong inputs from layer IVCα. The upper subdivision of layer V

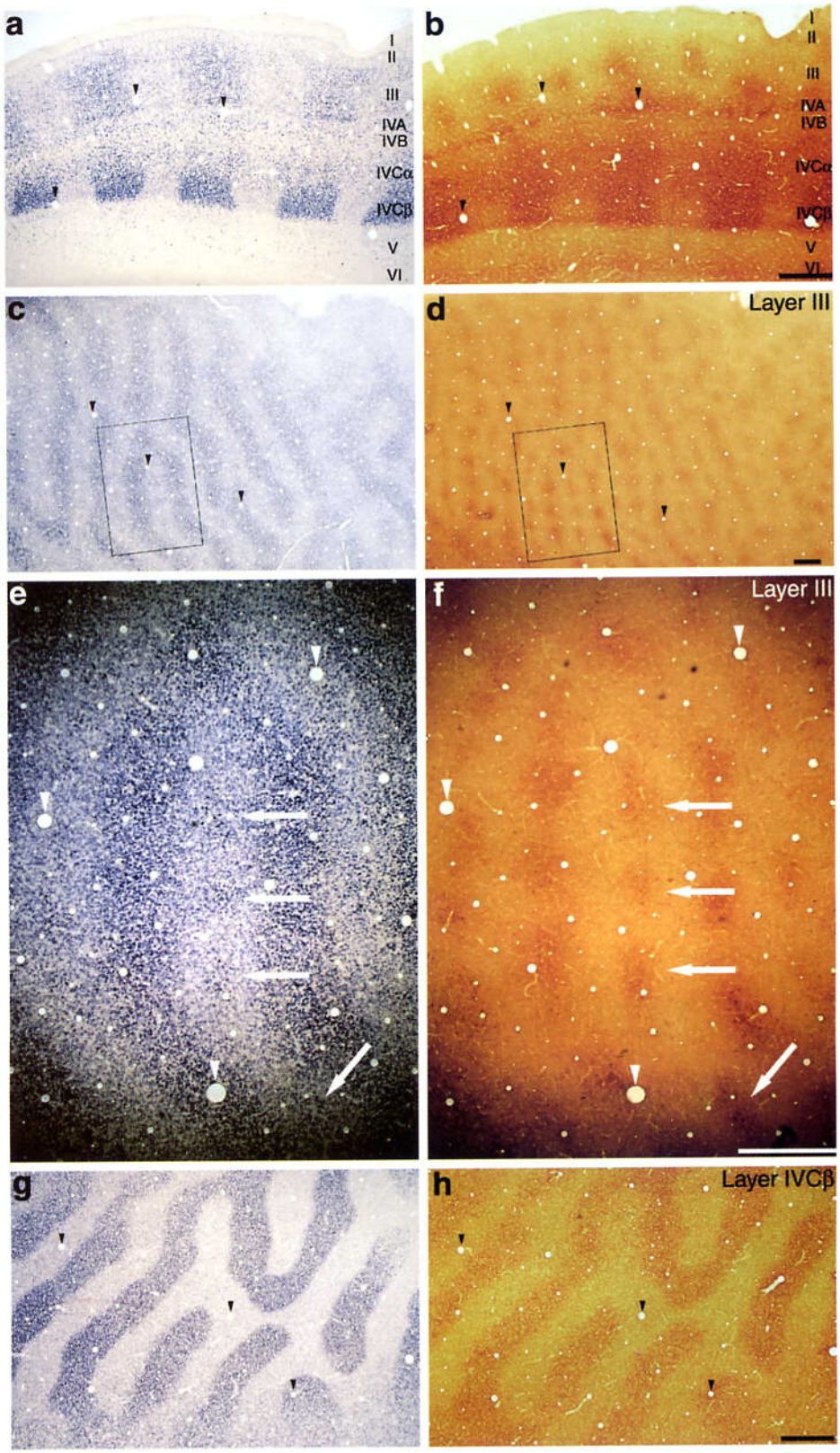

FIG. 10. Change in the transcription of *occ1* in adult area 17 following monocular deprivation. Sections are stained for *occ1* (left panels) and CO (right panels). (a and b) A coronal section through area 17 of a monkey monocularly deprived for 14 days. The change was detected in layers III, IVA, IVB, IVCα, IVCβ and V. (c–f) Tangential sections through layer III. The boxed areas in (c and d) are magnified in (e and f), respectively. (g and h) Tangential sections through layer IVCβ. By comparing the positions of the same blood vessel profiles in these sections (arrowheads), the remarkable reduction of *occ1* mRNA was found in the perturbed columns. Arrows in (e and f) indicate the representative patchy stainings in the perturbed columns in each section. Scale bars, 500 μm.

makes prominent connections to the thalamic recipient layers IVA, IVCα, IVCβ and VI (Lund, 1988; Callaway, 1998).

occ1 *expression and a functional subdivision of the visual thalamus*

We observed that the *occ1* expression in LGN is more frequent in the magnocellular layers in which the cells with broad band spectral qualities are selectively localized (Wiesel & Hubel, 1966) than in the other layers. *occ1* is also preferentially expressed in a functional subdivision of a thalamic nucleus. Some markers, for example Cat-301 and SMI-32, are known to primarily label the magnocellular layers (Hendry *et al.*, 1988b; Chaudhuri *et al.*, 1996). *occ1* can also be used as a marker to visualize a subset of neurons in those layers of the LGN and contribute to the classification of neurons in the LGN.

The function of occ1 *in cortical plasticity*

The data presented here clearly indicate that *occ1* mRNA is preferentially expressed in posterior regions of the neocortex, especially in area 17, in an activity-dependent manner. Activity-dependent gene expression, resulting in changes in neuronal phenotypes, plays an important role in neuronal plasticity of brain function and development (Marty *et al.*, 1997; Lee & Sheng, 2000). Many molecules are expressed in an activity-dependent manner, but none of them shows such a characteristic regional expression pattern in the neocortex as that of *occ1*. Although the function of OCC1 (FRP, TSC-36) remains unknown to date, it has been suggested that the follistatin motifs of follistatin, agrin and SC1 might play similar functions in the differentiation of the nervous system by accumulating, protecting and modulating the activity of growth factors (Patthy & Nikolics, 1993). This suggestion also presents the possibility that OCC1 could function by binding other molecule(s) and affecting its (their) activity(ies). The results of the expression study with COS-7 cells suggest that OCC1 might function in a secreted form. These together imply that OCC1 can work to mediate activity-dependent interactions between specific subsets of neurons through modulating the functions of other proteins in response to changes in neuronal activity in particular neuronal circuits. Further studies on the nature of OCC1 and to elucidate the role of the molecule in neuronal function will shed new light on the functional structure of the cerebral neocortex.

A few molecular markers for specific neuronal subtypes in the rodent brain have been identified and characterized, such as the limbic system-associated membrane protein (LAMP) and latexin (Levitt, 1984; Zacco *et al.*, 1990; Arimatsu *et al.*, 1992; Arimatsu, 1994). LAMP is a glycoprotein that is expressed in subsets of neurons in the adult rat brain that are associated with classic limbic structures (Reinoso *et al.*, 1996). Latexin-immunoreactive neurons are confined essentially to the infra-granular layers of lateral cortical areas in the rat neocortex (Arimatsu *et al.*, 1999). Among these markers, the distribution of LAMP in the primate brain has been examined, and it has been shown that LAMP can also be effective in visualizing neuronal subsets in the primate limbic system (Cote *et al.*, 1996). This result suggests that the characterization of *occ1*-positive neurons in the brains of rodents and other mammals could show the similarity and the difference of the neuronal organization between the primate and other mammalian brains. This kind of knowledge will contribute to understanding the nature of neurons expressing *occ1* in future studies.

A systematic survey for marker molecules in the primate neocortex described here presents a successful example of such an approach. Histochemical analyses using new molecular markers combined with various other techniques could become powerful tools in deciphering the functional organization of the neocortex.

Acknowledgements

This work was supported by a Grants-in-Aid from the Ministry of Education, Science, Sports, and Culture of Japan and a grant from the Mitsubishi Foundation (both to T.Y). We thank H. Horie, S. Abe and S. Hashizume of the Japan Poliomyelitis Research Institute for providing the monkey tissues, F. Ono of the Corporation for Production and Research of Laboratory Primates and K. Terao of the Tsukuba Primate Center, National Institute of Infectious Diseases for supplying the animals, M. Ida-Hosonuma and S. Koike at the Tokyo Metropolitan Institute for Neuroscience for help with the over-expression study, and H. Komatsu of the National Institute for Physiological Sciences in Japan for critical reading of the manuscript.

Abbreviations

CaMKII α, the α-subunit of type II calcium/calmodulin-dependent protein kinase; bp, base pairs; CO, cytochrome oxidase; DD, differential display; FRP, follistatin-related protein; LGN, lateral geniculate nucleus; PBS, phosphate-buffered saline.

References

Arimatsu, Y. (1994) Latexin: a molecular marker for regional specification in the neocortex. *Neurosci. Res.*, **20**, 131–135.

Arimatsu, Y., Kojima, M. & Ishida, M. (1999) Area- and lamina-specific organization of a neuronal subpopulation defined by expression of latexin in the rat cerebral cortex. *Neuroscience*, **88**, 93–105.

Arimatsu, Y., Miyamoto, M., Nihonmatsu, I., Hirata, K., Uratani, Y., Hatanaka, Y. & Takiguchi-Hayashi, K. (1992) Early regional specification for a molecular neuronal phenotype in the rat neocortex. *Proc. Natl. Acad. Sci. USA*, **89**, 8879–8883.

Benson, D.L., Isackson, P.J., Gall, C.M. & Jones, E.G. (1992) Contrasting patterns in the localization of glutamic acid decarboxylase and Ca2+/calmodulin protein kinase gene expression in the rat central nervous system. *Neuroscience*, **46**, 825–849.

Benson, D.L., Isackson, P.J., Hendry, S.H. & Jones, E.G. (1991) Differential gene expression for glutamic acid decarboxylase and type II calcium-calmodulin-dependent protein kinase in basal ganglia, thalamus, and hypothalamus of the monkey. *J. Neurosci.*, **11**, 1540–1564.

Blasdel, G.G. & Lund, J.S. (1983) Termination of afferent axons in macaque striate cortex. *J. Neurosci.*, **3**, 1389–1413.

von Bonin, G. & Bailey, P. (1947). *The Neocortex of Macaca Mulatta*. University of Illinois Press, Urbana.

Callaway, E.M. (1998) Local circuits in primary visual cortex of the macaque monkey. *Annu. Rev. Neurosci.*, **21**, 47–74.

Chaudhuri, A., Zangenehpour, S., Matsubara, J.A. & Cynader, M.S. (1996) Differential expression of neurofilament protein in the visual system of the vervet monkey. *Brain Res.*, **709**, 17–26.

Chomczynski, P. & Sacchi, N. (1987) Single-step method of RNA isolation by acid guanidium thiocyanate-phenol-chloroform extraction. *Anal. Biochem.*, **162**, 156–159.

Cote, P.Y., Levitt, P. & Parent, A. (1996) Limbic system-associated membrane protein (LAMP) in primate amygdala and hippocampus. *Hippocampus*, **6**, 483–494.

Curcio, C.A. & Harting, J.K. (1978) Organization of pulvinar afferents to area 18 in the squirrel monkey: evidence for stripes. *Brain Res.*, **143**, 155–161.

Dyck, R.H. & Cynader, M.S. (1993) An interdigitated columnar mosaic of cytochrome oxidase, zinc, and neurotransmitter-related molecules in cat and monkey visual cortex. *Proc. Natl. Acad. Sci. USA*, **90**, 9066–9069.

Fairen, A., DeFelipe, J. & Regidor, J. (1984) Nonpyramidal neurons. General account. In Peters, A. & Jones, E.G. (eds), *Cerebral Cortex*, **Vol. 1** Cellular Components of the Cerebral Cortex. Plenum, New York, pp. 201–253.

Fitzpatrick, D., Itoh, K. & Diamond, I.T. (1983) The laminar organization of the lateral geniculate body and the striate cortex in the squirrel monkey (Saimiri sciureus). *J. Neurosci.*, **3**, 673–702.

Guermah, M., Crisanti, P., Laugier, D., Dezelee, P., Bidou, L., Pessac, B. & Calothy, G. (1991) Transcription of a quail gene expressed in embryonic retinal cells is shut off sharply at hatching. *Proc. Natl. Acad. Sci. USA*, **88**, 4503–4507.

Hendrickson, A.E., Wilson, J.R. & Ogren, M.P. (1978) The neuroanatomical organization of pathways between the dorsal lateral geniculate nucleus and visual cortex in Old World and New World primates. *J. Comp. Neurol.*, **182**, 123–136.

Hendry, S.H.C. & Calkins, D.J. (1998) neuronal chemistry and functional organization in the primate visual system. *Trends Neurosci.*, **21**, 344–349.
Hendry, S.H.C., Hockfield, S., Jones, E.G. & MacKay, R. (1984) Monoclonal antibody that identifies subsets of neurons in the central visual system of monkey and cat. *Nature*, **307**, 267–269.
Hendry, S.H. & Jones, E.G. (1986) Reduction in number of immunostained GABAergic neurones in deprived-eye dominance columns of monkey area 17. *Nature*, **320**, 750–753.
Hendry, S.H. & Jones, E.G. (1988) Activity-dependent regulation of GABA expression in the visual cortex of adult monkeys. *Neuron*, **1**, 701–712.
Hendry, S.H., Jones, E.G. & Burstein, N. (1988a) Activity-dependent regulation of tachykinin-like immunoreactivity in neurons of monkey visual cortex. *J. Neurosci.*, **8**, 1225–1238.
Hendry, S.H., Jones, E.G., Hockfield, S. & McKay, R.D. (1988b) Neuronal populations stained with the monoclonal antibody Cat-301 in the mammalian cerebral cortex and thalamus. *J. Neurosci.*, **8**, 518–542.
Hendry, S.H. & Kennedy, M.B. (1986) Immunoreactivity for a calmodulin-dependent protein kinase is selectively increased in macaque striate cortex after monocular deprivation. *Proc. Natl. Acad. Sci. USA*, **83**, 1536–1541.
Hendry, S.H., Schwark, H.D., Jones, E.G. & Yan, J. (1987) Numbers and proportions of GABA-immunoreactive neurons in different areas of monkey cerebral cortex. *J. Neurosci.*, **7**, 1503–1519.
Hendry, S.H.C. & Yoshioka, T. (1994) A neurochemically distinct third channel in the macaque dorsal lateral geniculate nucleus. *Science*, **264**, 575–577.
Hockfield, S., Kalb, R.G., Zaremba, S. & Fryer, H. (1990) Expression of Neural proteoglycans correlates with the acquisition of mature neuronal properties in the mammalian brain. *Cold Spring Harbor Symp. Quant. Biol.*, **55**, 505–514.
Hof, P.R. & Morrison, J.H. (1995) Neurofilament protein defines regional patterns of cortical organization in the macaque monkey visual system: a quantitative immunohistochemical analysis. *J. Comp. Neurol.*, **352**, 161–186.
Horton, J.C. (1984) Cytochrome oxidase patches: a new cytoarchitectonic feature of monkey visual cortex. *Philos. Trans. R. Soc. Lond. B Biol. Sci.*, **304**, 199–253.
Horton, J.C. & Hubel, D.H. (1981) Regular patchy distribution of cytochrome oxidase staining in primary visual cortex of macaque monkey. *Nature*, **292**, 762–764.
Houser, C.R., Hendry, S.H., Jones, E.G. & Vaughn, J.E. (1983) Morphological diversity of immunocytochemically identified GABA neurons in the monkey sensory-motor cortex. *J. Neurocytol.*, **12**, 617–638.
Hubel, D.H. & Wiesel, T.N. (1972) Laminar and columnar distribution of geniculo-cortical fibers in the macaque monkey. *J. Comp. Neurol.*, **146**, 421–450.
Itaya, S.K., Itaya, P.W. & Van Hoesen, G.W. (1984) Intracortical termination of the retino-geniculo-striate pathway studied with transsynaptic tracer (wheat germ agglutinin-horseradish peroxidase) and cytochrome oxidase staining in the macaque monkey. *Brain Res.*, **304**, 303–310.
Johnston, I.G., Paladino, T., Gurd, J.W. & Brown, I.R. (1990) Molecular cloning of SC1: a putative brain extracellular matrix glycoprotein showing partial similarity to osteonectin/BM40/SPARC. *Neuron*, **4**, 165–176.
Jones, E.G., Hendry, S.H.C., DeFelipe, J. & Benson, D.L. (1994) GABA neurons and their role in activity-dependent plasticity of adult primate visual cortex. In Peters, A. & Rockland, K.S. (eds), *Cerebral Cortex*, **Vol. 10**, Primary Visual Cortex in Primates. Plenum, New York, pp. 61–140.
Lee, S.H. & Sheng, M. (2000) Development of neuron–neuron synapses. *Curr. Opin. Neurobiol.*, **10**, 125–131.
Levitt, P. (1984) A monoclonal antibody to limbic system neurons. *Science*, **223**, 299–301.
Liang, F., Hatanaka, Y., Saito, H., Yamamori, T. & Hashikawa, T. (2000) Differential expression of gamma-aminobutyric acid type B receptor-1a and -1b mRNA variants in GABA and non-GABAergic neurons of the rat brain. *J. Comp. Neurol.*, **416**, 475–495.
Liang, P. & Pardee, A.B. (1992) Differential display of eukaryotic messenger RNA by means of the polymerase chain reaction. *Science*, **257**, 967–971.
Liu, X.B. & Jones, E.G. (1996) Localization of alpha type II calcium calmodulin-dependent protein kinase at glutamatergic but not gamma-aminobutyric acid (GABAergic) synapses in thalamus and cerebral cortex. *Proc. Natl. Acad. Sci. USA*, **93**, 7332–7336.
Livingstone, M.S. & Hubel, D.H. (1982) Thalamic inputs to cytochrome oxidase-rich regions in monkey visual cortex. *Proc. Natl. Acad. Sci. USA*, **79**, 6098–6101.
Livingstone, M.S. & Hubel, D.H. (1983) Specificity of cortico-cortical connections in monkey visual system. *Nature*, **304**, 531–534.
Lund, J.S. (1988) Anatomical organization of macaque monkey striate visual cortex. *Annu. Rev. Neurosci.*, **11**, 253–288.
Marty, S., Berzaghi Mda, P. & Berninger, B. (1997) Neurotrophins and activity-dependent plasticity of cortical interneurons. *Trends Neurosci.*, **20**, 198–202.
Maurer, P., Hohenadl, C., Hohenester, E., Gohring, W., Timpl, R. & Engel, J. (1995) The C-terminal portion of BM-40 (SPARC/osteonectin) is an autonomously folding and crystallisable domain that binds calcium and collagen IV. *J. Mol. Biol.*, **253**, 347–357.
Motamed, K. (1999) SPARC (osteonectin/BM-40). *Int. J. Biochem. Cell Biol.*, **31**, 1363–1366.
Mrzljak, L., Levey, A.I. & Rakic, P. (1996) Selective expression of m2 muscarinic receptor in the parvocellular channel of the primate visual cortex. *Proc. Natl. Acad. Sci. USA*, **93**, 7337–7340.
Ohashi, T., Sato, S., Yoshiki, A. & Kusakabe, M. (1997) TSC-36 (follistatin-related polypeptide) gene expression in estrogen receptor positive osteoblastic cell line, CDO7F. *Calcif. Tissue Int.*, **61**, 400–403.
Okabayashi, K., Shoji, H., Onuma, Y., Nakamura, T., Nose, K., Sugino, H. & Asashima, M. (1999) cDNA cloning and distribution of the *Xenopus* follistatin-related protein. *Biochem. Biophys. Res. Commun.*, **254**, 42–48.
Patel, K., Connolly, D.J., Amthor, H., Nose, K. & Cooke, J. (1996) Cloning and early dorsal axial expression of Flik, a chick follistatin- related gene: evidence for involvement in dorsalization/neural induction. *Dev. Biol.*, **178**, 327–342.
Patthy, L. & Nikolics, K. (1993) Functions of agrin and agrin-related proteins. *Trends Neurosci.*, **16**, 76–81.
Phillips, D.J. & de Kretser, D.M. (1998) Follistatin: a multifunctional regulatory protein. *Front. Neuroendocrinol.*, **19**, 287–322.
Reinoso, B.S., Pimenta, A.F. & Levitt, P. (1996) Expression of the mRNAs encoding the limbic system-associated membrane protein (LAMP): I. Adult rat brain. *J. Comp. Neurol.*, **375**, 274–288.
Rockel, A.J., Hiorns, R.W. & Powell, T.P. (1980) The basic uniformity in structure of the neocortex. *Brain*, **103**, 221–244.
Shibanuma, M., Mashimo, J., Mita, A., Kuroki, T. & Nose, K. (1993) Cloning from a mouse osteoblastic cell line of a set of transforming- growth-factor-beta 1-regulated genes, one of which seems to encode a follistatin-related polypeptide. *Eur. J. Biochem.*, **217**, 13–19.
Sloper, J.J. (1973) An electron microscopic study of the neurons of the primate motor and somatic sensory cortices. *J. Neurocytol.*, **2**, 351–359.
Sloper, J.J., Hirons, R.W. & Powell, T.P.S. (1978) A qualitative and quantitative electron microscopic study of the neurons in the primate motor and somatic sensory cortices. *Philos. Trans. R. Soc. Lond. B Biol. Sci.*, **285**, 141–171.
Tanaka, M., Ozaki, S., Osakada, F., Mori, K., Okubo, M. & Nakao, K. (1998) Cloning of follistatin-related protein as a novel autoantigen in systemic rheumatic diseases. *Int. Immunol.*, **10**, 1305–1314.
Tighilet, B., Hashikawa, T. & Jones, E.G. (1998) Cell- and lamina-specific expression and activity-dependent regulation of type II calcium/calmodulin-dependent protein kinase isoforms in monkey visual cortex. *J. Neurosci.*, **18**, 2129–2146.
Tombol, T. (1974) An electron microscopic study of the neurons of the visual cortex. *J. Neurocytol.*, **3**, 525–531.
Wiesel, T.N. & Hubel, D.H. (1966) Spatial and chromatic interactions in the lateral geniculate body of the rhesus monkey. *J. Neurophysiol.*, **29**, 1115–1156.
Wiesel, T.N., Hubel, D.H. & Lam, D.M. (1974) Autoradiographic demonstration of ocular-dominance columns in the monkey striate cortex by means of transneuronal transport. *Brain Res.*, **79**, 273–279.
Wong-Riley, M. (1979) Changes in the visual system of monocularly sutured or enucleated cats demonstrable with cytochrome oxidase histochemistry. *Brain Res.*, **171**, 11–28.
Zacco, A., Cooper, V., Chantler, P.D., Fisher-Hyland, S., Horton, H.L. & Levitt, P. (1990) Isolation, biochemical characterization and ultrastructural analysis of the limbic system-associated membrane protein (LAMP), a protein expressed by neurons comprising functional neural circuits. *J. Neurosci.*, **10**, 73–90.
Zaremba, S., Guimaraes, A., Kalb, R.G. & Hockfield, S. (1989) Characterization of an activity-dependent, neuronal surface proteoglycan identified with monoclonal antibody cat-301. *Neuron*, **2**, 1207–1219.
Zwijsen, A., Blockx, H., Van Arnhem, W., Willems, J., Fransen, L., Devos, K., Raymackers, O., Van de Voorde, A. & Slegers, H. (1994) Characterization of a rat C6 glioma-secreted follistatin-related protein (FRP). Cloning and sequence of the human homologue. *Eur. J. Biochem.*, **225**, 937–946.